

**A Mathematical Model of Glucose Metabolism
in Hospitalized Patients with Diabetes and Stress Hyperglycemia**

A Thesis

Submitted to the Faculty

of

Drexel University

by

Brian Ray Hipszer

in partial fulfillment of the

requirements for the degree

of

Doctor of Philosophy

August 2008

© Copyright 2008
Brian R. Hipszer. All Rights Reserved.

DEDICATIONS

In memory of Aliene Emilie Hipszer

ACKNOWLEDGMENTS

I have encountered countless individuals that have helped me in my doctoral pursuit – I would like to express my sincere gratitude. It is humbling to reflect on the sacrifices others have made on my behalf.

By far the strongest and most constant force in this quest has been my wife, Laurel. She has been at my side, day in and day out, sharing my frustration and elation. I am so grateful for her love, support and resolve – her unwillingness to let me fail.

My parents, Ray and Elizabeth, also deserve special recognition. Only when you walk in their shoes do you realize the love parents have for their children.

On the surface, my advisors are as different as night and day. However, both Moshe and Jeff are passionate teachers and caring beings. Their dedication to their professions is truly admirable. I am privileged to have matured under their guidance.

Banu Onaral, Ph.D. opened the door to my graduate career. Her commitment to my success was unfailing. I am very grateful for the support I received from the School of Biomedical Engineering, Science and Health Systems.

A special thanks to my fellow lab rats, especially Li Bai, Lit-Hsin Loo, and Ram Achuthanan, your encouragement and camaraderie over the years is greatly appreciated.

TABLE OF CONTENTS

LIST OF TABLES	vii
LIST OF FIGURES	ix
ABSTRACT.....	xii
CHAPTER 1. INTRODUCTION	1
1.1. Glycemia in the Hospital	1
1.1.1. Prevalence of Diabetes and Stress Hyperglycemia.....	2
1.1.2. Evidence for Tight Inpatient Glycemic Control	3
1.1.3. Glycemic Management in the Hospital.....	8
CHAPTER 2. GLUCOSE METABOLISM IN A HOSPITALIZED PATIENT	12
2.1. Stress Response.....	13
2.1.1. Catecholamines	14
2.1.2. Cortisol.....	17
2.1.3. Growth Hormone	18
2.1.4. Glucagon.....	21
2.2. Modifiers of Glucose Metabolism	23
2.2.1. Anesthesia and Analgesia	24
2.2.2. Atypical Nutrition	26
2.2.3. Fluid Balance	27
2.2.4. Hypothermia	28
2.2.5. Hypoxia.....	30
2.2.6. Medications.....	30
2.2.7. Sepsis	32
2.2.8. Surgical Procedure	33
2.3. Perioperative Timeline.....	34

CHAPTER 3. A MODEL OF GLUCOSE METABOLISM	38
3.1. Compartmental Modeling	38
3.2. Model Equations	40
3.2.1. Glucose Subsystem	40
3.2.2. Insulin Subsystem	42
3.2.3. Glucagon Subsystem.....	43
3.3. Model Parameter Analyses	43
3.3.1. Parameter Dependencies.....	44
3.3.2. Sensitivity Analysis	49
CHAPTER 4. REFINING DYNAMIC GLUCOSE UPTAKE.....	65
4.1. Peripheral Glucose Uptake	65
4.2. Net Hepatic Glucose Balance	74
CHAPTER 5. MODELING STRESS-INDUCED HYPERGLYCEMIA	87
5.1. Epinephrine Kinetics.....	87
5.2. Epinephrine Pharmacodynamics.....	91
5.2.1. Insulin Release	91
5.2.2. Endogenous Glucose Production	94
5.2.3. Glucose Uptake.....	102
5.2.4. Blood Flow.....	106
5.2.5. Glucagon Release.....	108
5.3. Models of Epinephrine Kinetics	109
5.3.1. Two-compartment Model	109
5.3.2. Six-compartment Model	110
5.3.3. Model Accuracy in Steady-State and Transient Conditions.....	113
5.4. An Expanded Model of Glucose Metabolism.....	116

LIST OF REFERENCES.....	119
APPENDIX A: ORIGINAL MODEL EQUATIONS	140
APPENDIX B: EPINEPHRINE INFUSION STUDIES IN MAN.....	144
APPENDIX C: VALUES FOR EXTENDED MODEL PARAMETERS	146
VITA.....	148

LIST OF TABLES

Table 2.1: Hyperglycemic Actions of the Stress Hormones.....	23
Table 2.2: Modifiers of glucose metabolism during hospitalization	24
Table 2.3: Factors affecting intraoperative fluid balance (adapted from Rosenthal 1999 [1]).....	28
Table 2.4: Glycemia-altering drugs (adapted from Pandit 1993 [2]).....	31
Table 2.5: Severity of General and Orthopedic Procedures (adapted from Copeland 2002)	34
Table 3.1: Glucose metabolism model clarifications and corrections	40
Table 3.2: Volumetric flow rates for blood, glucose (water), and insulin (plasma). Rates in parentheses are redundant.....	46
Table 3.3: Blood, interstitial fluid and intracellular fluid volumes for the given tissue or organ.	47
Table 3.4 Independent Parameters of the Glucose Metabolism Model	51
Table 3.5: L^1 and L^∞ norms for all unique parameter sets (an odd or even value of k corresponds to the 10% decrease or the 10% increase in a parameter, respectively).....	57
Table 3.6: Percent change in α for 10% increase ($\Delta\alpha_i^+$) and a 10% decrease ($\Delta\alpha_i^-$) in parameter i	60
Table 3.7: Experimental data from seven published studies where constant intravenous insulin infusions were performed in normal man.	63
Table 4.1: Sources of glucose uptake	65
Table 4.2: Hyperbolic tangent equation parameter values for the insulin-mediated modifier of peripheral glucose uptake	66
Table 4.3: Data from published appendicular studies.....	68
Table 4.4: Assumptions used to translate appendicular glucose uptake data (in $\text{mg min}^{-1} 100\text{ml tissue}^{-1}$) to total peripheral tissue glucose uptake (mg/min).....	70
Table 4.5: Parameter estimates with 95% confidence limits in parentheses for the hyperbolic tangent and logistics equations and the (transformed) original parameter values for the hyperbolic tangent relationship between peripheral interstitial insulin concentration and peripheral glucose uptake.....	71

Table 4.6: Estimates of splanchnic glucose uptake from glucose/insulin clamp experiments.....	82
Table 4.7: The increase in endogenous glucose production (EGP) and circulating levels of glucagon, epinephrine, and cortisol after 5h [3] and 72h [4] of hormone infusion in healthy subjects.....	84
Table 5.1: Average (\pm SD) release rate and clearance of epinephrine in man at rest reported in the literature (n, number of subjects; ND, not determined).....	88
Table 5.2: Fractional extraction of epinephrine for specific regions reported in the literature	90
Table 5.3: Peak first-phase insulin response to a 5g intravenous arginine bolus at different plasma glucose (100, 150 and 250 mg/dl) and epinephrine concentrations [5].....	93
Table 5.4: Determination of the epinephrine modifier from data published by Rizza et al [6], Deibert [7] and Shamoon [3, 8].....	99
Table 5.5: Summary of published euglycemic insulin clamp studies in man that report on the effect of epinephrine on peripheral glucose uptake	104
Table 5.6: Coefficient values (V_{\max} and K_m) and goodness-of-fit for each published dataset and the average coefficient values. Fractional increase in cardiac output (ΔCO) and arterial epinephrine concentrations were fit to the equation $\Delta CO = V_{\max}(x-1)/(K_m + x-1)$ where V_{\max} and K_m are constants and x is the arterial epinephrine concentration divided by the basal arterial epinephrine concentration. Italicized coefficient values represent the values averaged from the four published studies.	107
Table 5.7: System of six first-order differential equations describing the kinetics of epinephrine.....	112
Table 5.8: Parameter Values for the 6 th order model of epinephrine kinetics	112
Table 5.9: Goodness-of-Fit of epinephrine kinetics models to clinical data as assessed by the root mean square error (RMSE).....	114

LIST OF FIGURES

Figure 2.1: Perioperative timeline.....	35
Figure 3.1: Simplified representation of a biological compartment used in the glucose metabolism model.....	39
Figure 3.2: Contour map of simulated steady-state plasma glucose concentrations (in mg/dl) for constant intravenous infusions of glucose and insulin.	54
Figure 3.3: Residual plots for insulin subsystem predicted steady-state plasma insulin concentration versus measured plasma insulin concentrations for various intravenous insulin infusion rates. Panel A contains the residuals for the subsystem using the original parameter values and panel B contains the residuals for the subsystem using update values for HCT and F_{LIC} . In each panel, the red dashed line is the mean of the residuals.	62
Figure 3.4: Log-transformed insulin infusion rate and plasma insulin concentration data from published experiments (gray circles), model simulations using the original (blue dot-dashed line) and updated (red dashed line), and the linear least-squares regression model of the experimental data (green line).	64
Figure 4.1: Pooled data from appendicular glucose uptake studies. Open and solid circles indicate leg and forearm glucose uptake studies, respectively. For each data point, horizontal and vertical error bars represent the standard deviations in measured plasma insulin concentrations and calculated rates of glucose uptake, respectively, among the subjects in the study.	69
Figure 4.2: Various response curves describing the relationship between peripheral interstitial insulin concentrations and peripheral glucose uptake (pooled data – filled black circles, original hyperbolic tangent relationship - solid black line, the hyperbolic tangent relationship with updated parameter values - dashed red line and the logistics relationship - dot-dash blue line).	72
Figure 4.3: Arterial (red) and venous (blue) blood supplying the liver where Q_G and Q_L represent the blood flow from the gut and liver, respectively, and Q_A represents the blood flow through the hepatic artery such that the sum of Q_A and Q_G equals Q_L ...	77
Figure 4.4: Model simulation (red dashed line) of a $6.5 \text{ mg kg}^{-1} \text{ min}^{-1}$ intravenous glucose infusion in normal man superimposed on plot of experimental data originally published in [9]	78
Figure 4.5: Data from Sorensen (1985) used to compute M_{HGU}^G . Data from glucose/insulin clamp studies (solid symbols) are circled in blue and data from oral glucose tolerance tests (open symbols) are circled in red.	80

- Figure 4.6: Steady-state rates of splanchnic glucose uptake at euglycemia (light blue) and hyperglycemia (dark blue) as a function of normalized insulin concentrations. The lines represent model estimates of uptake and points represent actual measurements. Panel A: model estimates..... 82
- Figure 4.7: Model simulation (red dashed line) of a $6.5 \text{ mg kg}^{-1} \text{ min}^{-1}$ intravenous glucose infusion in normal man superimposed on plot of experimental data originally reported in [9] after adjustment of the function parameters of glucose-mediated hepatic glucose uptake (gray line represents the simulation data with original parameter values)..... 83
- Figure 5.1: Average (\pm SD) plasma epinephrine concentrations in arterial, arterialized venous, and venous blood as reported in [3, 5, 10-33] (* $p < 0.005$ versus arterial) 89
- Figure 5.2: Percent decrease in first phase (red circles) and second phase (blue squares) insulin release as a function of arterial epinephrine concentration. The solid line represent the best fit of all data points to the equation $\Delta IR = V_{\max} (x-1)/(K_m + x-1)$ where V_{\max} and K_m are constants and x is the arterial epinephrine concentration divided by the basal arterial epinephrine concentration..... 92
- Figure 5.3: The time course of epinephrine-mediated hepatic glucose output in response to a constant intravenous epinephrine infusion as predicted from data from published by ●Rizza et al [6], ▲ Deibert [7] and ■ Shamoon [3, 8]. The red dashed line demarcates unity. 98
- Figure 5.4: A model of the time course of epinephrine-mediated hepatic glucose output (solid line) compared to the experimental data (■) from published by Shamoon [3, 8]. 101
- Figure 5.5: The epinephrine-dependent peripheral glucose uptake modifier. Blue circles represent the pooled clinical data from [201, 247-249] as shown in Table 5.5 and the red line represents equation 5.12 with $E_H^B = 60 \text{ pg/ml}$, $V_{\min} = 1$, $V_{\max} = 0.3$, $m = 1.5$, and $K_{50} = 6$ 105
- Figure 5.6: Percent change in cardiac output (l/min) as a function of arterial epinephrine concentration. The points represent data reported in [26, 28, 34, 35] and the lines represent the best fit to the equation $\Delta CO = V_{\max} (x-1)/(K_m + x-1)$ where V_{\max} and K_m are constants and x is the arterial epinephrine concentration divided by the basal arterial epinephrine concentration..... 107
- Figure 5.7: Two-compartment model of epinephrine kinetics adapted from [36]..... 110
- Figure 5.8: A six compartment model of epinephrine kinetics..... 111
- Figure 5.9: Model estimates of steady-state arterial (red circles) and venous (blue triangles) plasma epinephrine concentrations. Solid red line, arterial estimates of model A; red and blue dashed lines, arterial and venous estimates of model B; red

and blue dot-dashed lines, arterial and venous estimates of model C; magenta squares, arterialized venous plasma epinephrine concentrations..... 115

Figure 5.10: Comparison of experimental and simulated data for an intravenous epinephrine infusion at a rate of 0.83ug/kg per min over 60 minutes. Blue triangles, measured epinephrine levels from the brachial vein; solid blue line, model A; dashed blue line, model B; dot-dashed blue line, model C..... 115

Figure 5.11: Extended model equations categorized by subsystem with equations highlight gray associated with a particular organ or tissue in each subsystem. Equations and variables highlighted in green and yellow identify our contribution to the extended model with green representing modifications to the original model (equation 5.11 and F_{LIC} in 13.1) and yellow representing new equations (5.7-5.9, 8.3, 13.9, and 17-22). 118

ABSTRACT

A Mathematical Model of Glucose Metabolism
in Hospitalized Patients with Diabetes and Stress Hyperglycemia

Brian Ray Hipszer

Moshe Kam, Ph.D. and Jeffrey I. Joseph, D.O.

The human body employs several mechanisms to regulate the concentration of glucose in the bloodstream. The rates of glucose uptake and release from specific organs within the body are modulated directly by the concentrations of metabolites and hormones, and indirectly by the autonomic nervous system. The negative feedback relationship between glucose and the anabolic hormone, insulin, dominates the process of glycemic regulation. The binding of insulin to its receptor begins a cascade of intracellular events that increases glucose uptake into the liver and peripheral tissue and reduces glucose release from the liver. However, this mechanism can be overwhelmed during the acute stress typified by a moderate surgical procedure. Cellular damage and tissue trauma cause a surge in catabolic hormones and cytokines, leading to insulin resistance and marked hyperglycemia.

The focus of this study is the mathematical descriptions of the processes that regulate glucose production and uptake. Such descriptions model the complex relationships between metabolites and hormones and their effects on glycemia. Descriptive models that are accurate and robust have the potential to guide the development of tools designed to manage glycemia in hospitalized patients with diabetes and stress-induced hyperglycemia. Specifically, we investigate the validity of a glucose metabolism model published by John Sorensen in a 1985 doctoral thesis. The model is a set of 22 first-order time-invariant nonlinear differential equations describing the interaction of glucose,

insulin and glucagon and their effect on organ-level glucose uptake and release. We modified the model to incorporate recent experimental data, including data we have collected in clinical trials. The model was expanded to include a description of epinephrine and its effects on glycemia.

CHAPTER 1. INTRODUCTION

In order to develop a realistic representation of glycemia in the hospitalized patients, the mechanisms that alter the normal metabolism in this population need to be considered. Understanding the factors that affect net hepatic glucose balance is important in describing changes to endogenous glucose production. Factors that change to insulin sensitivity will also be discussed because of the dominate role insulin plays in the regulation of glycemia. Finally, something cannot be simply overlooked in the hospitalized, specifically the surgical, population are factors that change distribution volumes of glucose and insulin.

The mathematical descriptions developed herewith focus on the mechanisms that govern glycemic regulation in a perioperative surgical patient. There are a multitude of factors that influence glucose metabolism in this setting. This thesis attempts to choose those factors that play a predominant role in determining the course of glycemia.

Data is represented as mean \pm SD. When referenced data is reproduced in this text, data in mean \pm SEM format were converted to mean \pm SD.

1.1. Glycemia in the Hospital

The goals of diabetes management in the hospital are to avoid hypoglycemia, excessive hyperglycemia, lipolysis, ketogenesis, protein catabolism, dehydration, and electrolyte imbalance. Adequate levels of the anabolic hormone insulin are required to counter balance the surge of catabolic hormones (epinephrine, glucagon, cortisol, and growth hormone) that occur with stress and surgery [37-39]. The combination of insufficient insulin and excessive catabolism typically leads to diabetic ketoacidosis, hyperosmolar

nonketotic syndrome, or excessive lactic acid production [40]. Historically, patient care has focused almost entirely on the importance of maintaining sufficient plasma insulin levels to avoid overt metabolic decompensation [41]. Recently, several prospective clinical studies have demonstrated improved clinical outcome (decreased morbidity and mortality), decreased overall cost, and decreased length of hospital stay, when blood glucose levels are managed acutely within a narrow range for specific patient populations [42-48].

In this chapter, we will discuss the state of glycemic management in the hospital setting and review the evidence that acute tight glycemic control is clinically important.

1.1.1. Prevalence of Diabetes and Stress Hyperglycemia

In 2005, an estimated 20.8 million Americans had diabetes with over one third of this population unaware they have this disease [49]. An additional 41 million people are pre-diabetic, a classification in which a person displays abnormal glycemia but does not meet the formal definition of type 2 diabetes [50]. There is a disproportionate per capita expenditure in medical care for those with diabetes. Whereas those with diabetes comprise only 7.0% of the U.S. population, they are responsible for 18% of the \$413 billion spent on inpatient hospital care with \$40 billion directly attributable to the treatment of their disease [51]. In 2004, 5.4 million (short stay) diabetic patients were discharged from the hospital out of a total of 34.9 million discharges [52]. 15.6% of the inpatient population had a diagnosis of diabetes – more than twice the rate of diabetes in the general population. These statistics do not even account for the large pre-diabetic population who, under the stress of illness and/or medical procedure, will be acutely hyperglycemic during their hospital stay. Diabetic patients are more likely to be admitted

to the hospital and, once admitted, the costs associated with their care are greater. Recent prospective, controlled studies have demonstrated that short-term glycemic control in the hospital setting can reduce morbidity/mortality, shorten hospital stays, and decrease overall costs [44-47, 53].

Among adults with diagnosed diabetes, 16% take insulin only, 12% take both insulin and oral medication, 57% take oral medication only, and 15% do not take either insulin or oral medications. Many of patients with type 2 diabetes treated by diet and pills will require insulin during their hospital stay, due to the stress of anesthesia, surgery, and acute illness [54, 55]. Another 1.5 million patients have significant hyperglycemia while in the hospital, but do not have the diagnosis of diabetes [56]. Stress hyperglycemia has been clearly linked to excessive in-hospital mortality and an increased risk for congestive heart failure and cardiogenic shock [57, 58]. Recent prospective studies have demonstrated a significant decrease in morbidity and mortality when glucose levels are tightly controlled in the hospital setting [45, 46, 59-61]. In a report published by the Agency for Healthcare Research and Quality, aggressive glucose management was identified as one of the patient practices with great potential to improve patient safety and clinical outcome [62].

1.1.2. Evidence for Tight Inpatient Glycemic Control

Diabetes has been proven to be a major risk factor for perioperative myocardial infarction (MI), heart failure, infection, and death [46, 57]. Anesthesia and surgery initiates a general stress response characterized by a rapid (epinephrine, norepinephrine) and delayed (cortisol, growth hormone, thyroid hormones) release of catabolic hormones. Insulin levels are depressed and the liver and peripheral tissues exhibit a variable degree

of insulin resistance [63]. The result of this metabolic imbalance is an increase in hepatic glucose production, a decreased rate of peripheral glucose utilization, and protein catabolism [55, 63]. The level of hyperglycemia is related to the patient's prior diabetic status and the degree of metabolic stress. Blood glucose (BG) levels greater than 500 mg/dl are not uncommon following major stressful events (cardiopulmonary bypass, major trauma), including patients without a history of diabetes or glucose intolerance [55, 64]. In addition, diabetic patients requiring surgery are at increased risk for hypoglycemia due to prolonged fasting and a mismatch between intravenous glucose intake, endogenous glucose production, glucose utilization, and the timing/amount of insulin delivery. Inadequate delivery of intravenous (IV) glucose (< 5 gm/hr) will cause excessive proteolysis, lipolysis, and starvation ketosis. Increased amounts of IV glucose (>10 gm/hr), especially in the face of insulin resistance, will lead to significant hyperglycemia [55, 63]. Therapeutic regimens of glucose infusion, glucose monitoring, and insulin delivery have traditionally focused on the avoidance of hypoglycemia, and avoidance of acidosis.

Tight perioperative BG control has clearly been shown to decrease the risk for developing a post-operative sternal wound infection (60% risk reduction) following coronary artery bypass graft (CABG) surgery [45, 65]. BG levels above 200 mg/dl are known to greatly increase the risk for post-operative infection in general, including wound infection, urinary tract infection, and nosocomial pneumonia [66, 67]. Even transient episodes of hyperglycemia are known to reduce cellular and humoral immunity, including a marked inhibition of neutrophil/macrophage phagocytic function and decreased opsonin production. Immune function has been shown to quickly return to

normal following insulin therapy and normoglycemia [68]. Diabetic patients undergoing major surgical procedures are at a significantly increased risk for cardiovascular complications (MI, congestive heart failure, and arrhythmia) and death when compared to matched controls [46, 69, 70]. Kalin *et al.* (1998) prospectively evaluated the impact of tight BG control (IV insulin infusion controlled by frequent BG measurements) on clinical outcome in 400 diabetic patients undergoing CABG surgery compared to 876 non-diabetic patients. Hospital mortality was nearly identical in the tightly controlled diabetic and non-diabetic patients (1.75% versus 1.71%) [61]. During this same period, the National Cardiac Surgery Database reported a 50% higher mortality for patients with diabetes when compared with non-diabetic patients undergoing similar CABG surgery. Another study demonstrated a similar reduction in hospital mortality – MI, stroke, renal failure, and less need for an intraoperative aortic balloon pump when BG was tightly controlled using a continuous insulin infusion and frequent BG monitoring [71]. Lazar *et al.* (2000) treated diabetic patients aggressively with a variable glucose-insulin-potassium infusion (target BG 100 to 200 mg/dl) [44]. When compared to matched diabetic patients treated with conventional insulin therapy, the intensively treated patients demonstrated improved cardiac function, less need for inotropic and vasopressor support, less need for an intra-aortic balloon pump, less time on a ventilator, a lower incidence of atrial fibrillation, and shorter hospital stays. Hyperglycemia may also affect renal function in the perioperative period. In a prospective, multicenter study of 2,222 patients undergoing CABG surgery, preoperative hyperglycemia (>300 mg/dl) was associated with the highest relative risk for acute renal failure, especially in patients with pre-existing diabetic renal disease [46]. Mortality has also been correlated with elevated BG levels in

an observational study of 1,157 CABG surgery patients older than 75 years of age. BG levels greater than 300 mg/dl were a significant predictor of postoperative mortality [47].

Patients with diabetes account for a high percentage of all cardiovascular mortality [72]. Possible causes for this increased morbidity and mortality include: a higher incidence of multivessel atherosclerotic disease, decreased coronary flow reserve, decreased ejection fraction, subclinical cardiomyopathy, congestive heart failure, autonomic neuropathy, and ventricular arrhythmias [73, 74]. The short-term and long-term risk for death following an acute MI has been found to be significantly higher in patients with diabetes [46]. Even without symptoms, diabetic patients are known to have a 27-69% incidence of clinically significant diastolic dysfunction [75]. Even transient episodes of hyperglycemia are known to inhibit endothelial cell relaxation, and therefore local regulation of myocardial and cerebral blood flow. Local tissue levels of nitric oxide, oxygen free radicals, lactic acid, advanced glycosylation end products, and other intermediary metabolites interact dynamically to influence endothelial cell function [76]. The same factors may influence platelet activation and adhesion [77]. Even brief periods of inadequate insulin levels are known to cause an acute rise in blood free fatty acid levels, a switch to fatty acid oxidation within the myocardium, a significant rise in myocardial oxygen consumption, and an increased risk of ventricular arrhythmia [78]. Epidemiologic data demonstrate that diabetic and non-diabetic patients admitted to the hospital with hyperglycemia have an increased risk for death and cardiovascular complications during the stressful period of their illness [79]. Diabetic patients admitted to the hospital with a BG above 180 mg/dl nearly double their risk for in-hospital death and have a significantly increased risk for developing congestive heart failure and cardiogenic shock [58].

The Diabetes-Insulin-Glucose in Acute Myocardial Infarction (DIGAMI) trial prospectively studied 660 diabetic and non-diabetic patients admitted to the critical care unit (CCU) with a BG value greater than 198 mg/dl. Hyperglycemic patients experiencing an acute MI were randomized into an intensive insulin therapy group (24-hour IV insulin infusion titrated to frequent BG measurements following by tight BG control into the outpatient setting) or a conventional insulin therapy group. It was shown that the one-year mortality in diabetic patients after an acute MI could be reduced by 30% with intensive insulin treatment. A reduction in cardiovascular mortality could still be demonstrated at the five-year follow-up. In the subgroup of patients with a prior history of diabetes, in-hospital mortality decreased 58%, and 1-year mortality decreased 52%, compared to the conventionally treated group [80-84]. Capes *et al.* (2000) completed a meta-analysis of 15 studies that focused on stress hyperglycemia and the risk of death following an acute MI [58]. Non-diabetic patients with an acute MI and stress hyperglycemia had a four-fold increased risk for in-hospital mortality. Hyperglycemia is known to adversely affect platelet function, myocardial oxygen supply and demand, and pump function [57, 58, 63, 85].

In one of the most noted clinical trials regarding the inpatient hyperglycemia, University of Leuven researchers at conducted a prospective, randomized, controlled trial which evaluated 1548 post-surgical, trauma, and critically ill patients that had BG levels above 200 mg/dl upon admission to the ICU [43]. Approximately one-third of the patients where know to have diabetes, while the remaining patients developed hyperglycemia due to the metabolic stress of anesthesia, surgery, and critical illness. Hyperglycemia was managed in both groups with an IV infusion of regular insulin. Patients were randomized

to receive either intensive-insulin therapy (BG target 80-110 mg/dl) or conventional-insulin therapy (BG target 180-200 mg/dl) over 3-7 days. The group receiving intensive-insulin therapy experienced a 34% reduction in overall in-hospital mortality, 46% reduction in bacteremia, and a 41% reduction in acute renal failure. The greatest reduction in mortality occurred in patients requiring more than 5 days of ICU care (20.2% mortality with conventional-therapy versus 10.6% with intensive-insulin therapy). Mortality was decreased by preventing sepsis and multi-organ failure. Van den Berghe and her colleagues have since qualified their findings, stating that it is the normalization of BG levels, not the delivery of insulin, which improves outcome [59]. In a subsequent study of 1,200 medical ICU patients, these researchers were not able to show a significant decrease in the mortality rates between intensely treated patients versus those receiving conventional therapy [42]. However, morbidity was significantly reduced as seen in the prevention of newly acquired kidney injury, accelerated weaning from mechanical ventilation, and accelerated discharge from the ICU and the hospital.

1.1.3. Glycemic Management in the Hospital

Developing an insulin regimen to accommodate long periods of fasting and the stresses of major illness and surgery can be quite challenging [64, 86]. The anxiety and fear of hypoglycemia continues to dictate the way nurses and physicians manage diabetes. Hyperglycemia is tolerated because the factors that predispose one to clinically significant hypoglycemia (*e.g.*, long periods of fasting, inadequate and delayed food intake, changing insulin sensitivity, variability in subcutaneous insulin absorption, changing renal function) commonly occur in the hospital setting [64, 85]. The early signs and symptoms of neuroglycopenia may be masked by sedatives, general anesthesia, and

cardiovascular medications [55]. A program established by the US Pharmacopoeia to track hospital drug errors reported that errors involving insulin delivery ranked second in number, and ranked first as the leading cause of significant patient injury [87].

Improvement in the glycemic management of patients within the hospital is required.

This fact was highlighted by Golden *et al.* (1999) in a study involving 411 diabetic adults undergoing CABG surgery in an urban university teaching hospital [66]. Only six capillary BG measurements were taken during the 36-hour period following surgery.

More than 75% of the patients had a mean BG greater than 200 mg/dl. Although convenient for nursing and house-staff personnel, the “sliding-scale” method of insulin dose adjustment, based upon BG values obtained at fixed intervals, typically fails to maintain BG levels in the desired range [86, 88-90]. Limitations include highly variable insulin absorption from the subcutaneous tissue, infrequent capillary BG measurements, and a dosing schedule unrelated to meals and medical procedures [64]. A more physiological method of subcutaneous insulin delivery requires multiple daily adjustments of therapy (short acting insulin appropriately timed with meals) based upon frequent BG monitoring [85, 91]. IV insulin therapy has gained popularity because of the pharmacokinetic limitations of subcutaneous delivery [55, 90]. The injection of large bolus doses of regular insulin has been found to be one of the most commonly practiced methods of insulin delivery in the U.S. and abroad [40, 64, 92]. In one study at a university teaching hospital, 85% of type 1 diabetes patients requiring insulin therapy in the perioperative period were treated with intermittent IV boluses, rather than a continuous IV infusion [40]. Bolus dosing produces a rapid rise in plasma insulin to very high levels. The short plasma half-life (6 minutes) and short biological half-life (less than

20 minutes) of IV insulin leads to extremely low plasma and tissue insulin levels approximately 60 to 120 minutes following an IV bolus [93]. This “roller-coaster” method of BG control is unphysiological, leading to an increased rate of lipolysis, ketogenesis, and lactic acid production, and may predispose the patient to dangerous hypoglycemia [40, 55]. Finally, intermittent insulin bolus injections can cause a rapid extracellular-to-intracellular shift of electrolytes (potassium, phosphorus, and magnesium) that may predispose a patient to a life-threatening cardiac arrhythmia [55].

The continuous intravenous infusion of insulin, titrated to frequent BG measurements, has become the safest and most physiological way to manage glycemia during the stresses of major surgery and acute illness [94]. For a patient with type 1 diabetes, an IV infusion of regular insulin (at a concentration of 1.0 U/ml) is titrated to maintain BG levels within the desired range using a dedicated pump. Although the insulin dose for optimal control varies, the usual starting dose for the variable rate insulin infusion is 1.0 U/hr. Numerous clinical algorithms have been developed that account for changes in insulin sensitivity, renal function, and nutrient needs [55, 64, 85, 95, 96]. In June 2006, the Food and Drug Administration approved a computer software application (Glucommander Plus, GlucoTec, Inc., Greenville, SC) that automates the calculation of an appropriate dose of insulin as well as glucose, saline and other medications for patients on intravenous and subcutaneous insulin therapy [97].

The optimal frequency of BG measurement has not been determined. Many anesthesiologists, surgeons, and endocrinologists recommend hourly BG monitoring during periods of initial titration and stress, followed by less frequent monitoring (every 2-4 hours). BG measurements as frequently as every 20-30 minutes have been

recommended during cardiovascular and transplant surgery to minimize the risk of hypoglycemia and metabolic decompensation [64, 98]. Many physicians recommend a separate IV infusion of glucose to satisfy the basic nutritional needs of the fasting patient (5-10 g/hr) to minimize protein wasting and starvation ketosis, and to avoid hypoglycemia [55].

Recently, both the American College of Endocrinology (ACE) and the American Diabetes Association (ADA) have issued position statements supporting the need to reduce hyperglycemia in the hospital. The 2003 ACE statement recommends that fasting BG values should be maintained below 110 mg/dl while limiting excursions to a peak of 180 mg/dl [99]. A 2006 ACE/ADA statement indicates that continuous IV insulin administration is the best method to achieve near-normal glycemia in the hospital [100].

CHAPTER 2. GLUCOSE METABOLISM IN A HOSPITALIZED PATIENT

The development of a mathematical model that describes blood glucose levels in hospitalized patients starts with an understanding the factors that alter the normal glucose metabolism in this population. The stress response is primary cause of the imbalance between peripheral glucose uptake and endogenous glucose production that often leads to hyperglycemia. Conditions in the hospital can also increase the likelihood of hypoglycemic episodes. Food intake can be limited because of illness or surgical procedure. Lack of adequate exogenous glucose combined with inappropriate dosing of certain medications can easily lead to the development of hypoglycemia.

Abnormal glucose tolerance is common after trauma or illness in spite of normal or heightened insulin secretion. Despite the responsiveness of the pancreatic β -cells to secrete insulin in response to a glucose load, glucose intolerance and hyperglycemia persist, suggesting that certain target organs are relatively insensitive to the effects of circulating insulin. Because glucose consumption by central and peripheral nervous tissue, renal medulla, bone marrow, erythrocytes, and leukocytes is not insulin sensitive, the primary sites of insulin resistance are in the liver and peripheral tissues where insulin stimulates glucose uptake.

Endogenous glucose production sustains the body during periods of fasting. Glucose is supplied through the processes of glycogenolysis and gluconeogenesis. Glycogenolysis is the process by which stored glycogen is broken down to glucose. In the liver, this glucose is released into systemic circulation. Gluconeogenesis is the creation of glucose from substrates like pyruvate, lactate, glycerol, and amino acids (primarily alanine and

glutamine). It occurs primarily in the liver and, to a smaller extent, in the cortex of kidney. These processes are hyperactive in stressful periods typified by surgery and illness. The amount of glucose supplied to the body is disproportionate to its metabolic need. Coupled with decreased peripheral glucose uptake, hyperglycemia typically ensues.

In this chapter, the stress response will be described, concentrating on how it affects glucose metabolism. Factors that either exaggerate or attenuate the stress response in the hospital setting will be discussed. A typical surgical scenario will be used to illustrate the fluctuation in these glycemic modifiers. This information will be the basis for a modeling effort to describe glycemia in the perioperative setting.

2.1. Stress Response

The stress response refers to the hormonal, immunological and metabolic changes that occur after injury, trauma or illness. It is a coordinated response between the neuroendocrine and immune systems [101] that causes a catabolic state designed to stimulate and promote the process of healing following trauma. When the injury is minor, its effects are beneficial. However, when the injury is severe, its effects can be detrimental. Hypertension, tachycardia and arrhythmias strain the heart. Vasoconstriction can cause tissue hypoxia and acidosis. Increased circulating levels of epinephrine, cortisol, growth hormone, and glucagon increase both endogenous glucose production and peripheral insulin resistance, resulting in stress-induced hyperglycemia.

Stress activates the sympathetic nervous system. This activation increases the secretion of norepinephrine and epinephrine, as well as neuropeptides such as enkephalin and β -endorphin. In addition, hypothalamic corticotrophin-releasing hormone (CRF) and pituitary adrenocorticotropin hormone (ACTH) levels increase which, in turn, elevate the

levels of circulatory glucocorticosteroids. ACTH secretion is also enhanced through direct stimulation from the brain noradrenergic neurons. Other hormones involved in the stress response are prolactin and growth hormone. The response to stress is modulated by the type, duration and magnitude of stressor as well as the person's previous experience and control over stressor [102].

2.1.1. Catecholamines

Catecholamines include compounds dopamine, norepinephrine, and epinephrine. They are all derivatives of the amino acid, L-tyrosine. Besides being the precursor to norepinephrine and epinephrine, dopamine acts as a neurotransmitter. Both norepinephrine and epinephrine are found in sympathetic nerve fibers and the adrenal medulla. The adrenal medulla primarily secretes epinephrine into the circulatory system while the nervous system primarily uses norepinephrine to convey nerve impulses to effector organs. This distinction, epinephrine's release directly into the bloodstream, gives it rapid access to hepatic, muscle and adipose tissues.

Epinephrine and norepinephrine are classified as sympathetic agents. They bind to α - and β -adrenergic receptors on target organs. They cause vasoconstriction, which is selective in the case of epinephrine. Epinephrine will actually cause dilation in the blood vessels supplying muscle and the liver. They also cause circulating free fatty acid levels to rise. Epinephrine also increases the rate and force of contraction of the heart.

Epinephrine plays a significant role in the development of hyperglycemia associated with the stress response. It mobilizes glucose and fatty acids to fuel metabolism, increases the endogenous production of glucose by the liver, and inhibits pancreatic insulin secretion.

In the study of six normal subjects, epinephrine concentrations greater than 150 pg/ml caused an observable increase in blood glucose levels while epinephrine concentrations greater than 400 pg/ml suppressed insulin secretion [103]. In addition, epinephrine will also stimulate the release of glucagon from the pancreatic α -cells. These actions lead to hyperglycemia which feeds back to counteract epinephrine's effects on glycemia by stimulating insulin secretion and inhibiting glucagon secretion.

While plasma epinephrine levels range between 20 and 120 pg/ml in normal subjects [104-106], epinephrine levels range between 10 and 1,370 pg/ml in critically ill patients and between 360 and 237,000 pg/ml in patients successfully resuscitated after a heart attack [107]. In elective cardiac surgery patients, epinephrine levels return to normal within 48 hours after the operation [105]. Acute and chronic stress both can produce epinephrine levels great enough to cause both excessive endogenous glucose production and suppressed insulin release. Large variability in the epinephrine response to the same stress intensity makes it difficult to predict.

The direct effect of elevated epinephrine levels on hepatic glucose production appears transient. This increase in hepatic glucose production is independent of epinephrine-induced increase in circulating glucagon and its subsequent down-regulation does not stem from the depletion of glycogen or gluconeogenic substrates [6]. Glycogenolysis and gluconeogenesis contribute to hepatic glucose output. While epinephrine directly modulates glycogenolysis, it indirectly affects gluconeogenesis by increasing the abundance of the substrates (e.g., alanine, lactate, and glycerol) required for this process [108, 109]. Presented with additional gluconeogenic precursors, the liver will increase its rate of gluconeogenesis.

The ability of norepinephrine to elevate the glucose level is not as potent as that of other glucoregulatory hormones. Its role is primarily that of a neurotransmitter. It is localized in the synaptic clefts between neurons and their effector organs but can freely diffuse into circulation. The mean (\pm SD) resting plasma norepinephrine concentration was 228 ± 81 pg/ml and 526 ± 198 pg/ml (with maximum individual values of 406 pg/ml and 956 pg/ml) in the supine and upright positions [110]. When norepinephrine levels exceed 1,800 pg/ml, suppression of plasma insulin levels and the elevation of blood glucose levels are observed [110].

An increase in plasma norepinephrine levels increases the gluconeogenic precursors (increasing the rate of gluconeogenesis) but does not affect glycogenolysis [111]. During surgery and acute stress, plasma norepinephrine levels correlate well with epinephrine levels [105, 107]. However, norepinephrine levels remain elevated longer postoperatively than epinephrine [105]. In a study of catecholamine levels during cardiac bypass surgery, arterial norepinephrine peaked at 825 ± 84.2 pg/ml [112]. Although it is possible to achieve the norepinephrine levels required to affect glycemia, its role is secondary to that of epinephrine.

Circulating epinephrine (and, to a lesser extent, norepinephrine) will greatly influence glycemia. An acute increase in catecholamines is observed during surgery and immediately postoperatively [105, 112]. Circulating levels during these periods surpass (greatly in the case of epinephrine) the thresholds required to alter insulin secretion and resistance, and endogenous glucose production. Typically, catecholamines will return to preoperative levels in 48 hours postoperatively.

2.1.2. Cortisol

Cortisol is a steroid hormone that is released by the adrenal cortex. Its secretion is mediated by ACTH. There are two specific brain corticosteroid receptors. The mineralocorticoid receptors are nearly always fully occupied even at basal levels of circulating steroids. The glucocorticoid receptors become occupied during acute periods of stress and are responsible for down regulating sympathetic and hypothalamic-pituitary-adrenal activity [113].

Cortisol is a key mediator of the catabolic actions in the stress response. It promotes protein breakdown and hepatic gluconeogenesis while reducing peripheral glucose uptake so glucose can be spared for the brain and spinal cord. Cortisol increases insulin resistance in hepatic and peripheral tissues by diminishing insulin's post-receptor effects [114]. In addition, it promotes lipolysis which provides additional substrates for gluconeogenesis. Cortisol also stimulates of glucagon release [115, 116]. However, it inhibits the release of catecholamines, the potent hyperglycemic agents, as demonstrated in antecedent hypoglycemia studies [117, 118].

The normal circadian rhythm of cortisol release will produce circulating plasma concentrations of 0-20 $\mu\text{g}/\text{dl}$ with elevated levels occurring while awake or waking [119]. During surgery, total cortisol can peak at 55 $\mu\text{g}/\text{dl}$. A large majority of circulating cortisol is bound to corticosteroid-binding globulin (70-75%) and albumin (20-25%). Free cortisol is only 5 percent in controls but this percentage can be 3-fold higher following cardiac surgery [120]. Total cortisol levels in critically ill patients were twofold greater than in controls while free cortisol levels were fivefold greater [121]. The

disproportionate increase in free cortisol levels corresponds to a decrease in the binding proteins (corticosteroid-binding globulin and albumin).

When compared to the time course of catecholamine levels in critical illness, cortisol remains elevated longer. In 30 critically-ill patients, total cortisol levels averaged $22.6 \pm 8.9 \mu\text{g/dl}$ 6.4 ± 5.6 days after hospitalization [121]. In 54 patients admitted to the hospital for a ruptured aorta, total cortisol levels were $21.0 \pm 8.1 \mu\text{g/dl}$ within 24 hours of admission [122].

In a study of six normal subjects, a 24-hour cortisol infusion ($2 \mu\text{g/kg/min}$) produced a mean plasma cortisol level of $37 \mu\text{g/dl}$. Elevated plasma glucose levels ($126 \pm 2 \text{ mg/dl}$ with cortisol infusion versus $97 \pm 2 \text{ mg/dl}$ with saline infusion) and plasma insulin levels ($16 \pm 2 \text{ mU/l}$ with cortisol infusion versus $10 \pm 1 \text{ mU/l}$ with saline infusion) were observed [114]. However, short term exposure (2-6 hrs) to elevated cortisol levels either decreased or did not alter glucose production and utilization [123]. In the hospital setting, it is possible for cortisol levels to remain elevated over days to weeks – long enough to disrupt the normal regulation of glycemia.

2.1.3. Growth Hormone

Growth hormone stimulates protein synthesis and lipolysis, inhibits proteolysis, and increases peripheral insulin resistance and glycogenolysis. Synthesized within the pituitary gland, growth hormone is a 191-amino acid protein with a molecular weight of 22 kDa. Its release is controlled by GH-releasing hormone, somatostatin, and ghrelin. Growth hormone is secreted in a pulsatile fashion after the onset of sleep and postprandially. Peak plasma concentrations range from 5 to 35 ng/mL and typically last

one to two hours before returning to basal levels (<3 ng/ml) [119]. The amount and pattern of growth hormone secretion change throughout life. Adults average about 5 peaks per day while children and adolescents average about 8 peaks per day with children typically having higher basal levels as well.

In a study of 18 male non-diabetic patients, the magnitude and duration of increases in plasma growth hormone were directly related to the severity of the surgery [124]. The cohort undergoing aorto-femoral bypass (the highest surgical stress in the study) experienced sustained peak levels ($\sim 24 \pm 17$ ng/ml) post anesthesia that remained elevated past the eighth postoperative day.

In a forearm glucose uptake study involving seven fasted non-diabetic male subjects, an intravenous bolus (0.14 ng) of growth hormone produced a peak plasma level of 21 ± 8 ng/ml [125]. While plasma levels of insulin, C-peptide, and glucagon did not differ from controls throughout the study, forearm glucose utilization decreased significantly (more than 50% from baseline) for the first 20 minutes following the growth hormone bolus. Further studies could not demonstrate a dose-dependent response [126]. The growth hormone bolus also exhibited a significant capacity to increase circulating lipids ~ 30 minutes after administration. However, euglycemic insulin clamp studies with prolonged growth hormone infusions did not exhibit the same rise in circulating free fatty acids in 11 non-diabetic male subjects [127]. These studies demonstrated a suppression of glucose uptake that increased with the length of growth hormone infusion and an antagonistic effect of growth hormone on the insulin's suppression of endogenous glucose production. Hyperglycemic clamp studies with the same subjects demonstrated that elevation of growth hormone levels for 2-12 hours did not affect beta-cell sensitivity. Thus, prolonged

elevation of growth hormone will cause hepatic and peripheral insulin resistance but will not affect the ability of the pancreas to respond to hyperglycemia, thus, allowing insulin to counter lipolytic action of growth hormone under normal circumstances. In the separate euglycemic insulin clamp studies, a one-hour growth hormone infusion prior to the start of the clamp demonstrated the ability of growth hormone to elevate circulating free fatty acid levels [128]. However, upon initiation of an intravenous insulin infusion (0.5 mU/kg/min), free fatty acids levels promptly fell below baseline levels. In addition, the use of three separate rates of growth hormone infusion (2, 4, and 8 ng/kg/hr producing peak levels of 16 ± 5 , 26 ± 6 , 51 ± 13 ng/ml) illustrates dose-dependent responses in glucose uptake and production. The two highest infusion rates prolonged the suppression of glucose uptake with significant (compared to controls) suppression of glucose uptake 6 hours after the start of growth hormone infusion versus 4 hours for the lowest growth hormone infusion rate. Only the highest growth hormone infusion rate showed a significant increase in endogenous glucose production.

Whereas studies with acute boluses of growth hormone could not demonstrate any effect of elevated growth hormone on endogenous glucose production, a study with an extended infusion has shown that the chronic elevation of the hormone (20.8 ± 9.3 ng/ml in 6 subjects receiving a 4-hour exogenous intravenous infusion at a rate of 40 ng/kg/min) prevented a fall in the rate of glycogenolysis compared to fasting controls [129].

In trauma and illness, the loss of the normal circadian rhythm of growth hormone (in addition to its chronic elevation) may have a significant influence on glucose metabolism through its influence on circulating levels of insulin-like growth factor [130].

2.1.4. Glucagon

Glucagon is catabolic hormone (29 amino acids in length, 3.5kDa in weight) secreted by the α -cells of the pancreas. Its primary function is to counterbalance insulin's effects, protecting against hypoglycemia. It is secreted into the portal vein and its actions occur primarily in the liver, promoting glycogenolysis and gluconeogenesis. The mechanism by which glucagon promotes gluconeogenesis is separate from that which is used by adrenergic mediators [131]. Other stress hormones (epinephrine, growth hormone, and cortisol) will stimulate glucagon release [116, 132]. In man, plasma glucagon levels range between 20 and 100 pg/ml.

In the study of 21 surgical patients, immunoreactive glucagon¹ (IRG) increased twofold during the operation and remained elevated for up to 8 days postoperatively while those patients that experienced complications during surgery had peak glucagon levels 6-18 times greater than preoperative levels [133]. In a study of 40 patients, the patients were grouped by their surgical severity. Three stress categories (mild, moderate, and severe) were defined by the length of the operation. Average pre-, intra- and postoperative IRG levels for the three groups correlated with the degree of surgical stress [134]. Whereas IRG levels in mild group did not differ significantly from fasted healthy subjects, those of the moderate group increased starting in surgery and peaked on the second postoperative day and those in the severe group were significant elevated preoperative and peaked on the first postoperative day. IRG levels returned to preoperative levels between the fifth and seventh postoperative day in both the moderate and severe groups.

¹ The 3.5kDa glucagon molecule is one of several moieties (<2.0, 3.5, 9.0, and >40.0 kDa) of immunoreactive glucagon (IRG). The isolation and measurement of the 3.5kDa molecule was not performed until the late 1970s. As such, if specific plasma values of pancreatic glucagon (3.5kDa moiety) could not be discerned, the results are only discussed in general terms in this text.

The postoperative increase in plasma glucagon may not be completely attributable to stress. Plasma glucagon levels are elevated in the fasted state as well. In a study of 15 obese subjects, IRG levels rose twofold, peaking on the 3rd day of fasting [135]. It becomes difficult to separate the factors that contribute to the subsequent rise in glucagon levels since patients are instructed to withhold consumption of any solid food prior to surgery. Regardless of the cause, the course of patient care in the hospital creates the proper milieu to support a sustained increase in plasma glucagon levels.

In pancreatic-pituitary clamp experiments, low- and high-dose glucagon infusions (0.7 and 2.8 pg/kg/min) produced plasma glucagon levels of 64 ± 7 and 125 ± 61 pg/ml after 4 hours (compared to 44 ± 12 pg/ml in fasted control subjects). The high-dose infusion produced increases in both glycogenolysis and gluconeogenesis while the low-dose infusion produced a significant increase in glycogenolysis only [136]. The ability of glucagon to increase endogenous glucose production is greatly attenuated by elevated levels of circulating insulin [137] and hyperglycemia [114, 138]. However, the combination of elevated glucocorticoids (*e.g.*, cortisol) and glucagon elicits a notable increase in endogenous glucose production in spite of hyperinsulinemia, demonstrating that cortisol increases hepatic insulin resistance and/or hepatic glucagon sensitivity [139].

The actions of the stress hormones can easily produce a hyperglycemic state. These hormones increase endogenous glucose production, suppress insulin secretion, and decrease glucose uptake (Table 2.1). The anti-hyperglycemic actions these hormones exhibit (*i.e.*, cortisol will inhibit epinephrine release [117, 118] and glucagon hypersensitizes the pancreatic beta cells to glycemic changes [140]) are overwhelmed by their catabolic effects. Their concerted actions produces a hyperglycemic state greater

than the sum of the individual contributions of each hormone [141]. Epinephrine and glucagon are potent simulators of endogenous glucose production while cortisol and growth hormone cause severe hepatic and peripheral insulin resistance. The increase in the supply of glucose into systemic circulation and the inability for glucose and insulin to promote the glucose uptake result in sustained hyperglycemia during stress.

Table 2.1: Hyperglycemic Actions of the Stress Hormones

	Glycogenolysis	Gluconeogenesis	Lipolysis ^a	Proteolysis ^a	Glucagon Release	Peripheral Glucose Disposal	Pancreatic Insulin Secretion
Epinephrine	+	+ ^b	+	+	+	-	-
Norepinephrine		+ ^b	+	+		-	-
Cortisol		+	+	+	+	-	-
Growth Hormone	+		+	-	+	-	
Glucagon	+	+					+

a. lipolysis and proteolysis relate to gluconeogenesis in that these processes liberate gluconeogenic substrates

b. indirectly increases the rate of gluconeogenesis by increasing the substrates converted into glucose by the liver

Outside the classical endocrine stress response, the immune system also responds to trauma and illness through significant alterations in the release of multiple cytokines [142]. Cytokines (*i.e.*, interleukin 6) closely parallel changes to insulin sensitivity measured in postoperative patients [143].

2.2. Modifiers of Glucose Metabolism

By directly or indirectly increasing endogenous glucose production and inhibiting peripheral and hepatic glucose uptake, stress hormones create a glucose imbalance that

typically leads to hyperglycemia. Factors that typically alter the stress response, or glucose metabolism directly, in the hospitalized patient are summarized in Table 2.2.

Table 2.2: Modifiers of glucose metabolism during hospitalization

- Anesthesia and Analgesia
- Atypical Nutrition
- Fluid Balance
- Hypothermia
- Hypoxia
- Medications
- Sepsis
- Surgical Procedure

2.2.1. Anesthesia and Analgesia

Pain control and sedation in the hospitalized patient are focused on providing comfort and reducing the stress response without suppressing the immune system. Proper anesthetic and analgesic management can suppress the surge of catecholamines, cortisol, growth hormone and glucagon. Opioids such as morphine, codeine, and fentanyl are frequently administered for acute pain management in the hospital. Large doses of fentanyl (50-100 $\mu\text{g}/\text{kg}$) or morphine (>3 mg/kg) are necessary to abolish the stress response encountered during major cardiac surgery [144]. Patients receiving an epidural block during general anesthesia had significantly reduced cortisol and glucagon levels (as well as a reduction in endogenous glucose production and overall glycemia) intraoperatively when compared to controls [145]. However, the reduction in these levels was not sustained postoperatively even though the epidural block was maintained implying it was not exclusively attributable to the epidural block.

The type of general anesthesia affects the magnitude and time-course of the stress response. Sevoflurane was shown to reduce the catecholamine surge observed in patients treated with isoflurane while cortisol and glucagon profiles remained indistinguishable between the groups [146]. However, the perioperative glycemic profiles for both groups were similar and the catecholamine levels in the sevoflurane increased postoperatively to match those in the isoflurane group. An intraoperative study of seven elderly patients undergoing intra-abdominal surgery using sevoflurane-nitrous oxide anesthesia displayed similar profiles for epinephrine, norepinephrine, and cortisol (glucagon was not measured) [147].

In a study comparing epidural analgesia combined with general anesthesia (n=8), fentanyl and midazolam anesthesia (n=8), or inhaled anesthesia with isoflurane (n=7), endogenous glucose production and uptake (along with glucagon, cortisol, epinephrine and norepinephrine) were measured 110 minutes after incision in patients undergoing cystoprostatectomy [145]. Compared to preoperative measurements, the epidural group had a significant decrease, and the isoflurane group had a significant increase, in endogenous glucose production while all groups had significant decrease glucose uptake. Epidural analgesia abolished the stress response (*i.e.*, epinephrine, norepinephrine, cortisol and glucagon were not significantly different from preoperative values). While the decrease in glucose uptake in the isoflurane and fentanyl/midazolam groups could be explained by the intact (albeit blunted in the fentanyl/midazolam group) stress response, this reasoning cannot explain the decrease in the epidural group. Alternatively, sedation *per se* can reduce energy expenditure [148] which would correspond to a decrease in glucose uptake (*i.e.*, a reduction in muscle tone accompanies general anesthesia would

result in a decrease metabolic need). Although proper anesthesia can reduce (or even abolish) the stress-mediated increase in glucose production and decrease in insulin sensitivity, it causes an acute decrease in the body's metabolic need which also predisposes surgical patients to hyperglycemia.

The choice of anesthetic and analgesic agents can impact the evolution of the stress response. The ability to block afferent neural stimuli for the site of incision (*e.g.*, epidural analgesia) can completely suppress the surge of stress hormones during surgery and alter course of glycemia during a patient's hospital stay. Typically, the stress response will be blunted by anesthesia during surgery but will develop in the immediate postoperative period.

2.2.2. Atypical Nutrition

Before elective surgery, it is common practice for a patient to fast overnight so the digestive tract is empty prior to the surgical procedure thereby avoiding aspiration of stomach contents into the lungs which can cause pneumonia. However, upon fasting for 12-16 hours, liver glycogen stores are largely depleted and body metabolism is in a fasted state, with an increased breakdown of fat and protein to support increased gluconeogenesis and fat oxidation. This practice contributes, in part, to the increased insulin resistance and glucose intolerance in the hospitalized patient population [149].

Preoperative oral carbohydrate administration reduces the relative decreases in insulin sensitivity and whole body glucose uptake in patients undergoing elective total hip replacement [150]. In this study, cortisol levels were indistinguishable between the carbohydrate and placebo groups whereas nonesterified fatty acid levels were significantly depressed in the carbohydrate group. Elevated perioperative cortisol is a

common component between the treatment groups and will account for the part of the reduction in insulin sensitivity. However, fatty acid levels also influence endogenous glucose production and uptake [151] and a longer period in the fasted state accounts for the greater relative insulin resistance in the placebo group.

Inadequate nutrition in the perioperative period can profoundly affect insulin sensitivity. In a hospital setting, stress caused by the trauma of a surgical procedure combined with hypocaloric nutrition can lead to a state of severe glucose intolerance.

2.2.3. Fluid Balance

In health, water makes up 60% of total body weight. Its relative distribution between the vascular, interstitial and intracellular spaces is 10, 30, and 60 percent, respectively. In a study of 8 healthy volunteers, these volumes were 72 ± 7 , 204 ± 26 , and 417 ± 78 ml/kg for the vascular, interstitial and intracellular spaces [152].

The redistribution of fluid in the perioperative period is highly variable [153]. Capillary permeability increases in response to surgery, causing fluid to shift from the vasculature to the interstitial space [154]. Crystalloid solutions are administered intravenously to replace lost fluids, maintain adequate tissue perfusion and prevent anesthetic-induced hypotension. The stress response impairs the body's ability to excrete excess salt and water [155]. Compared to normal volunteers, extracellular volume increased (15 and 55 percent increase in vascular and interstitial volumes, respectively) while intracellular volume decreased postoperatively in trauma patients that were, on average, 15 liters positive [152].

Both hyper- and hypovolemia are associated with negative outcomes in the surgical patients [156, 157]. The need to maintain adequate blood pressure and volume during anesthesia typically leads to positive fluid balance intraoperatively. The amount of fluid given to a patient depends on several factors (Table 2.3). On average, patients undergoing major surgery will gain 3-7 kg during the procedure [156]. In the postoperative period, diuretic therapy can be used to restore fluid balance [158]. Within a relatively short period of time, a patient can experience considerable changes in the distribution and amount of total water.

Table 2.3: Factors affecting intraoperative fluid balance (adapted from Rosenthal 1999 [1])

- | | |
|----------------------------------------|---------------------------------------|
| • Preoperative intravascular volume | • Operative fluid management protocol |
| • Preoperative cardiovascular function | • Duration of surgery |
| • Anesthetic agent and technique | • Operative site |
| • Patient position | • Surgical technique |
| • Thermoregulation | • Splanchnic ischemia |
| • Capillary permeability | • Intraoperative cardiac function |

The dynamic nature of relative and absolute volumes of the intravascular, interstitial, and intracellular spaces in the perioperative period may have a significant effect on glycemia and, more importantly, the distribution of insulin. In addition, renal insufficiency will alter the elimination of insulin.

2.2.4. Hypothermia

Thermoregulation maintains core body temperature between 36.1 and 37.5°C.

Hypothermia is defined as a core temperature below 35°C. Accidental hypothermia is routinely encountered in trauma victims upon their arrival at the hospital. It is also

common for a patient to become hypothermic in the time around the procedure. The benefit of hypothermia on patient outcome is mixed. On one hand, it attenuates the inflammatory response, but it also compromises the ability of the immune system to protect against infection [159].

Hypothermia is an unavoidable consequence of the current standard practices within the hospital. Within the hospital, ambient air temperature is maintained below 25°C to minimize the infection risk posed by air-borne pathogens. The Center for Disease Control recommends a cool temperature standard with temperatures of 20-23°C within operating rooms and 21-24°C within holding areas and recovery rooms [160]. In addition to being placed in a cool environment, patients are sedated. Sedation decreases resting energy expenditure [161] which reduces endogenous heat production especially when the shivering reflex is ablated during anesthesia. Poor insulation (patients are scantily clothed prior to surgery and are placed naked on the operation table) increases the loss of heat. Convective heat loss is further increased by peripheral vasodilation as a result of anesthesia. Additional heat loss occurs from evaporation at the site of incision. Measures to limit the degree of hypothermia include the use of heated blankets [162].

Whether intentional or accidental, hypothermia is common in surgical patients. Of interest to us is the effect of hypothermia on the ability of the body to maintain euglycemia. Although hypothermia *per se* will cause an increase in catecholamine levels, hypothermic patients undergoing cardiopulmonary bypass had lower hormone levels (insulin, glucagon, cortisol, catecholamines) when compared to normothermic patients [163]. In addition, endogenous glucose production in hypothermic patients was decreased [164]. However, intraoperative hyperglycemia developed under both conditions. So,

although hypothermia attenuates the stress response, it is accompanied by a decrease in pancreatic insulin release [165] and metabolic need [166]. In addition, exogenous insulin administration cannot overcome the severe hypothermia-induced insulin resistance while leading to hypoglycemia after the rewarming period [167].

2.2.5. Hypoxia

Hypoxia is one of multiple factors in perioperative milieu that stimulates sympathetic activity in this setting. Hypoxia elicits a sympathetic response that significantly raises epinephrine levels as compared to normoxic same-subject controls [168]. Its role in decreased insulin sensitivity is well-defined in obstructive sleep apnea [169]. The hormonal and immunological changes that accompany intermittent hypoxia typify the classical stress response.

2.2.6. Medications

Insulin and oral agents are used to manage glycemia in the outpatient treatment of diabetes mellitus and within the hospital. However, hospitalized patients are often exposed to medications that inadvertently alter glucose production, insulin secretion and insulin sensitivity (Table 2.4).

Anesthesia increases the sympathetic tone of the cardiovascular system, causing an undesired drop in blood pressure. Ephedrine (which stimulates norepinephrine release) and epinephrine may be given to increase a patient's blood pressure. These medications will compound the effects of the endogenous catecholamines. Corticosteroids are typically given to decrease the inflammatory response following traumatic injuries and serious surgery. These medications cause both an increase in hepatic gluconeogenesis and a decrease in insulin sensitivity [170].

Table 2.4: Glycemia-altering drugs (adapted from Pandit 1993 [2])

Drug	Hyperglycemia	Hypoglycemia
β-blockers	•	•
fibric acid derivatives	•	•
fluoroquinolones	•	•
octeotide	•	•
atypical antipsychotics	•	
calcium channel blockers	•	
cyclosporine	•	
diazoxide	•	
ephedrine and epinephrine	•	
glucocorticoids	•	
nicotinic acid and niacin	•	
phenytoin	•	
protease inhibitors	•	
sex hormones	•	
Thiazides	•	
thyroxine	•	
ACE inhibitors		•
β ₂ agonists		•
β-adrenergic agonists		•
disopyramide		•
ethanol		•
MAOIs and tricyclics		•
pentamidine		•
quinine, chloroquine		•
salicylates and acetaminophen		•
streptozotcin		•
sulfamethoxazole		•

β-blockers and thiazides diuretics typically prescribed to treat hypertension. The mechanisms by which β-blockers cause hyperglycemia include the reduction of peripheral blood flow, a decrease in the first-phase of insulin release, and a decrease in insulin clearance which leads to hyperinsulinemia and a downregulation in insulin receptors [171]. Thiazides can cause hypokalemia which inhibits insulin secretion [172].

Fluoroquinolones are broad spectrum antibiotics that are commonly used in the hospital to treat infection. Drugs in this class (*i.e.*, moxifloxacin, gatifloxacin, levofloxacin, and ciprofloxacin) appear to stimulate insulin secretion, leading to hypoglycemic episodes. The combination with oral glucose-lowering agents increases the potency of these drugs [173, 174]. Gatifloxacin has also been associated with hyperglycemia [175].

Protease inhibitors are prescribed to treat viral infections, most commonly human immunodeficiency virus and hepatitis C. In healthy volunteers, the protease inhibitor, Indinavir, reduced the insulin-mediated increase in peripheral blood flow [176]. In this population, no difference in peripheral insulin sensitivity could be observed after four weeks of protease inhibitor treatment compared to baseline. However, there was also no significant difference in plasma lipid, insulin and glucose levels before and after treatment. But, protease inhibitors have been associated with increased insulin resistance in patients with HIV, which may be linked to their dyslipidemic effects [177]. There is also evidence that these drugs may attenuate insulin release [178].

2.2.7. Sepsis

Sepsis results from the immune response to a severe infection. It is associated with tachycardia, hyperthermia, hyperventilation and an abnormal white blood count. Sepsis causes a marked decrease in insulin sensitivity due, in part, to an exaggerated stress response.

Sepsis will inhibit the responsiveness of the pancreatic beta-cells and exaggerate the stress response. Peak insulin secretion in response to an intravenous glucose challenge was significantly decreased in septic postoperative patients (20.4 ± 6.8 mU/l, n=8) when compared to controls (51 ± 14 mU/l, n=6) and postoperative patients (42.4 ± 31 mU/l,

n=5) even though all groups had similar basal insulin levels [179]. In a comparison of postoperative patients categorized as septic (n=22) or nonseptic (n=12), the average levels of cortisol, catecholamines, and glucagon were greater in the septic patients (statistically significant for glucagon and catecholamines) [180].

2.2.8. Surgical Procedure

The emotional anxiety prior to surgery, the magnitude of tissue trauma sustained during surgery and the length of the procedure all modulate the severity of the stress response. Limiting the amount of tissue trauma has been shown to decrease the levels of plasma stress hormone levels and cytokines [181-183].

The magnitude of surgical procedure shows a positive correlation to the degree of subsequent insulin resistance. This resistance can be independent of changes in circulating cortisol, catecholamines, and glucagon. The resistance is localized in the skeletal muscle and it appears to involve the translocation of GLUT-4 transporters. Insulin resistance can change 20-60% postoperatively compared to preoperative measurements and it may require days to weeks to return to baseline [184].

Assessing the risk of death or complications in the course of patient care has given rise to several scoring systems [185]. The Physiological and Operative Severity Score for enUmeration of Mortality and morbidity (POSSUM) tracks 12 physiological variables and six variables related to the operation [186]. POSSUM ranks the severity of the procedure by placing it into one of four groups, minor, moderate, severe, and severe + (Table 2.5).

Table 2.5: Severity of General and Orthopedic Procedures (adapted from Copeland 2002)

Minor	Moderate	Severe	Severe +
<ul style="list-style-type: none"> • hernia • varicose vein • minor perianal surgery • scrotal surgery • minor transurethral tumor resection • excision of large subcutaneous lesion • fasciotomy • ganglion/bursa • tenotomy/tendon repair • endoscopic joint surgery • carpal tunnel/nerve release • removal of wire/nail • closed reduction of fracture 	<ul style="list-style-type: none"> • mastectomy • open cholecystectomy • laparoscopic cholecystectomy • appendectomy • excision of lesion requiring grafting or minor excision • minor amputation • thyroid lobectomy • excision/osteotomy of small bone • minor joint replacement • amputation of digit • closed reduction with external fixation • open reduction of small bone fracture 	<ul style="list-style-type: none"> • laparotomy and small bowel resection • colonic resection or anterior resection • major amputation • nonaortic vascular surgery • cholecystectomy and exploration of bile duct • total thyroidectomy • osteotomy of long bone • ligamentous reconstruction and prosthesis • arthrodesis of large joint • major joint replacement • amputation of limb • disk surgery • open reduction of long bone fracture 	<ul style="list-style-type: none"> • abdominoperineal resection • pancreatic or liver resection • oesophagogastrectomy • abdominoperineal excision of rectum • aortic surgery • whipple resection • radical total gastrectomy • radical tumorectomy • major spinal reconstruction • revision prosthetic replacement of major joint • hind limb/forelimb amputation

2.3. Perioperative Timeline

A patient's physiology is very dynamic in the time leading up to, during, and following surgery. A multitude of factors predispose a hospitalized patient to abnormal glycemia – predominantly hyperglycemia. This section describes the relative order of events (Figure 2.1) in the perioperative period in order to understand the evolution of the stress response and the development of hyperglycemia.

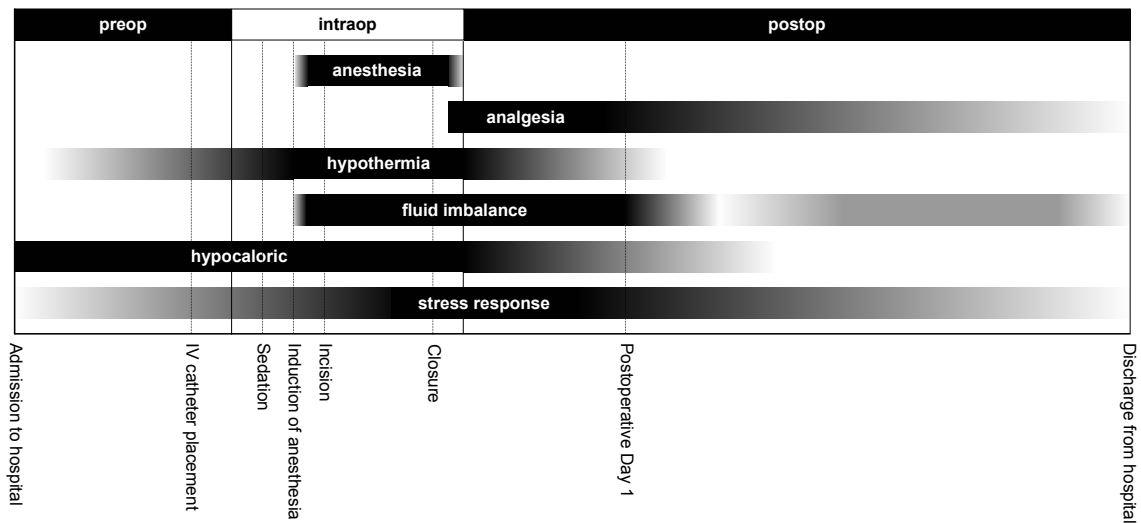


Figure 2.1: Perioperative timeline

Prior to admission into the hospital, the patient's diet is restricted. Typically, the patient will not have eaten 12-18 hours before undergoing surgery. In certain gastrointestinal procedures, a patient may be hypocaloric for several days to cleanse the bowel before surgery. In this prolonged fasted state, glycogen stores are depleted, circulating levels of free fatty acid levels are elevated. To spare protein, circulating levels of growth hormone are elevated in response to the patient's hypocaloric state as well. Cortisol levels are elevated, especially if the surgery is scheduled in the morning when this hormone naturally peaks. Patient anxiety over the impending surgical procedure can also elevate catecholamine levels before any physical tissue trauma is incurred. As a result, the surgical patient is insulin resistance before any tissue trauma occurs.

After admission to the hospital, a patient changes into a standardized robe which provides easy access for physical examination but little warmth. Prior to entering the operating room, the patient is confined to a bed in a preoperative holding area. Catheters are placed

to access to the bloodstream, allowing medications and maintenance fluids to be delivered to, and blood to be sampled from, the patient. Placed in a cool environment, inadequately clothed and delivered maintenance fluids at room temperature (typically below 25°C), a patient becomes susceptible to hyperthermia-induced insulin resistance.

Within the operating room, the patient is sedated through an intravenous administration of fentanyl or similar agent prior to the induction of general anesthesia. Under general anesthesia, a breathing tube is inserted in the throat and the patient is ventilated with a mixture of inhaled anesthetic and oxygen-rich air. The anesthetic agent is carefully titrated to control the patient's sympathetic tone - maintaining adequate blood pressure while ensuring adequate sedation during the procedure. The reduced sympathetic tone causes vasodilation and "leaky" capillaries. Crystalloid solutions are infused to maintain vascular volume and perfusion pressures. In addition, glucose-containing solutions are infused to provide a substrate for basal metabolism (~5g/hr for adults). The large amount of intravenous fluids given during surgery leads to a positive fluid balance (excessive fluid retention). At the site of incision, cells release inflammatory and necrotic factors while nerves alert the central nervous system to the tissue trauma. The degree of tissue trauma and the length of the procedure will determine, in part, the strength the stress response. The use of regional anesthesia can block transmission of pain before it reaches the central nervous system, further attenuating the stress response. While anesthesia will attenuate the stress response in the intraoperative period, it will interfere with thermal regulation. With the patient partially or fully disrobed and a low ambient room temperature, the patient's core body temperature will decrease.

The patient emerges from anesthesia cold and shivering. No longer suppressed by the anesthetic agent, a surge in circulating stress hormones occurs in response to the trauma incurred during the operation. Analgesic agents are administered for pain management. After surgery, the patient is transported to a recovery area within the hospital – the surgical severity and the patient's condition will determine the degree of care and monitoring the patient requires. Fluid restriction and diuretic therapy is employed to restore fluid balance. Other medications may inadvertently increase insulin resistance (*e.g.*, steroid therapy is prescribed to attenuate the inflammatory response). Caregivers must verify gastric motility prior to starting enteral nutrition. After a minor surgical procedure, a patient typically returns to enteral nutrition within 6-12 hours. In severe procedures, the patient may not begin eating for 24-48 hours. While patients are encouraged to ambulate primarily to promote gastrointestinal motility, muscle contraction will increase peripheral insulin sensitivity. As the patient recovers, the stress response will subside. However, complications can slow the recovery progress. Most notable, systemic infection is a life-threatening complication that will exacerbate the stress response. To compound the situation, medications used to treat sepsis will cause insulin resistance.

Subsequent chapters will attempt to quantify the effects of the stress response on glucose metabolism by focusing on tissue-specific changes to insulin sensitivity and endogenous glucose production.

CHAPTER 3. A MODEL OF GLUCOSE METABOLISM

The present effort will review and improve upon the model of glucose metabolism developed by John Sorensen [187] to describe glucose metabolism during periods of stress. As published, the model is a set of 22 first-order time-invariant nonlinear differential equations describing the interaction of glucose, insulin and glucagon. The model can be separated into three *subsystems*: glucose, insulin, and glucagon. Each subsystem divides the body into various compartments representing the capillary blood space of one or several biological tissues. The influx and outflow of mass (*i.e.*, glucose, insulin or glucagon) is modeled for each compartment.

3.1. Compartmental Modeling

In general, arterial blood enters and venous blood drains the capillary space. Mass is exchanged between the capillary and interstitial spaces, and between the interstitial and intracellular spaces. At most, the glucose metabolism model describes the flow of mass in the capillary and interstitial spaces (Figure 3.1). Mass that leaves the interstitial space either returns to the capillary space or is irrevocably removed from circulation once it is taken up by a cell. The general form of the equations governing the exchange of mass in a compartment is:

$$V_B \frac{dC_{Bo}}{dt} = Q_B (C_{Bi} - C_{Bo}) + PA(C_I - C_{Bo}) - r_{RBC} \quad 3.1$$

$$V_I \frac{dC_I}{dt} = PA(C_{Bo} - C_I) - r_I \quad 3.2$$

where V_B and V_I are the volumes of the capillary blood and interstitial fluid; Q_B is the volumetric flow rate; PA is the permeability-area product; C_{Bi} , C_{Bo} and C_I are the mass

(*i.e.*, glucose, insulin or glucagon) concentrations in the arterial blood, capillary (and venous) blood and the interstitial fluid; and r_{RBC} and r_I are the rates of mass uptake from the red blood cells and cells bathed by the interstitial fluid. In certain instances, the permeability of the capillary membrane is great enough to merge the capillary and interstitial spaces, forming one differential equation to describe the whole compartment. Auxiliary equations may be appended to the compartmental equations to describe rates of uptake or production.

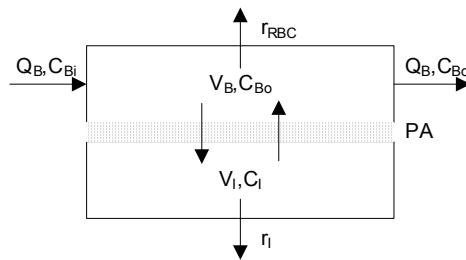


Figure 3.1: Simplified representation of a biological compartment used in the glucose metabolism model

The complexity of each subsystem varies. The glucose subsystem contains six compartments: the brain, heart and lungs, gut, liver, kidney, and peripheral tissues. It is described by eight first-order differential equations. Four rates (*i.e.*, hepatic glucose uptake, hepatic glucose production, peripheral glucose uptake, and renal glucose excretion) are described by a set of nonlinear auxiliary equations, including three additional first-order differential equations. The insulin subsystem contains the same six compartments. It is described by seven linear first-order differential equations. A nonlinear model of pancreatic insulin release is also included, adding three differential

equations to the subsystem. The glucagon subsystem contains only one compartment. It is described by one nonlinear first-order differential equation.

3.2. Model Equations

The equations for the model of glucose metabolism as they appear in the 1985 doctoral thesis of John Sorensen are provided here and in Appendix A. In general, time-varying variables (*e.g.*, G_H and r_{PIR}) are italicized whereas time-invariant quantities (*e.g.*, Q_L^1 and r_{RBCU}) are not. Some minor corrections and clarifications are described in Table 3.1.

Table 3.1: Glucose metabolism model clarifications and corrections

- In equation 3.11 that describes the kidney glucose excretion rate r_{KGE} , the quantity 0.011 multiplying the expression (G_K-460) within the hyperbolic tangent function was incorrectly reported in some sections of Sorensen's thesis.
- In one of the equations describing pancreatic insulin release (equation 3.37), the superscript 0+ in the expression $(X-I)^{0+}$ denotes that the expression only takes on positive values and is zero otherwise.

3.2.1. Glucose Subsystem

$$\frac{d}{dt} G_{BV} = \frac{1}{V_{BV}^G} \left[Q_B^G (G_H - G_{BV}) - \frac{V_{BI}^G}{T_B} (G_{BV} - G_{BI}) \right] \quad 3.3$$

$$\frac{d}{dt} G_{BI} = \frac{1}{V_{BI}^G} \left[\frac{V_{BI}^G}{T_B} (G_{BV} - G_{BI}) - r_{BGU} \right] \quad 3.4$$

$$\frac{d}{dt} G_H = \frac{1}{V_H^G} \left[Q_B^G G_{BV} + Q_L^G G_L + Q_K^G G_K + Q_P^G G_{PV} - Q_H^G G_H - r_{RBCU} \right] \quad 3.5$$

$$\frac{d}{dt} G_G = \frac{1}{V_G^G} \left[Q_G^G (G_H - G_G) - r_{GGU} \right] \quad 3.6$$

$$\frac{d}{dt} G_L = \frac{1}{V_L^G} \left[Q_A^G G_H + Q_G^G G_G - Q_L^G I_L + r_{HGP} - r_{HGU} \right] \quad 3.7$$

$$\frac{d}{dt} G_K = \frac{1}{V_K^G} \left[Q_K^G (G_H - G_K) - r_{KGE} \right] \quad 3.8$$

$$\frac{d}{dt} G_{PV} = \frac{1}{V_{PV}^G} \left[Q_P^G (G_H - G_{PV}) - \frac{V_{PI}^G}{T_P^G} (G_{PV} - G_{PI}) \right] \quad 3.9$$

$$\frac{d}{dt} G_{PI} = \frac{1}{V_{PI}^G} \left[\frac{V_{PI}^G}{T_P^G} (G_{PV} - G_{PI}) - r_{PGU} \right] \quad 3.10$$

$$r_{KGE} = \begin{cases} 71 + 71 \tanh[0.011(G_K - 460)], & 0 \leq G_K \leq 460 \\ -330 + 0.872G_K, & G_K > 460 \end{cases} \quad 3.11$$

$$r_{PGU} = I_{PGU}^B M_{PGU}^G M_{PGU}^I \quad 3.12$$

$$M_{PGU}^G = \frac{G_{PI}}{G_{PI}^B} \quad 3.13$$

$$M_{PGU}^I = 7.03 + 6.52 \tanh \left[0.338 \left(\frac{I_{PI}}{I_{PI}^B} - 5.82 \right) \right] \quad 3.14$$

$$r_{HGU} = r_{HGU}^B M_{HGU}^G M_{HGU}^I \quad 3.15$$

$$M_{HGU}^G = 5.66 + 5.66 \tanh \left[2.44 \left(\frac{G_L}{G_L^B} - 1.48 \right) \right] \quad 3.16$$

$$\frac{d}{dt} M_{HGU}^I = \frac{1}{\tau_1} [M_{HGU}^{I\infty} - M_{HGU}^I] \quad 3.17$$

$$M_{HGU}^{I\infty} = 2.0 \tanh \left[0.55 \frac{I_L}{I_L^B} \right] \quad 3.18$$

$$r_{HGP} = I_{HGP}^B M_{HGP}^G M_{HGP}^I M_{HGP}^\Gamma \quad 3.19$$

$$M_{HGP}^G = 1.42 - 1.41 \tanh \left[0.62 \left(\frac{G_L}{G_L^B} - 0.497 \right) \right] \quad 3.20$$

$$\frac{d}{dt} M_{HGP}^I = \frac{1}{\tau_1} [M_{HGP}^{I\infty} - M_{HGP}^I] \quad 3.21$$

$$M_{HGP}^{I\infty} = 1.21 - 1.14 \tanh \left[1.66 \left(\frac{I_L}{I_L^B} - 0.89 \right) \right] \quad 3.22$$

$$M_{HGP}^\Gamma = M_{HGP}^{\Gamma 0} - f_2 \quad 3.23$$

$$M_{HGP}^{\Gamma 0} = 2.7 \tanh[0.39\Gamma^N] \quad 3.24$$

$$\frac{d}{dt} f_2 = \frac{1}{\tau_\Gamma} \left[\frac{M_{HGP}^{\Gamma 0} - 1}{2} - f_2 \right] \quad 3.25$$

$V_{BV}^G = 3.5 \text{ dl}$	$Q_B^G = 5.9 \text{ dl/min}$	$T_B = 2.1 \text{ min}$	$G_H^B = 91.89 \text{ mg/dl}$
$V_{BI}^G = 4.5 \text{ dl}$	$Q_A^G = 2.5 \text{ dl/min}$	$T_P^G = 5.0 \text{ min}$	$G_L^B = 101.0 \text{ mg/dl}$
$V_H^G = 13.8 \text{ dl}$	$Q_H^G = 43.7 \text{ dl/min}$		$G_{PI}^B = 86.81 \text{ mg/dl}$
$V_L^G = 25.1 \text{ dl}$	$Q_L^G = 12.6 \text{ dl/min}$	$\tau_I = 25 \text{ min}$	$r_{PGU}^B = 35 \text{ mg/min}$
$V_G^G = 11.2 \text{ dl}$	$Q_G^G = 10.1 \text{ dl/min}$	$\tau_T = 65 \text{ min}$	$r_{HGU}^B = 20 \text{ mg/min}$
$V_K^G = 6.6 \text{ dl}$	$Q_K^G = 10.1 \text{ dl/min}$		$r_{HGP}^B = 155 \text{ mg/min}$
$V_{PV}^G = 10.4 \text{ dl}$	$Q_P^G = 15.1 \text{ dl/min}$		$r_{BGU} = 70 \text{ mg/min}$
$V_{PI}^G = 67.4 \text{ dl}$			$r_{RBCU} = 10 \text{ mg/min}$
			$r_{GGU} = 20 \text{ mg/min}$

3.2.2. Insulin Subsystem

$$\frac{d}{dt} I_B = \frac{1}{V_B^I} [Q_B^I (I_H - I_B)] \quad 3.26$$

$$\frac{d}{dt} I_H = \frac{1}{V_H^I} [Q_B^I I_B + Q_L^I I_L + Q_K^I I_K + Q_P^I I_{PV} - Q_H^I I_H] \quad 3.27$$

$$\frac{d}{dt} I_G = \frac{1}{V_G^I} [Q_G^I (I_H - I_G)] \quad 3.28$$

$$\frac{d}{dt} I_L = \frac{1}{V_L^I} [Q_A^I I_H + Q_G^I I_G - Q_L^I I_L + r_{PIR} - r_{LIC}] \quad 3.29$$

$$\frac{d}{dt} I_K = \frac{1}{V_K^I} [Q_K^I (I_H - I_K) - r_{KIC}] \quad 3.30$$

$$\frac{d}{dt} I_{PV} = \frac{1}{V_{PV}^I} \left[Q_P^I (I_H - I_{PV}) - \frac{V_{PI}^I}{T_P^I} (I_{PV} - I_{PI}) \right] \quad 3.31$$

$$\frac{d}{dt} I_{PI} = \frac{1}{V_{PI}^I} \left[\frac{V_{PI}^I}{T_P^I} (I_{PV} - I_{PI}) - r_{PIC} \right] \quad 3.32$$

$$r_{LIC} = F_{LIC} [Q_A^I I_H + Q_G^I I_G + r_{PIR}] \quad 3.33$$

$$r_{KIC} = F_{KIC} Q_K^I I_K \quad 3.34$$

$$r_{PIC} = \frac{I_{PI}}{\frac{1}{Q_P^I} \left(\frac{1 - F_{PIC}}{F_{PIC}} \right) - \frac{T_P^I}{V_{PI}^I}} \quad 3.35$$

$$r_{PIR} = r_{PIR}^B \frac{S(G_H)}{S_\infty(G_H^B)} \quad 3.36$$

$$S(G_H) = Q(M_1 Y + M_2 (X - I)^{0+}) \quad 3.37$$

$$S_{\infty}(G_H^B) = \frac{(\gamma P_{\infty} + KQ_0)M_1 Y}{K + M_1 Y} \quad 3.38$$

$$X(G) = \frac{G^{3.27}}{132^{3.27} + 5.93G^{3.02}} \quad 3.39$$

$$Y = P_{\infty} = X^{1.11} \quad 3.40$$

$$\frac{d}{dt} P = \alpha(P_{\infty} - P) \quad 3.41$$

$$\frac{d}{dt} I = \beta(X - I) \quad 3.42$$

$$\frac{d}{dt} Q = K(Q_0 - Q) + \gamma P - S \quad 3.43$$

$V_B^I = 0.261$	$Q_B^I = 0.45 \text{ l/min}$	$T_p^I = 20 \text{ min}$	$\alpha = 0.0482 \text{ min}^{-1}$
$V_H^I = 0.991$	$Q_H^I = 3.12 \text{ l/min}$	$F_{LIC} = 0.40$	$\beta = 0.931 \text{ min}^{-1}$
$V_L^I = 0.941$	$Q_L^I = 0.90 \text{ l/min}$	$F_{KIC} = 0.30$	$\gamma = 0.575 \text{ U/min}$
$V_G^I = 1.141$	$Q_G^I = 0.72 \text{ l/min}$	$F_{PIC} = 0.15$	$K = 0.00794 \text{ min}^{-1}$
$V_K^I = 0.511$	$Q_K^I = 0.72 \text{ l/min}$	$I_H^B = 15.15 \text{ mU/l}$	$M_1 = 0.00747 \text{ min}^{-1}$
$V_{PV}^I = 0.741$	$Q_P^I = 1.05 \text{ l/min}$	$I_L^B = 21.43 \text{ mU/l}$	$M_2 = 0.0958 \text{ min}^{-1}$
$V_{PI}^I = 6.741$	$Q_A^I = 0.18 \text{ l/min}$	$I_{PI}^B = 5.304 \text{ mU/l}$	$Q_0 = 6.33 \text{ U}$
			$r_{PIR}^B = 20 \text{ mU/min}$

3.2.3. Glucagon Subsystem

$$\frac{d}{dt} \Gamma^N = \frac{r_{MFC}}{V^{\Gamma}} [M_{PT\Gamma}^G M_{PT\Gamma}^I - \Gamma^N] \quad 3.44$$

$$M_{PT\Gamma}^G = 2.93 - 2.10 \tanh \left[4.18 \left(\frac{G_H}{G_H^B} - 0.61 \right) \right] \quad 3.45$$

$$M_{PT\Gamma}^I = 1.31 - 0.61 \tanh \left[1.06 \left(\frac{I_H}{I_H^B} - 0.47 \right) \right] \quad 3.46$$

$$V^{\Gamma} = 11310 \text{ ml} \quad r_{MFC} = 9.10 \text{ ml/min}$$

3.3. Model Parameter Analyses

As originally published, the glucose metabolism model has 59 parameters. Nearly all the parameters can be categorized as distribution volumes, flow rates, time constants, basal values, or fractional clearances for glucose, insulin and glucagon.

3.3.1. Parameter Dependencies

Several model parameters are dependent. In a majority of the cases, dependency arises because parameters from different subsystems are based on the same underlying physiological quantities. These physiological quantities have been scaled or combined together so the model equations can be written in a compact form. The volumetric flow rates and distribution volumes both exhibit this type of dependency. Between all three subsystems, there are 14 volumetric flow rate parameters and 16 distribution volume parameters. Out of these 30 parameters, only 19 are independent.

Here, the volumetric flow rates and distribution volumes are denoted by $\mathbf{Q} = Q_j^i$ where $i = \{G, I\}$ and $j = \{B, H, L, G, K, P, A\}$ and $\mathbf{V} = V_j^i$ where $i = \{G, I, \Gamma\}$ and $j = \{B, BV, BI, H, L, G, K, P, PV, PI\}$, respectively. Here the superscript i represents the subsystem: glucose (G), insulin (I), or glucagon (Γ). The first character of the subscript j represents the compartment: brain (B), heart and lungs (H), liver (L), gut (G), kidneys (K), periphery (P), and hepatic artery (A). If present, the second character differentiates between the vascular (V) and interstitial (I) parts of the compartment.

The anatomy of the human circulatory system is the basis of four dependencies in \mathbf{Q} . Without any formal representation of the lymphatic system, the model assumes that all blood supplying the tissues and organs of the body returns to the heart. In order to avoid any accumulation of blood any given tissue, all the flow rates to these tissue beds must equal the flow rate returning to the heart. As shown in equation 3.47, Q_H^G and Q_H^I are dependent on the flow rates to the brain, liver, kidneys, and peripheral tissues.

$$Q_H^i = Q_B^i + Q_L^i + Q_K^i + Q_P^i \quad 3.47$$

Blood supplied to the liver is composed of arterial blood from the hepatic artery and venous blood that drains into the portal vein from the gastrointestinal tract. The oxygen-rich arterial blood and the venous blood (laden with nutrients following a meal) are brought together within the liver and return to the heart through the inferior vena cava. As shown in equation 3.48, Q_L^G and Q_L^I are dependent parameters.

$$Q_L^i = Q_A^i + Q_G^i \quad 3.48$$

The cause of remaining dependencies in \mathbf{Q} is that parameters in both the glucose and insulin subsystems are scaled quantities of the same flow rates. The distribution space of glucose in the blood is water and it was estimated that water comprises 84% of the total volume of whole blood (water content percentage, WCP), which includes the intracellular fluid of the red blood cells. If Q_j represents the rate at which whole blood flows into compartment j , Q_j is reduced by 16% to generate the glucose subsystem flow rate, Q_j^G . The glucose subsystem's flow rate, Q_j^G , in dl/min for $j = \{B, H, L, G, K, P, A\}$ is given by the following equation:

$$Q_j^G = \frac{10 \text{ dl}}{1} \times \text{WCP} \times Q_j \quad 3.49$$

Similarly, the insulin distribution space in whole blood is limited to the plasma since insulin does not cross the plasma membrane of the circulating red blood cells. Therefore, Q_j is reduced by the fraction of the space occupied by red blood cells in a fixed volume of blood, or the hematocrit (HCT). The hematocrit was estimated at 40%. The insulin

subsystem's flow rate, Q_j^I , in l/min for $j = \{B, H, L, G, K, P, A\}$ is given by the following equation:

$$Q_j^I = (1 - \text{HCT}) \times Q_j \quad 3.50$$

The values for the blood flow rates and the flow rates used by Sorensen for the glucose and insulin subsystems of the glucose metabolism model are summarized in Table 3.2. These values were based on the quantities for a 70kg man in the postabsorptive state. The 16 parameters in \mathbf{Q} can be described by smaller set of 7 independent physiologic parameters (Q_j for $j = \{B, G, K, P, A\}$, WCP, and HCT).

Table 3.2: Volumetric flow rates for blood, glucose (water), and insulin (plasma). Rates in parentheses are redundant.

Tissue or Organ	Subscript j	Flow Rate (l/min)		
		Blood Q_j	Glucose Q_j^G	Insulin Q_j^I
Brain	B	0.70	0.59	0.42
Heart & Lungs	H	(5.20)	(4.37)	(3.12)
Liver	L	(1.50)	(1.26)	(0.90)
Gut	G	1.20	1.01	0.72
Kidney	K	1.20	1.01	0.72
Periphery	P	1.80	1.51	1.08
Hepatic Artery	A	0.30	0.25	0.18

The values of \mathbf{V} can also be derived from a common set of independent physiological parameters. This set includes WCP, HCT, and volumes representing the blood, interstitial fluid, and intracellular fluid. The volumes for blood, interstitial fluid and intracellular fluid used by Sorensen in the glucose metabolism model are given in Table 3.3. Italicized values were not used in the calculation of any parameter in \mathbf{V} but were provided for completeness.

Table 3.3: Blood, interstitial fluid and intracellular fluid volumes for the given tissue or organ.

Tissue or Organ	Compartment <i>j</i>	Volume (l)		
		Blood $V_{j,B}$	Interstitial Fluid $V_{j,ISF}$	Intracellular Fluid ^b $V_{j,ICF}$
Brain	B	0.41	0.45	8.60
Heart & Lungs ^a	H	1.64	-	-
Liver	L	0.90	0.60	1.15
Gut	G	0.71	0.52	1.01
Kidney	K	0.68	0.09	0.18
Periphery	P	1.26	6.74	19.65

^a heart and lung tissues lumped with the periphery

^b intracellular fluid volumes are neglected in the distribution volume of a compartment except for the liver

There are no compact expressions to relate these independent parameters to \mathbf{V} . For the subsequent discussion, the blood, interstitial fluid and intracellular fluid volumes will be denoted by $V_{j,k}$ where $j = \{B, H, L, G, K, P\}$ refers to the compartment and $k = \{B, ISF, ICF\}$ refers to blood, interstitial fluid, or intracellular fluid component of the compartment. Except for $V_{L,ICF}$ which was used in the calculation V_L^G , intracellular fluid volumes were not used in the calculation of the distribution spaces for glucose, insulin and glucagon. The expressions relating \mathbf{V} to $V_{j,k}$ are given in the following equations:

Glucose Subsystem

$$V_{BV}^G = \frac{10 \text{ dl}}{1} \times WCP \times V_{B,B} \quad 3.51$$

$$V_{BI}^G = \frac{10 \text{ dl}}{1} \times V_{B,ISF} \quad 3.52$$

$$V_H^G = \frac{10 \text{ dl}}{1} \times WCP \times V_{H,B} \quad 3.53$$

$$V_L^G = \frac{10 \text{ dl}}{1} (WCP \times V_{L,B} + V_{L,ISF} + V_{L,ICF}) \quad 3.54$$

$$V_G^G = \frac{10 \text{ dl}}{1} (WCP \times V_{G,B} + V_{G,ISF}) \quad 3.55$$

$$V_K^G = \frac{10 \text{ dl}}{1} (WCP \times V_{K,B} + V_{K,ISF}) \quad 3.56$$

$$V_{PV}^G = \frac{10 \text{ dl}}{1} \times WCP \times V_{P,B} \quad 3.57$$

$$V_{PI}^G = \frac{10 \text{ dl}}{1} \times V_{P,ISF} \quad 3.58$$

Insulin Subsystem

$$V_B^I = (1 - HCT) \times V_{B,B} \quad 3.59$$

$$V_H^I = (1 - HCT) \times V_{H,B} \quad 3.60$$

$$V_L^I = (1 - HCT) \times V_{L,B} + V_{L,ISF} \quad 3.61$$

$$V_G^I = (1 - HCT) \times V_{G,B} + V_{G,ISF} \quad 3.62$$

$$V_K^I = (1 - HCT) \times V_{K,B} + V_{K,ISF} \quad 3.63$$

$$V_{PV}^I = (1 - HCT) \times V_{P,B} \quad 3.64$$

$$V_{PI}^I = V_{P,ISF} \quad 3.65$$

Glucagon Subsystem

$$V^\Gamma = \frac{1000 \text{ ml}}{1} \times \sum_j V_j^I \text{ for } j = \{B, H, L, G, K, PV, PI\} \quad 3.66$$

Since WCP and HCT were included in the independent parameter set describing \mathbf{Q} , the 16 parameters in \mathbf{V} can be described by 12 independent parameters.

The last parameter dependency that will be discussed here is that of the basal rate of peripheral glucose uptake, r_{PGU}^B . Here, r_{PGU}^B describes the rate at which peripheral tissue takes glucose from systemic circulation. The peripheral tissue is comprised of muscle and adipose tissue including the heart and lung tissues. The basal rate of peripheral glucose uptake was fixed between 22.7 and 88.9 mg/min using data from published forearm glucose metabolism studies. This estimate was made under the assumptions that (1) a nonobese 70 kg man has 30 kg of muscle and 10 kg of adipose tissue, (2) muscle and adipose tissue constitute 64 and 8 percent of the total forearm volume, and (3) muscle and adipose tissue constitute 89 and 11 percent of forearm glucose uptake. The need to

balance glucose uptake with hepatic glucose production in the fasted basal state lead Sorensen to set r_{PGU}^B equal to basal rate of hepatic glucose production less all other sources of glucose uptake (equation 3.67).

$$r_{PGU}^B = r_{HGP}^B - r_{HGU}^B - r_{BGU}^B - r_{GGU}^B - r_{RBCU}^B \quad 3.67$$

3.3.2. Sensitivity Analysis

To study the effect of parameter uncertainty on the overall behavior of the glucose metabolism model, the model's sensitivity to changes in parameter values was investigated. Analytical approaches to this analysis were considered impracticable. The mathematical complexity of the glucose metabolism model makes it impossible to find the explicit expression relating the sensitivity of the model's output to parameter changes. Instead, a sampling-based approach was chosen. The sampling-based approach involves running the model for a set of input/parameter combinations (sample points) and estimating the sensitivity using the model output at those points.

In this analysis, only one parameter value was changed at a time to identify the subset of parameters to which the model was most sensitive. The glucose metabolism model was studied with the pancreatic insulin release rate, r_{PIR} , set to zero. By excluding the equations governing endogenous insulin secretion, the model's sensitivity to changes in a small subset of parameters was not assessed. Plasma insulin and glucose concentrations were directly manipulated using external inputs.

The external inputs can be described as intravenous infusions of glucose and insulin. The glucose infusion rate, RG , in units of mg/min was added as an input to the heart & lung compartment of the glucose subsystem (equation 3.68). This compartment represents the

blood volume in the cardiopulmonary system and the major arteries. The heart & lung compartment is the most appropriate location for the external inputs since an infusion catheter placed in a vein (most commonly, in the antecubital region) will mix with blood draining from other tissue beds as it returns to the heart. The insulin infusion rate, RI , in units of mU/min was added as an input to the heart & lung compartment of the insulin subsystem (equation 3.69).

$$\frac{d}{dt} G_H = \frac{1}{V_H^G} \left[Q_B^G G_{BV} + Q_L^G G_L + Q_K^G G_K + Q_P^G G_{PV} - Q_H^G G_H - r_{RBCU} + RG \right] \quad 3.68$$

$$\frac{d}{dt} I_H = \frac{1}{V_H^I} \left[Q_B^I I_B + Q_L^I I_L + Q_K^I I_K + Q_P^I I_{PV} - Q_H^I I_H + RI \right] \quad 3.69$$

As originally published, the glucose metabolism model has 59 parameters. Eight parameters appear in the equations describing pancreatic insulin release. The remaining 51 parameters can be categorized as physiological quantities such as volumes, flow rates, time constants, basal values, and fractional clearances. Several dependencies exist among these parameters. A set of 39 independent parameters (Table 3.4) is sufficient to calculate the 51 parameters. The complete description of the parameter dependencies and the independent parameter set is given in the previous section.

Table 3.4 Independent Parameters of the Glucose Metabolism Model

Volumes (l) $V_{B,B} = 0.41$ $V_{B,ISF} = 0.45$ $V_{G,B} = 0.71$ $V_{G,ISF} = 0.52$ $V_{H,B} = 1.64$ $V_{K,B} = 0.68$ $V_{K,ISF} = 0.09$ $V_{L,B} = 0.90$ $V_{L,ISF} = 0.60$ $V_{L,ICF} = 1.15$ $V_{P,B} = 1.26$ $V_{P,ISF} = 6.74$	Volumetric Flow (l/min) $Q_A = 0.3$ $Q_B = 0.7$ $Q_G = 1.2$ $Q_K = 1.2$ $Q_P = 1.8$	Time Constants (min) $T_I = 25$ $T_B = 2.1$ $T_P^G = 5$ $T_\Gamma = 65$ $T_P^I = 20$
	Mass Flow (mg/min) $r_{HGP}^B = 155$ $r_{HGU}^B = 20$ $r_{BGU} = 70$ $r_{GGU} = 20$ $r_{RBCU} = 10$	Basal Values $G_H^B = 91.89 \text{ mg/dl}$ $G_L^B = 101 \text{ mg/dl}$ $G_{PI}^B = 86.81 \text{ mg/dl}$ $I_H^B = 15.15 \text{ mU/l}$ $I_L^B = 21.43 \text{ mU/l}$ $I_{PI}^B = 5.304 \text{ mU/l}$
	Fractional Clearances $F_{KIC} = 0.30$ $F_{LIC} = 0.40$ $F_{PIC} = 0.15$	Other $HCT = 0.40$ $WCP = 0.84$
Metabolic Clearance Rate $r_{MTC} = 9.10 \text{ ml/min}$		

The model output is the plasma glucose concentration G . In the glucose metabolism model, whole blood water glucose concentration is the basis for the vascular glucose distribution. Therefore, the state variable G_H must be multiplied by 92.5% to convert it to the concentration of glucose in the plasma (equation 3.70).

$$G = 0.925G_H \quad 3.70$$

The sensitivity analysis was restricted to steady-state conditions. The change in G was used to assess the model's sensitivity to a change in a single parameter under a variety of input combinations.

3.3.2.1. Steady-State Single Parameter Sensitivity Analysis

In the steady-state sensitivity analysis, the effect of changing a single parameter on the steady-state value of G (denoted by G_{ss}) was assessed. The value of each parameter was

increased by 10% and decreased by 10% from its original value (see Table 3.4) such that any set of parameter values differs from the original set by only one parameter value. For each parameter set, G_{ss} was calculated under various insulinemic and glycemc conditions achieved by choosing the constant rates for RI and RG in equations 3.71 and 3.72. All possible combinations of RI and RG were used.

$$RI(i) = (i-1) \text{ mU/min for } i = 1 \dots 201 \quad 3.71$$

$$RG(j) = 5 \times (j-1) \text{ mg/min for } j = 1 \dots 401 \quad 3.72$$

Given N_1 and N_2 unique values for RI and RG , an $N_1 \times N_2 \times 2P$ matrix of G_{ss} values was constructed for P parameter values, $G_{ss}(i,j,k)$ where $i = 1 \dots N_1$, $j = 1 \dots N_2$ and $k = 1 \dots 2P$. For each sample point (i,j,k) , only one parameter value was changed. Odd values of k indicate that the changed parameter was decreased by 10% and even values of k indicate that the changed parameter was increased by 10%. $N_1 \times N_2$ sample points (and G_{ss} values) are associated with each parameter set. $G_{ss}(i,j,0)$ denotes the G_{ss} values using the original parameter set.

The percent change in G_{ss} (denoted by ΔG_{ss}) is defined in equation 3.73. The difference between $G_{ss}(i,j,k)$ and $G_{ss}(i,j,0)$ was scaled by the reciprocal of $G_{ss}(i,j,0)$ in order to balance the influence of large differences when G_{ss} itself was large.

$$\Delta G_{ss}(i, j, k) = [G_{ss}(i, j, k) - G_{ss}(i, j, 0)] / G_{ss}(i, j, 0) \quad 3.73$$

The L^1 and L^∞ norms of ΔG_{ss} for each parameter set are defined in equations 3.74 and 3.75. If the input values, $RI(i)$ and $RG(j)$, produced G_{ss} less than 0 mg/dl for any k , ΔG_{ss} was excluded from the calculation of the norms for all k .

$$L^1 = \|\Delta G_{ss}(k)\|_1 = \frac{1}{N_1 \times N_2} \sum_{i,j} |\Delta G_{ss}(i,j,k)| \quad 3.74$$

$$L^\infty = \|\Delta G_{ss}(k)\|_\infty = \max_{i,j} |\Delta G_{ss}(i,j,k)| \quad 3.75$$

Each norm reduced the $N_1 \times N_2$ values of ΔG_{ss} to one summary statistic for each parameter set which was used to determine the effect of changing a single parameter value on G_{ss} .

In total, 79 parameter sets were studied (the original set and 78 sets with one parameter that was different from its original value). 80,601 G_{ss} values were calculated for each parameter set. Figure 3.2 plots the contour lines of $G_{ss}(i,j,0)$ for the constant rates of RI and RG . The 0 mg/dl contour line demarcates a region of sample points (loosely described by $RI > 38$ mU/min and $RG < 75$ mg/min) that was excluded from L^1 and L^∞ norm calculations since G_{ss} was negative in that region.

The L^1 and L^∞ norms for each parameter set are given in Table 3.5. Two parameter sets are associated with a change in one parameter value. The k (where k is odd) and $k+1$ parameter sets correspond to a 10% decrease and a 10% increase in the associated parameter, respectively. Nine parameters (r_{MFC} , $V_{B,B}$, $V_{G,B}$, $V_{P,B}$, $V_{B,ISF}$, $V_{G,ISF}$, T_B , T_1 , T_Γ) did not produce any change in G_{ss} . These parameters did not appear in the model equations when they were solved for steady-state conditions. Seven other parameters (Q_B , $V_{H,B}$, $V_{K,B}$, $V_{L,B}$, $V_{K,ISF}$, $V_{L,ISF}$, $V_{L,ICF}$) produced difference less than 0.0001 mg/dl between $G_{ss}(i,j,k)$ and $G_{ss}(i,j,0)$ for all i and j . The parameter sets that produced the five largest L^1 norms were $k = 18, 17, 21, 77, 22$ (corresponding to parameters r_{HGP}^B , r_{HGP}^B , r_{BGU} , F_{PIC} , r_{BGU}). The parameter sets that produced the five largest L^∞ norms were $k = 73, 14, 4, 74, 21$ (corresponding to parameters F_{LIC} , I_L^B , HCT , F_{LIC} , r_{BGU}).

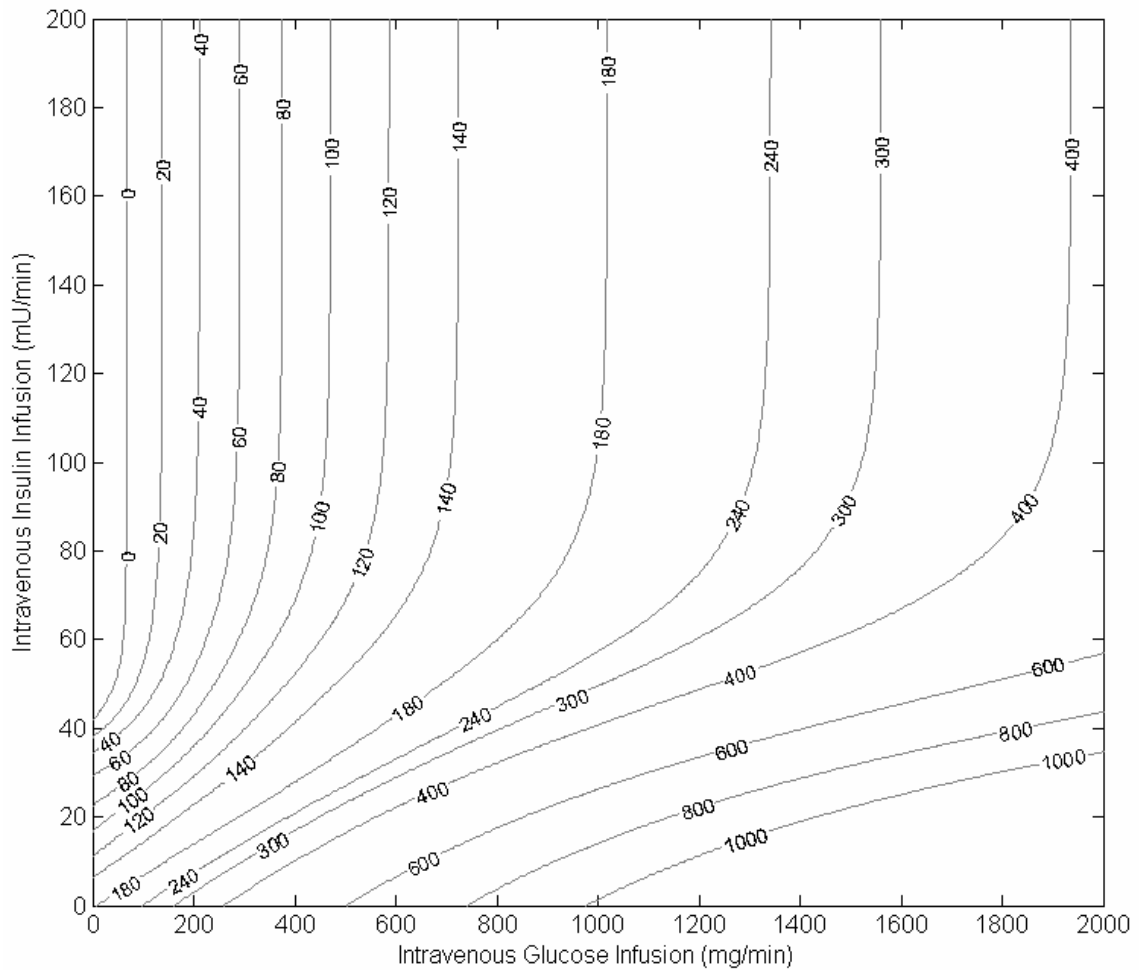


Figure 3.2: Contour map of simulated steady-state plasma glucose concentrations (in mg/dl) for constant intravenous infusions of glucose and insulin.

The combination of the top five parameters as ranked by the L^1 and L^∞ norms yields six unique parameters in which a 10% change in that parameter had a largest effect on steady-state glycemia. Of this set of 6 parameters, half are directly related to the liver. Clinical experimentation has firmly established its prominent role in glycemic regulation. The steady-state sensitivity analysis highlights its importance within the model in terms of hepatic glucose production (r_{HGP}^B), insulin-mediated effects on net hepatic glucose

balance (as expressed through the affect of I_L^B on hepatic glucose production and utilization) and hepatic insulin clearance (F_{LIC}).

The rate of glucose uptake by the brain (r_{BGU}) is the only parameter to appear in the five most sensitive parameters as measured by both the L^1 and L^∞ norms. At basal conditions, the rate at which the brain utilizes glucose is twice as much as any other tissue compartment. The central nervous system represents the only collection of tissues that are completely reliant on glucose as the sole source of fuel for metabolism. An accurate determination of r_{BGU} is vital to ensure the model's realism.

This analysis also illustrated the model's sensitivity to changes in the fractional rate of insulin clearance by peripheral muscle and adipose tissues (F_{PIC}). Peripheral tissue is the most insulin-sensitive tissue in the body with the rate of glucose uptake changing by an order of magnitude over the range of physiological insulin concentrations. The rate of peripheral insulin clearance determines, in part, the insulin concentration in the periphery. The model's description of peripheral glucose uptake is depends on the amount of insulin in the peripheral interstitial fluid. As modeled, increasing F_{PIC} will lower the steady-state value of I_{PI} which will, in turn, reduce insulin-mediated modifier of peripheral glucose uptake, M_{PGU}^1 . However, as insulin binds to its receptor on the cell membrane, it sets off a cascade of events that increases the concentration of glucose transport proteins (specifically, GLUT4) on the cell membrane thereby enhance the cell's ability to take up glucose for the surrounding interstitial space. To be removed from the interstitial space, the entire insulin/receptor complex is internalized and degraded with the cell. Unless a

post-receptor defect is present, it stands to reason that an increase in F_{PIC} should increase peripheral glucose uptake rather than decrease it.

The steady-state glucose concentration was also sensitive to changes in hematocrit as measured by the L^∞ norm. Hematocrit (HCT) is the volume of red cells in the body divided by the total blood volume. Normal HCT values range from 40 to 53 percent and 36 to 48 percent in adult males and females, respectively [188]. An increase in HCT means a greater fraction of the blood volume is occupied by red blood cells and less space is available for insulin. With all other parameters fixed, an increase in HCT will cause an increase in plasma insulin concentrations for a given exogenous insulin infusion rate. Greater insulin concentrations will, in turn, increase insulin-mediated glucose uptake and reduce steady-state plasma glucose concentrations.

Table 3.5: L^1 and L^∞ norms for all unique parameter sets (an odd or even value of k corresponds to the 10% decrease or the 10% increase in a parameter, respectively)

parameter	k	L^1 norm	L^∞ norm	k	L^1 norm	L^∞ norm
WCP	1	0.0120	0.0179	2	0.0146	0.0218
HCT	3	0.0401	0.7116	4	0.0523	1.1982
G_{PI}^B	5	0.0401	0.0713	6	0.0418	0.0729
G_L^B	7	0.0196	0.0915	8	0.0205	0.0929
G_H^B	9	0.0007	0.0525	10	0.0008	0.0583
I_H^B	11	0.0264	0.1387	12	0.0248	0.1331
I_L^B	13	0.0095	1.2826	14	0.0092	0.9137
I_{PI}^B	15	0.0001	0.0084	16	0.0001	0.0091
Γ_{HGP}^B	17	0.1303	0.2345	18	0.2743	0.494
Γ_{HGU}^B	19	0.0104	0.0465	20	0.0106	0.0487
Γ_{BGU}	21	0.0861	0.9455	22	0.0621	0.7444
Γ_{BCU}	23	0.0105	0.120	24	0.0101	0.1160
Γ_{GGU}	25	0.0218	0.2403	26	0.0199	0.2247
Γ_{MFC}	27	0	0	28	0	0
$V_{B,B}$	29	0	0	30	0	0
$V_{H,B}$	31	<0.0001	<0.0001	32	<0.0001	<0.0001
$V_{L,B}$	33	<0.0001	<0.0001	34	<0.0001	<0.0001
$V_{G,B}$	35	0	0	36	0	0
$V_{K,B}$	37	<0.0001	<0.0001	38	<0.0001	<0.0001
$V_{P,B}$	39	0	0	40	0	0
$V_{B,ISF}$	41	0	0	42	0	0
$V_{L,ISF}$	43	<0.0001	<0.0001	44	<0.0001	<0.0001
$V_{G,ISF}$	45	0	0	46	0	0
$V_{K,ISF}$	47	<0.0001	<0.0001	48	<0.0001	<0.0001
$V_{P,ISF}$	49	0.0374	0.1492	50	0.0585	0.2460
$V_{L,ICF}$	51	<0.0001	<0.0001	52	<0.0001	<0.0001
Q_B	53	<0.0001	<0.0001	54	<0.0001	<0.0001
Q_G	55	0.0149	0.5723	56	0.0145	0.4621
Q_K	57	0.0083	0.3137	58	0.0081	0.2776
Q_P	59	0.0489	0.5461	60	0.0369	0.3649
Q_A	61	0.0037	0.1327	62	0.0037	0.1258
T_B	63	0	0	64	0	0
T_P^G	65	0.012	0.0217	66	0.0122	0.0218
T_I	67	0	0	68	0	0
T_P^I	69	0.0401	0.2077	70	0.0284	0.1525
T_Γ	71	0	0	72	0	0
F_{LIC}	73	0.0262	1.8745	74	0.0232	0.9955
F_{KIC}	75	0.0064	0.2325	76	0.0066	0.2216
F_{PIC}	77	0.0668	0.6540	78	0.0422	0.3978

3.3.2.2. Insulin Subsystem Example

Additional steady-state sensitivity analysis has been performed to illustrate its utility.

Analysis of the glucose metabolism model's insulin subsystem identified those parameters which have the greatest influence on the steady-state value of the peripheral venous insulin concentration (I_{PV}). Estimates of selected parameters are revised based on published information. Clinical data is used to demonstrate an improvement in the subsystem's prediction of steady-state plasma insulin levels.

The insulin subsystem is a 7th order system of ordinary differential equations (excluding the equations governing insulin secretion from the pancreas). This analysis assesses the sensitivity of I_{PV} to a change in a single parameter value. As with the sensitivity analysis of glucose metabolism model, r_{PIR} is set to zero. The sole external input in this example is RI as defined in equation 3.68. The insulin subsystem contains 20 of the 39 independent parameters in Table 3.4. Of those 20 parameters, only 8 parameters (HCT , Q_G , Q_K , Q_P , Q_A , F_{LIC} , F_{KIC} , F_{PIC}) determine the steady-state value of I_{PV} .

Under steady-state conditions, RI is constant (denoted by RI_{ss}) and I_{PV} (denoted by I_{ss}) is a linear function of RI_{ss} ,

$$I_{ss} = \frac{RI_{ss}}{(1 - HCT)(1 - F_{PIC}) \left((Q_A + Q_G)F_{LIC} + \frac{Q_K F_{KIC}}{F_{KIC} + 1} + Q_P F_{PIC} \right)}. \quad 3.76$$

The linear relationship between the I_{ss} and RI_{ss} eliminates the need to evaluate the subsystem over the range of values (as described in equation 3.71). This, in turn, eliminates the need to calculate the L^1 and L^∞ norms. To calculate the sensitivity of I_{ss} to a change in a parameter value, a term α is defined as

$$\alpha = \frac{1}{(1 - \text{HCT})(1 - F_{\text{PIC}}) \left((Q_A + Q_G)F_{\text{LIC}} + \frac{Q_K F_{\text{KIC}}}{F_{\text{KIC}} + 1} + Q_P F_{\text{PIC}} \right)}. \quad 3.77$$

where $I_{\text{ss}} = \alpha R I_{\text{ss}}$. The change in α for a change in a single parameter value is determined. The sensitivity of I_{ss} to a change in a single parameter value corresponds directly to that of α since I_{ss} is simply a scale quantity of α where the scaling factor is $R I_{\text{ss}}$.

The percent changes in α for a 10% increase or a 10% decrease in parameter i are defined as

$$\Delta\alpha_i^+ = \frac{\alpha_i^+ - \alpha_0}{\alpha_0} \quad \text{and} \quad \Delta\alpha_i^- = \frac{\alpha_i^- - \alpha_0}{\alpha_0} \quad 3.78$$

where α_0 is the value of α using the published parameter values in Table 3.4, α_i^+ is the value for α when the value for parameter i is increased 10% above its published value, α_i^- is the value for α when the value for parameter i is decreased 10% below its published value and i is a parameter in the set $\{\text{HCT}, Q_G, Q_K, Q_P, Q_A, F_{\text{LIC}}, F_{\text{KIC}}, F_{\text{PIC}}\}$.

Table 3.6 lists the results of the steady-state sensitivity analysis for the insulin subsystem. Ranking the parameters based on the magnitude of $\Delta\alpha_i^+$ or $\Delta\alpha_i^-$ produces the same order. I_{ss} is most sensitive to changes in HCT and F_{LIC} . A 10% increase in the HCT produces a 7.1% increase I_{ss} while a 10% decrease in HCT results in a 6.3% decrease in I_{ss} . A 10% increase in the F_{LIC} produces a 5.0% decrease I_{ss} while a 10% decrease in F_{LIC} results in a 5.5% increase in I_{ss} .

Table 3.6: Percent change in α for 10% increase ($\Delta\alpha_i^+$) and a 10% decrease ($\Delta\alpha_i^-$) in parameter i

parameter i	$\Delta\alpha_i^+$	$\Delta\alpha_i^-$
HCT	0.071	-0.063
Q_K	-0.024	0.025
Q_P	-0.023	0.024
Q_A	-0.010	0.011
Q_G	-0.040	0.044
F_{KIC}	-0.018	0.019
F_{LIC}	-0.050	0.055
F_{PIC}	-0.005	0.006

Next, we demonstrate how these results can be used to refine the insulin subsystem. The selected parameters (HCT and F_{LIC}) are revised and the subsystem's estimates of steady-state insulin concentrations are compared to clinical data. Here we will use clinical data collected in subjects with type 1 diabetes who participated in meal studies at the Artificial Pancreas Center (Thomas Jefferson University, Philadelphia, PA). In previously published analysis, data were used to compare insulin kinetics models consisting of one, two, and three first-order linear differential equations [189]. A first-order linear insulin kinetics model was sufficient to describe the clinical data. The model had a fractional insulin loss rate of $0.112 \pm 0.063 \text{ min}^{-1}$ and a distribution volume of $15.6 \pm 4.0 \text{ L}$.

Briefly, the meal studies consist of seven experiments on five human subjects with type 1 diabetes (one subject was studied on three separate occasions). The data consists of the variable rate of insulin delivery and plasma insulin concentrations every ten minutes over the 510-minute experiment as well as subject height, weight, age, sex and average daily insulin requirement. During each experiment, each subject consumed an identical 829 Kcal meal of solid food for breakfast and lunch, followed by exercise on a stationary

bicycle. Regular human insulin was infused into a peripheral vein at a basal rate (0.5 U/h) for the entire study. Coinciding with the consumption of each meal, insulin was infused at a higher rate for 120 min (average dose 8.5 ± 2.1 U). The bolus dose was based upon preprandial and 60-min postprandial blood glucose measurements and a sliding scale regimen. Blood glucose levels were allowed to fluctuate throughout the protocol (mean 174 mg/dL, range 55–340 mg/dL). A total of 346 plasma samples were assayed to measure the concentration of human insulin.

A portion of the clinical data collected in the meal study will be used here, namely, paired points consisting of the insulin infusion rate and steady-state plasma insulin concentration. Steady-state plasma insulin concentrations were determined to be those points collected at least 20 minutes after a change in the insulin infusion rate (greater than 4 half-lives for insulin). In [189], one subject (subject 4) was identified as an outlier and data collected from this subject will be excluded from analysis here.

While HCT can be determined with a simple blood test, the subjects that participated in the meal study did not have their HCT measured. Therefore, mean HCT values based on sex and ethnicity were used: 45.5 for adult Caucasian males and 40.2 for adult Caucasian females [188]. A review of the literature also indicates that the value for F_{LIC} was underestimated – the fractional clearance of insulin by the liver was revised to 60% [190]. Using the new values for HCT and F_{LIC} , the average value of the residuals was -0.57 ± 6.55 mU/l compare to 4.60 ± 7.39 mU/l using the original parameter values (Figure 3.3).

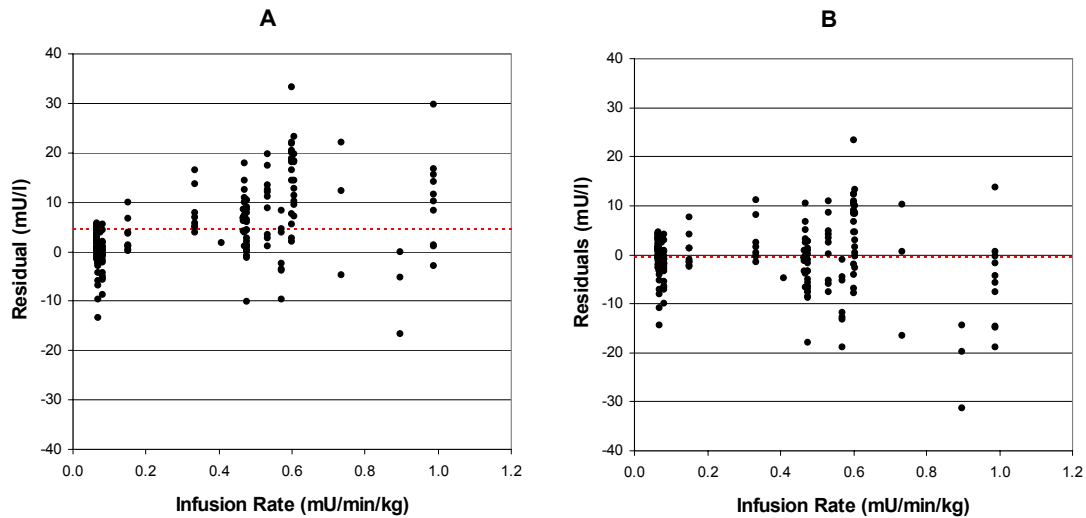


Figure 3.3: Residual plots for insulin subsystem predicted steady-state plasma insulin concentration versus measured plasma insulin concentrations for various intravenous insulin infusion rates. Panel A contains the residuals for the subsystem using the original parameter values and panel B contains the residuals for the subsystem using update values for HCT and F_{LIC} . In each panel, the red dashed line is the mean of the residuals.

The new parameter values were also validated with data collected from seven published insulin studies employing intravenous infusions of insulin. The constant infusion rates and steady-state plasma insulin concentrations are given in Table 3.7. Several studies (Gottesman 1983, Best 1981, Yki-Jarvinen 1987) used a concurrent somatostatin infusion to suppress endogenous insulin release. For the remaining studies, it was assumed that the exogenous insulin infusion sufficiently suppressed endogenous insulin release. Plasma insulin concentrations were simulated using the original and updated parameter values for HCT (0.4 vs. 0.46) and F_{LIC} (0.4 vs. 0.6). All data were log-normalized. The regression line ($y = 1.07x + 1.82$) produced the best fit to the log-transformed data in the least-squares sense. Compared to the original parameter set, the simulated data from the updated parameter set fit the regression line better (Figure 3.4), and reduced the bias (calculated as the average difference between the log-transformed plasma insulin and the

log-transformed simulated plasma insulin concentrations) by a factor of ten (-0.101 vs. -0.011).

Table 3.7: Experimental data from seven published studies where constant intravenous insulin infusions were performed in normal man.

number of subjects	basal insulin concentration (mU/l)	infusion rate (mU/min/kg)	plasma insulin concentration (mU/l)	Reference
6	1 ± 1	0.2	18 ± 5	Best 1981
5		0.5	47 ± 11	
4	8 ± 4	0.3	26 ± 3	Bonadonna 1993
5		0.9	61 ± 7	
4		4.3	427 ± 54	
4		8.6	1371 ± 138	
4	11 ± 5	0.9	42 ± 20	Brooks 1984
7		1.7	106 ± 16	
6		3.5	183 ± 47	
4		8.7	564 ± 50	
5	n/a	0.2	18 ± 2	Gottesman 1983
4		1.0	84 ± 10	
5		2.0	156 ± 5	
6	5 ± 2	0.5	18 ± 7	Laakso 1992
6		0.9	42 ± 10	
6		1.8	86 ± 15	
6		13.8	1350 ± 401	
6		27.5	3017 ± 951	
6	8 ± 4	1.6	65 ± 4	Williams 2001
4		4.8	183 ± 18	
5	7 ± 5	0.8	45 ± 2	Yki-Jarvinen 1987
6		2.8	170 ± 31	
5		18.9	1710 ± 561	

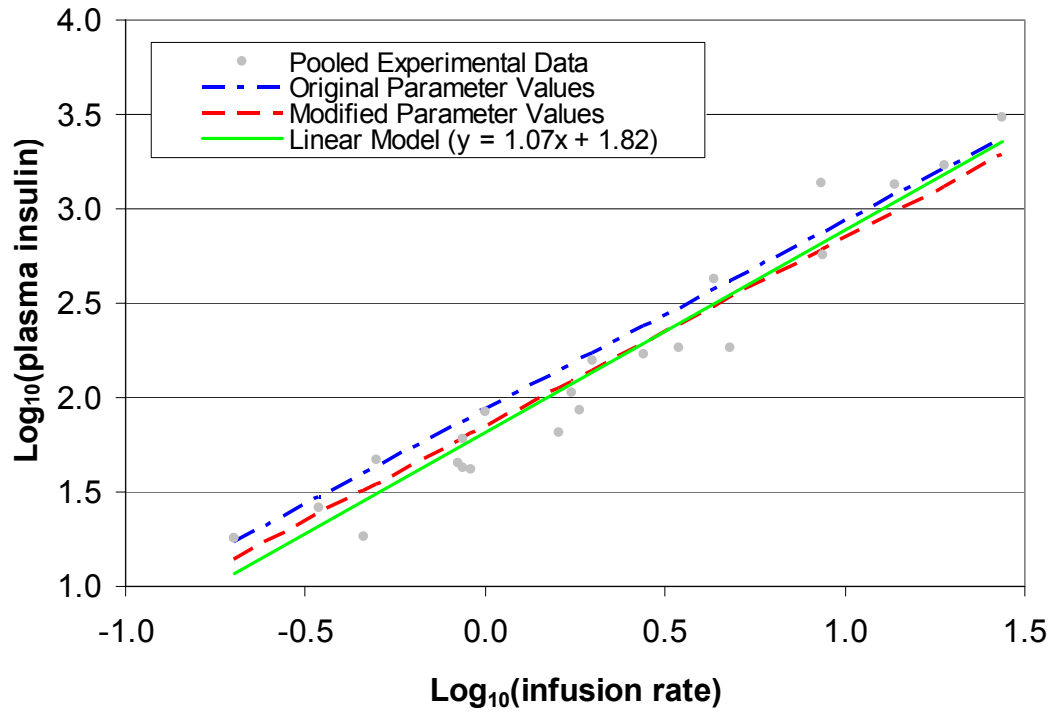


Figure 3.4: Log-transformed insulin infusion rate and plasma insulin concentration data from published experiments (gray circles), model simulations using the original (blue dot-dashed line) and updated (red dashed line), and the linear least-squares regression model of the experimental data (green line).

CHAPTER 4. REFINING DYNAMIC GLUCOSE UPTAKE

Glucose utilization in peripheral muscle and the liver change dramatically when glucose and insulin concentrations vary (Table 4.1). As such, these tissues are primarily responsible for maintaining glycemia under various conditions (*e.g.*, fasting versus postprandial). It is important to accurately describe the processes within these two organs that alter circulating levels of insulin and glucose in order to have a realistic model of glucose metabolism. This chapter is devoted to the review of relevant clinical data to improve the model's description of these processes.

Table 4.1: Sources of glucose uptake

Parameter		Basal Rate (mg/min)	Range [†] (mg/min)	Mediators
r_{BGU}	Brain Glucose Uptake	70	-	constant
r_{PGU}	Peripheral Glucose Uptake	35	10 - 1600	insulin, glucose
r_{HGU}	Hepatic Glucose Uptake	20	0.2 - 400	insulin, glucose
r_{GGU}	Gut Glucose Uptake	20	-	constant
r_{RBCU}	Red Blood Cell Glucose Uptake	10	-	constant
r_{KGE}	Kidney Glucose Excretion	0.05	0.02 - 10	glucose

[†] minimum and maximum steady-state glucose uptake rates for plasma insulin between 1 and 100 mU/l, and plasma glucose concentrations between 40 and 300 mg/dl

4.1. Peripheral Glucose Uptake

The rate at which glucose is transported into muscle tissue is very sensitive to changes in circulating insulin concentrations. The relationship between rate of peripheral glucose uptake and plasma insulin concentrations has been the focus of several clinical studies. As originally published in the glucose metabolism model, this relationship is described using a hyperbolic tangent function,

$$M_{PGU}^I = A + B \tanh \left[C \left(\frac{I_{PI}}{I_{PI}^B} - D \right) \right] \quad 4.1$$

where I_{PI} is the insulin concentration in the interstitial fluid bathing the peripheral tissue, I_{PI}^B is the value of I_{PI} under basal conditions and the parameters $\{A, B, C, D\}$ were estimated from forearm glucose uptake studies (see Table 4.2). The rate of peripheral glucose uptake, $r_{PGU} = r_{PGU}^B M_{PGU}^G M_{PGU}^I$, is a combination of M_{PGU}^I , M_{PGU}^G and r_{PGU}^B , the insulin-mediated modifier of peripheral glucose uptake, the glucose-mediated modifier of peripheral glucose uptake and the basal rate of peripheral glucose uptake, respectively. Under euglycemic conditions, $M_{PGU}^G = 1$ and r_{PGU} is reduced to $\bar{r}_{PGU} = r_{PGU}^B M_{PGU}^I$.

Table 4.2: Hyperbolic tangent equation parameter values for the insulin-mediated modifier of peripheral glucose uptake

A	B	C	D
7.03	6.52	0.338	5.82

Laakso *et al.* (1990) have used an alternative formulation of the relationship between the concentration of insulin and its effect on peripheral glucose uptake, described by the logistics equation:

$$\bar{r}_{PGU} = V_{\min} + \frac{V_{\max} - V_{\min}}{1 + \left(\frac{I_{PI}}{K_{50}} \right)^m} \quad 4.2$$

where I_{PI} is the interstitial plasma insulin concentration, V_{\min} and V_{\max} are the minimal and maximal rates of glucose uptake, K_{50} is the insulin concentration at which uptake is halfway between V_{\min} and V_{\max} , and m is a slope factor [191]. Using the hyperbolic

tangent relationship in equation 4.1 rewritten to incorporate parameters analogous to that in equation 4.2, \bar{r}_{PGU} can also be written as:

$$\bar{r}_{\text{PGU}} = \frac{1}{2} \left((V_{\text{max}} + V_{\text{min}}) + (V_{\text{max}} - V_{\text{min}}) \tanh(m(I_{\text{PI}} - K_{50})) \right) \quad 4.3$$

where $V_{\text{max}} = r_{\text{PGU}}^{\text{B}}(A + B)$, $V_{\text{min}} = r_{\text{PGU}}^{\text{B}}(A - B)$, $K_{50} = I_{\text{PI}}^{\text{B}}D$, $m = \frac{C}{I_{\text{PI}}^{\text{B}}}$. Whereas the parameters $\{V_{\text{max}}, V_{\text{min}}, K_{50}, m\}$ in the hyperbolic tangent equation have the same interpretation as the logistics equation, only the values of V_{max} , V_{min} and K_{50} can be directly compared between equations 4.2 and 4.3.

Appendicular (forearm and leg) studies have been used to estimate the rate of glucose uptake by muscle for a range of insulin concentrations. The majority of insulin-mediated peripheral glucose uptake data reported in the literature has been collected under steady-state conditions. In these studies, exogenous glucose and insulin are infused intravenously to maintain euglycemia and achieve a desired level of insulinemia. Glucose uptake is computed as a product of the blood flow rate and glucose concentration gradient across the tissue (measured as the difference between measured arterial and venous glucose concentrations that supply and drain a specific tissue). These data have been pooled to evaluate the model's ability to describe insulin-mediated peripheral glucose uptake (Table 4.3). Except for [192], all measured insulin concentrations are from arterial (or arterialized) blood. In [193], somatostatin was also infused to produce a state of hypoinsulinemia such that plasma insulin levels were not detectable below the 2.2 mU/l threshold of the assay.

Table 4.3: Data from published appendicular studies

Reference	limb	n	insulin infusion rate (mU/kg/min)	insulin concentration (mU/l)	glucose concentration (mg/dl)	glucose uptake (mg/min/100ml)
Louard 1992 [†] [192]	arm	10	0	6 ± 3	78 ± 6	0.18 ± 0.06
	arm	7	0.01	33 ± 11	69 ± 10	0.21 ± 0.7
	arm	7	0.02	40 ± 13	79 ± 10	0.32 ± 0.14
	arm	8	0.035	67 ± 23	78 ± 5	0.43 ± 0.20
	arm	7	0.05	124 ± 29	78 ± 5	0.85 ± 0.33
Williams 2001 [194]	leg	4	0	8 ± 4	88 ± 4	0.04 ± 0.02
	leg	6	1.61	65 ± 4	96 ± 13	0.87 ± 0.69
	leg	4	4.82	183 ± 18	92 ± 4	1.13 ± 0.28
Bonadonna 1993a [193]	arm	4	0	< 2.2 [‡]	88 ± 10	0.10 ± 0.05
	arm	6	0	7.5 ± 3.9	90 ± 3	0.10 ± 0.07
	arm	4	0.35	26.9 ± 2.6	90 ± 10	0.18 ± 0.08
	arm	5	0.86	60.5 ± 7.1	90 ± 10	0.48 ± 0.18
	arm	4	4.32	426.5 ± 53.5	90 ± 10	0.99 ± 0.15
	arm	4	8.64	1371 ± 138	90 ± 10	1.10 ± 0.39
Bonadonna 1993b [195]	arm	5	0	6 ± 2	92 ± 5	0.08 ± 0.05
	arm	5	34.6	68 ± 7	94 ± 13	0.68 ± 0.32
Laakso 1990 [191]	leg	6	0	5 ± 2	81 ± 4	0.04 ± 0.01
	leg	6	0.46	18 ± 7	76 ± 4	0.11 ± 0.06
	leg	6	0.92	42 ± 10	79 ± 9	0.52 ± 0.22
	leg	6	1.83	86 ± 15	79 ± 9	1.06 ± 0.36
	leg	6	13.76	1350 ± 401	81 ± 9	1.52 ± 0.54
	leg	6	27.52	3017 ± 951	81 ± 9	1.55 ± 0.50
Yki-Jarvinen 1987 [196]	arm	6	0	7 ± 5	91 ± 5	0.17
	arm	5	0.84	45 ± 2	90 ± 2	0.40
	arm	6	2.76	170 ± 31	89 ± 2	1.19
	arm	5	18.87	1710 ± 561	90 ± 2	1.55
Fugmann 1998 [197]	arm	9	0	15 ± 4	92	0.08 ± 0.05
	arm	9	2.49	92 ± 12	92	0.58 ± 0.4
Brooks 1984 [198]	arm	21	0.00	11 ± 5	96 ± 5	0.06 ± 0.09
	arm	4	0.98	42 ± 20	91 ± 6	0.61 ± 0.20
	arm	7	1.97	106 ± 16	92 ± 5	0.76 ± 0.32
	arm	6	3.93	183 ± 47	92 ± 5	1.10 ± 0.27
	arm	4	9.83	564 ± 50	94 ± 8	1.13 ± 0.36

[†] insulin concentrations were measured from deep vein blood

[‡] Somatostatin was infused to produce a state of hypoinsulinemia, insulin concentration was below detectable limit of assay

As illustrated in Figure 4.1, a ten-fold increase in the glucose uptake rate can occur within physiological insulin concentrations (5-200 mU/l). At any given insulin concentration, the rates of peripheral glucose uptake measured in these studies demonstrate a large variability. This variability is caused, in part, to the coarse methods used to measure glucose uptake (*i.e.*, errors introduced through inaccuracies in blood flow and glucose gradient measurements). However, this variability can also be partially attributed to the random effect of each subject – highlighting the existence of a continuum of curves that describes the relationship between insulin concentrations and peripheral glucose uptake for the whole population.

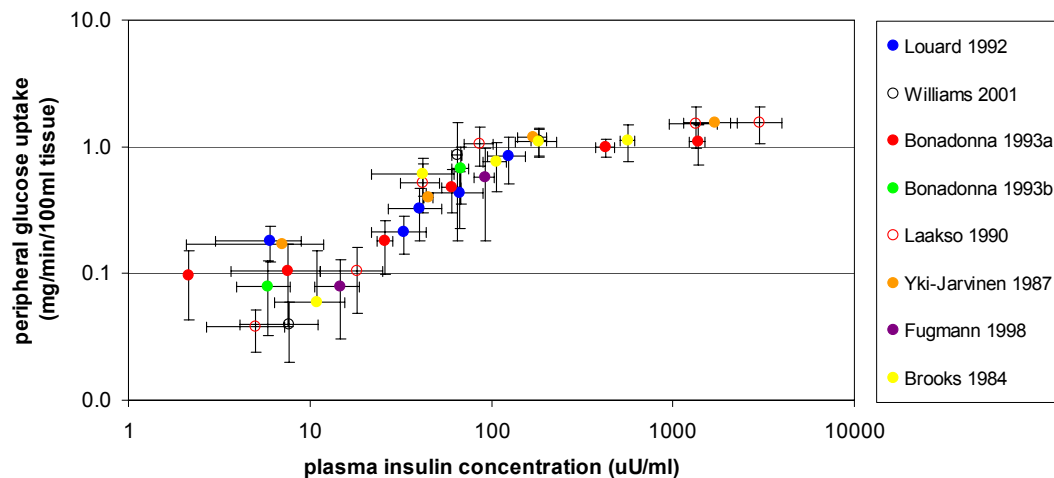


Figure 4.1: Pooled data from appendicular glucose uptake studies. Open and solid circles indicate leg and forearm glucose uptake studies, respectively. For each data point, horizontal and vertical error bars represent the standard deviations in measured plasma insulin concentrations and calculated rates of glucose uptake, respectively, among the subjects in the study.

Glucose uptake data are reported in units of $\text{mg min}^{-1} 100\text{ml tissue}^{-1}$, $\text{mg min}^{-1} \text{arm}^{-1}$, or $\text{mg min}^{-1} \text{leg}^{-1}$. The assumptions listed in Table 4.4 made it possible to compare clinical

data to the model estimate of peripheral glucose uptake (tissue densities in assumption 1 were found at <http://physics.nist.gov/cgi-bin/Star/compos.pl>, assumptions 2-4 were taken directly from [187] and assumption 5 was derived from [199]).

Table 4.4: Assumptions used to translate appendicular glucose uptake data (in $\text{mg min}^{-1} 100\text{ml tissue}^{-1}$) to total peripheral tissue glucose uptake (mg/min).

-
1. Muscle and adipose tissue densities are 1.04 g/ml and 0.92 g/ml
 2. Total muscle and adipose masses in a 70 kg man are 30 kg and 10 kg, respectively
 3. Muscle and adipose tissue account for 89 and 11 percent of basal glucose uptake, respectively
 4. Muscle and adipose tissue constitute 64 and 8 percent of total forearm volume in nonobese subjects
 5. Muscle and adipose tissue constitute 58 and 40 percent of total leg volume in nonobese subjects
-

Published appendicular glucose uptake data was pooled to estimate the parameters in the two proposed functional relationships (equations 4.2 and 4.3). The assumptions in Table 4.4 were used to standardize the rate of peripheral glucose uptake in units of mg/min. In addition, plasma insulin concentrations (I_H) were converted to peripheral interstitial insulin concentrations (I_{PI}) using

$$I_{PI} = I_H \left(1 - F_{PIC} \left(\frac{Q_P^I T_P^I}{V_{PI}^I} - 1 \right) \right) \quad 4.4$$

which was derived from the model's insulin subsystem equations under steady-state conditions.

Parameter estimates were computed using a nonlinear least-squares fitting routine in the curve fitting toolbox (version 1.1) of Matlab (version 6.5). Parameters were constrained

to positive values and each data point was weighted by the reciprocal of the variance of the measured peripheral glucose uptake rate².

The parameter estimates for each equation is given in Table 4.5 along with the (transformed) parameter values for the hyperbolic tangent equation originally reported in [187]. Goodness-of-fit (R^2) was 0.949 and 0.935 for the logistics and hyperbolic tangent equations, respectively. Estimates for V_{\max} and K_{50} were similar for both equations. Evaluating \bar{r}_{PGU} at $I_{\text{PI}}=0$ (rather than comparing V_{\min} estimates) provides similar estimates between the two equation (28 and 34 mg/min for the logistics and hyperbolic tangent equations, respectively).

Both equations adequately describe the relationship between peripheral interstitial insulin concentration and peripheral glucose uptake. For both functional relationships, V_{\max} and K_{50} are greater than the original parameter values (Table 4.5). The original model would have underestimated peripheral glucose uptake at supra-physiological insulin concentrations. However, all three relationships are similar at basal insulin concentrations (Figure 4.2).

Table 4.5: Parameter estimates with 95% confidence limits in parentheses for the hyperbolic tangent and logistics equations and the (transformed) original parameter values for the hyperbolic tangent relationship between peripheral interstitial insulin concentration and peripheral glucose uptake.

Equation	V_{\min}	V_{\max}	K_{50}	m
Logistics	28 (5, 50)	647 (571, 723)	46 (36, 56)	1.94 (1.23, 2.64)
Hyperbolic Tangent	0 [†]	598 (539, 656)	43 (36, 49)	0.033 (0.025, 0.041)
Original Hyperbolic Tangent	18	474	31	0.064

[†] confidence limits not reported by Matlab curve fitting function

² Yki-Jarvinen *et al.* (1987) did not report the variance in their computed uptake rates and these points were weighted arbitrarily based on the weights of data points from other studies with similar uptake rates.

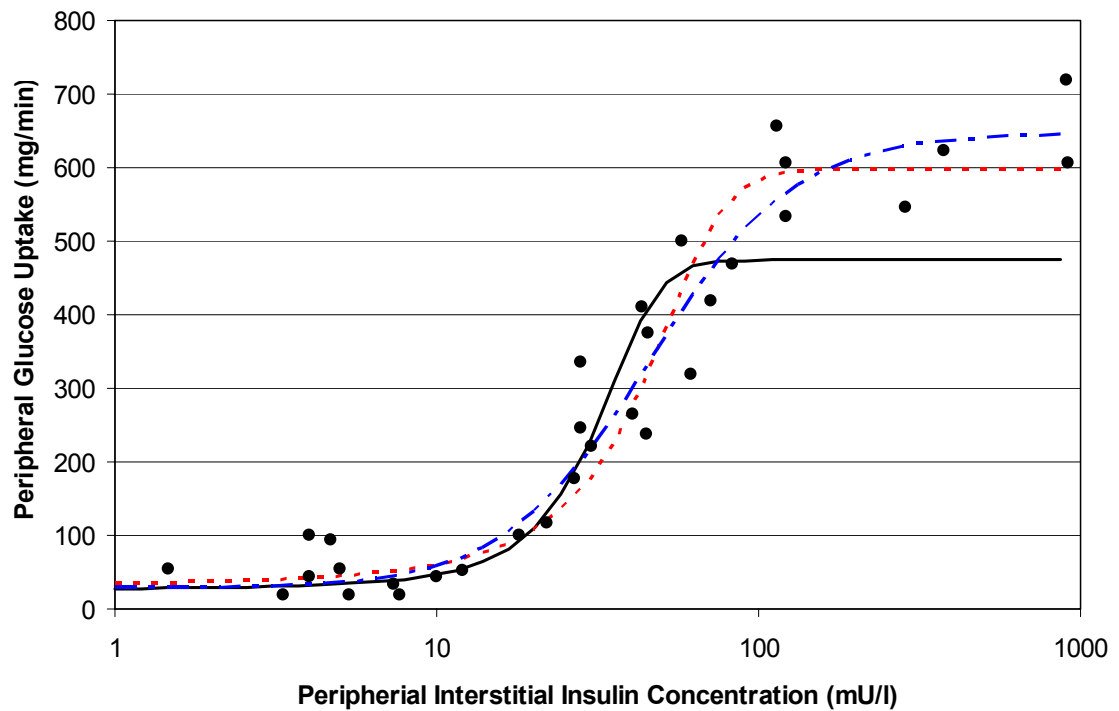


Figure 4.2: Various response curves describing the relationship between peripheral interstitial insulin concentrations and peripheral glucose uptake (pooled data – filled black circles, original hyperbolic tangent relationship - solid black line, the hyperbolic tangent relationship with updated parameter values - dashed red line and the logistics relationship - dot-dash blue line).

Data describing peripheral glucose uptake under the stress of trauma and surgery are limited. In a study of nine healthy male subjects, an intravenous infusion of hydrocortisone, glucagon and epinephrine was given over four days to mimic the stress response [4]. With subjects acting as their own controls, steady-state levels for cortisol, glucagon and epinephrine were $40 \pm 4 \mu\text{g/dl}$, $507 \pm 65 \text{ pg/ml}$ and $417 \pm 52 \text{ pg/ml}$ during the hormone infusion and $12 \pm 1 \mu\text{g/dl}$, $79 \pm 14 \text{ pg/ml}$ and $22 \pm 5 \text{ pg/ml}$ during the saline infusion. These levels are comparable to those reported in studies of the in-hospital patient population as reviewed herewith in. At the end of the study period, a

hyperinsulinemic, euglycemic clamp was performed to evaluate forearm glucose uptake. The mean forearm glucose uptake was reduced by 50% in the simulated state of stress (0.48 ± 0.36 versus 1.03 ± 0.27 mg/100 ml tissue/min). In forearm glucose uptake measurements performed on trauma patients, no basal glucose uptake was observed in four patients that were studied in the immediate postoperative period [198]. When measured under hyperinsulinemic glucose clamp conditions, the forearm glucose uptake in these post-traumatic patients varied greatly although the mean uptake value was reduced more than 50% relative to healthy controls. Under similar conditions, Little *et al.* (1987) demonstrated a 40% reduction in insulin-mediated forearm glucose uptake in trauma patients 5-10 days postoperative [200]. These data demonstrate the response of insulin-mediated peripheral glucose uptake to stress is significantly attenuated after severe injury (*i.e.*, V_{\max} acutely decrease around the stressful event). However, no data exists to describe the relationship between the surgical severity and the degree of peripheral glucose uptake attenuation.

Laakso *et al.* (1992) performed euglycemic insulin-mediated leg glucose uptakes studies in six healthy lean non-diabetic subjects with and without an epinephrine infusion [201]. With the subjects acting as their own controls, the epinephrine-infusion experiments achieve an average arterial epinephrine concentration of 390 pg/ml (compared to an average basal concentration of 38 pg/ml). Leg glucose uptake was determined at several insulin levels and the data was fitted to a logistic equation. While V_{\max} decreased and K_{50} increased during the epinephrine-infusion group, the changes did not reach statistical significance. However, there were profound (statistically significant) changes in the underlying mechanisms that contribute to glucose uptake: glucose extraction decreased

while blood flow increased in the epinephrine-infusion group. It can be postulated that a decrease in peripheral blood flow during the perioperative period coupled with decrease in glucose extraction will lead to an overall decrease in peripheral glucose uptake.

4.2. Net Hepatic Glucose Balance

The liver acts as both a sink and source for glucose, typically removing glucose from circulation in the hours following a meal and adding it to circulation otherwise. The flux of glucose in and out of hepatocytes is regulated by the abundance of glucose and other substrates in circulation, various hormones secreted by the pancreas and other organs, and direct neural stimulation. The liver has the capability to store glucose as glycogen, a highly branched polymer that may contain upwards of 60,000 glucose molecules. A healthy adult liver contains 90 grams of glucose (stored as glycogen) in the hours following a meal [202]. The breakdown of glycogen (glycogenolysis) provides a source of glucose that can be released rapidly into the bloodstream. Alternatively, the liver can also convert specific substrates (*i.e.*, lactate, gluconeogenic amino acids, and glycerol) into glucose in a process referred to as gluconeogenesis.

The basal hepatic glucose production rate of a healthy adult is $2.2 \text{ mg kg}^{-1} \text{ min}^{-1}$ [203] which decreases with a prolonged fast [204]. In the postabsorptive state, glycogenolysis and gluconeogenesis contribute equally to the endogenous production of glucose [205]. However, as glycogen are depleted during fasting, the role of gluconeogenesis increases so that, after 42 hours of fasting, over 90% of endogenous glucose production is from gluconeogenesis [206].

The fate of intracellular glucose is controlled by a myriad of factors that directly or indirectly modulate the processes of glucose storage and production in the liver. Glucose,

insulin, glucagon, epinephrine and cortisol directly affect enzyme function and/or expression within hepatocytes. The distinction between these two forms of regulation is temporal. Controlling the activity of an enzyme (i.e., enhancing or inhibiting its function) has an immediate effect, whereas controlling the expression (transcription and translation) of these enzymes has a delayed effect, on the rate of the reaction. Glucose *per se* decreases the output of glucose by the liver by reducing the activity of glycogen phosphorylase which is responsible for glycogen breakdown [207]. When hepatic glycogen concentrations are reduced (as with a prolonged fast), a reduction in gluconeogenesis can be observed during hyperglycemia [208].

Insulin decreases the release of hepatic glucose by increasing the activities of key enzymes involved glycogen production, glycogen synthase and glucokinase [207, 209]. Insulin will also suppress the genetic expression of key gluconeogenic enzymes, phosphoenolpyruvate carboxykinase (PEPCK) and glucose-6-phosphatase [210]. The effect of insulin on glycogenolysis is more profound than on gluconeogenesis[211]. The counterregulatory hormones (glucagon and epinephrine) oppose insulin's actions. Glucagon acts solely on the liver. It increases the activity of glycogen phosphorylase, increasing the rate of glycogenolysis, [212]. It also increases the activity and transcription of PEPCK, which increases the rate of gluconeogenesis, and downregulates the activity and transcription of pyruvate kinase, which decreases the metabolism of glucose within the cell, making more glucose available for release from the liver [212]. Like glucagon, epinephrine also increases glycogenolysis by increasing glycogen phosphorylase activity. In fact, adrenergic and glucagon receptors are coupled to the same type of G-protein that initiates the cascade of events that ultimately lead to the activation of glycogen

phosphorylase. Unlike glucagon, epinephrine indirectly increases the rate of gluconeogenesis by increasing the supply of glucogenic precursors in the bloodstream [108]. Cortisol directly and indirectly increases the rate of gluconeogenesis by promoting the expression of enzymes involved in the process and increasing the supply of gluconeogenic amino acids [213, 214]. Acute cortisol stimulation does not cause significant alterations in hepatic glucose release because (1) its regulation relies on increasing enzyme expression and (2) new glucose is shuttled directly into glycogen in the short term. In contrast, prolonged cortisol stimulation results in an increased hepatic glucose output and glycogen stores despite increased phosphorylase activity, probably as a consequence of a greater stimulation of synthetase activity coupled with a marked augmentation of gluconeogenesis [123].

The release of glucose from hepatocytes into the bloodstream is offset by their uptake. The transport of glucose across the plasma membrane of the hepatocyte is facilitated by glucose transporters (GLUT-2) which do not increase their membrane-bound numbers in an insulin-dependent manner unlike GLUT-4 which is found in insulin-sensitive muscle and adipose tissue [215]. Inside the hepatocyte, glucose is phosphorylated predominantly by glucokinase to produce glucose 6-phosphate which is not released back into circulation. Insulin modulates glucose uptake by increasing glucokinase expression [216] thereby exerting an influence on the ability to retain glucose within the cell once it is taken out of circulation.

Quantification of the hepatic glucose uptake in man is hindered by the limited access to the portal vein which supplies the liver with blood draining from the gut which comprises the gastrointestinal tract, pancreas and spleen (Figure 4.3). Without access to the portal

vein, it is virtually impossible to measure gut glucose uptake, the pancreatic insulin release and the appearance of glucose from the intestines. As such, much of the insight into the control of hepatic glucose metabolism has been gained through animal experimentation. In man, direct measurements of hepatic glucose uptake are typically reported for the region as a whole. Referred to as splanchnic glucose uptake, it is the sum of glucose uptake from the gut and the liver.

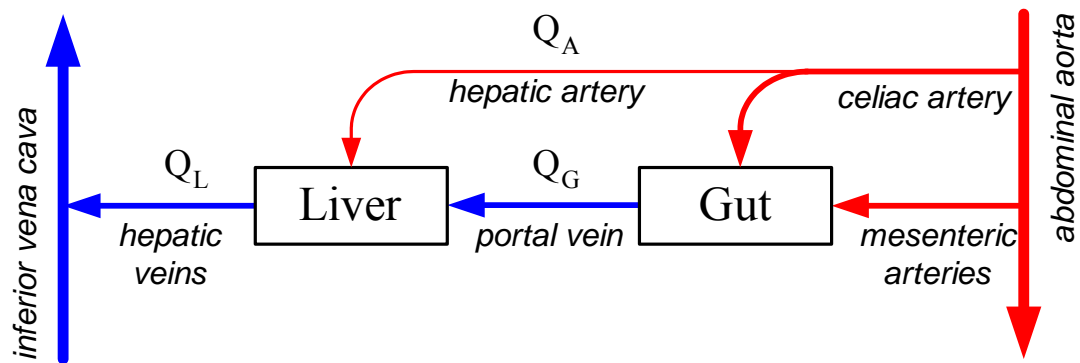


Figure 4.3: Arterial (red) and venous (blue) blood supplying the liver where Q_G and Q_L represent the blood flow from the gut and liver, respectively, and Q_A represents the blood flow through the hepatic artery such that the sum of Q_A and Q_G equals Q_L .

Sacca *et al.* (1982) studied splanchnic glucose balance in experiments with normal male subjects. Using a combination of hepatic vein catheterization, labeled and unlabeled glucose infusions and hormone infusions, the rates of hepatic glucose production, splanchnic glucose uptake and peripheral (all non-splanchnic) glucose uptake were measured [9]. The model was employed to simulate the data from a set of experiments which consisted of a 90-minute glucose infusion at a rate of $6.5 \text{ mg/kg min}^{-1}$ into a peripheral vein (control experiments). The simulated data are superimposed on the mean (\pm SE) data collected in five subjects (Figure 4.4). The glucose infusion was started at

time 0. The model accurately depicts the time course of hepatic glucose output (*i.e.*, hepatic glucose production) and it slightly underestimates of peripheral (all non-splanchnic) glucose uptake. However, there is considerable difference in the estimation of splanchnic glucose uptake such that the steady-state values (between 60-90 minutes) were twofold greater.

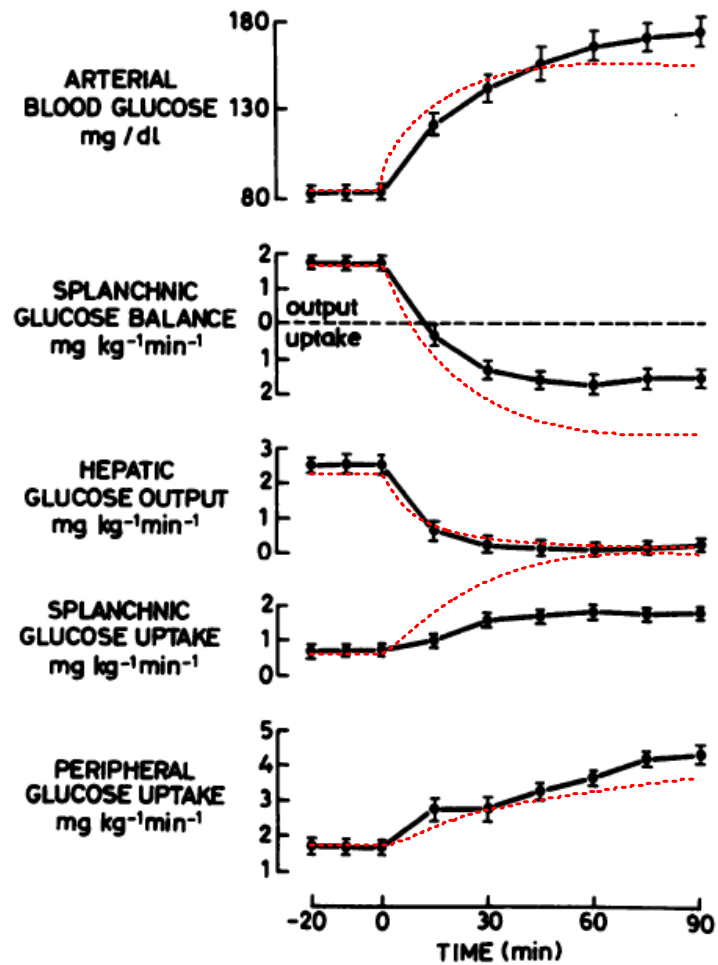


Figure 4.4: Model simulation (red dashed line) of a $6.5 \text{ mg kg}^{-1} \text{ min}^{-1}$ intravenous glucose infusion in normal man superimposed on plot of experimental data originally published in [9]

As modeled, the rate of hepatic glucose uptake (r_{HGU}) is controlled by insulin and glucose. The model describes their control of r_{HGU} through the variables $M_{\text{HGU}}^{\text{G}}$ and $M_{\text{HGU}}^{\text{I}}$ in the equation

$$r_{\text{HGU}} = r_{\text{HGU}}^{\text{B}} M_{\text{HGU}}^{\text{G}} M_{\text{HGU}}^{\text{I}}$$

where $r_{\text{HGU}}^{\text{B}}$ is the basal rate of hepatic glucose uptake. The value of $M_{\text{HGU}}^{\text{G}}$ is based on the instantaneous hepatic glucose concentration, G_{L} , described in the equation

$$M_{\text{HGU}}^{\text{G}} = 5.66 + 5.66 \tanh \left[2.44 \left(\frac{G_{\text{L}}}{G_{\text{L}}^{\text{B}}} - 1.48 \right) \right]$$

where G_{L}^{B} is the basal hepatic glucose concentration. The value of $M_{\text{HGU}}^{\text{I}}$ is based on the hepatic insulin concentration, I_{L} , subjected to a delay, τ_{I} , described in the differential equation

$$\frac{d}{dt} M_{\text{HGU}}^{\text{I}} = \frac{1}{\tau_{\text{I}}} \left[2.0 \tanh \left(0.55 \frac{I_{\text{L}}}{I_{\text{L}}^{\text{B}}} \right) - M_{\text{HGU}}^{\text{I}} \right]$$

where I_{L}^{B} is the basal hepatic insulin concentration. As discussed previously in this section, insulin's regulation of glucokinase expression introduces the lag in its effect of glucose uptake.

To define the relationship between glucose and its uptake by the liver, Sorensen (1985) combined data from experiments that derived r_{HGU} from (i) clamp studies where insulin and glucose levels were fixed by the intravenous infusion of glucose and either insulin or somatostatin and (ii) oral glucose tolerance tests where a fixed dose of labeled glucose

was ingested and plasma glucose and insulin levels were allowed to vary (Figure 4.5). The route of glucose administration does not alter the rate at which the liver takes up glucose [217, 218] but portal insulin and glucose concentrations are not measured directly because this compartment is not readily accessible. In a glucose/insulin clamp study, portal concentrations of glucose and insulin can be assumed to be equivalent to arterial concentrations. There is no glucose appearance from the gut and pancreatic insulin release is suppressed through the infusion of exogenous somatostatin or insulin. In oral glucose tolerance tests, glucose absorption from the gut and pancreatic insulin release occur which will elevate the concentrations of glucose and insulin in portal circulation. These quantities must be measured in order to estimate portal glucose and insulin concentrations. As seen in Figure 4.5, hepatic glucose uptake estimates from oral glucose tolerance tests are distinctly higher than clamp study estimates.

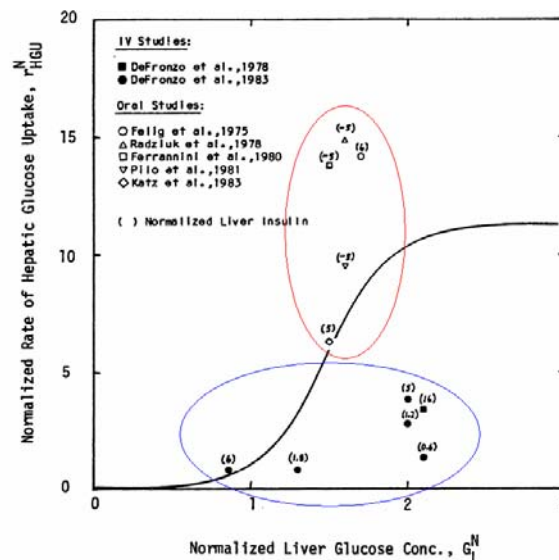


Figure 4.5: Data from Sorensen (1985) used to compute M_{HGU}^G . Data from glucose/insulin clamp studies (solid symbols) are circled in blue and data from oral glucose tolerance tests (open symbols) are circled in red.

The use of glucose/insulin clamp data is preferred to derive the relationship between portal glucose concentrations and hepatic glucose uptake. Hepatic glucose uptake in humans must be derived using measurements of splanchnic glucose uptake since blood supplying the liver is not accessible. Splanchnic glucose uptake (r_{SGU}) is the sum of hepatic and gut glucose uptake,

$$r_{SGU} = r_{HGU} + r_{GGU}.$$

Since the model assumes a constant rate of gut glucose uptake (r_{GGU}), a direct comparison between reported measures and model estimates of r_{SGU} are possible. Data from two published studies are given in Table 4.6.

After insulin concentrations are normalized by basal insulin concentrations, these data are compared to model estimates of r_{SGU} at steady-state (Panel A of Figure 4.6). As with the experimental data from Sacca *et al.* (1982), these data also illustrate an overestimation of the influence of glucose to promote hepatic glucose uptake. There is insufficient data to derive the parameters {A, B, C} of the functional relationship in the form

$$M_{HGU}^G = A + A \tanh \left[B \left(\frac{G_L}{G_L^B} - C \right) \right].$$

Therefore, A was adjusted to fit the experimental data. Then, C was adjusted so

$M_{HGU}^G \Big|_{G_L=G_L^B} = 1$. As illustrated in panel B of Figure 4.6, the new parameterization

(A=1.89, B=2.44 and C=1.27) improves the model's fit to the experimental data. In

addition, the new parameter values for M_{HGU}^G also rectify the overestimation of hepatic glucose uptake in the control experiments (Figure 4.7).

Table 4.6: Estimates of splanchnic glucose uptake from glucose/insulin clamp experiments

	number of subjects	systemic insulin infusion rate (mU/kg/min)	arterial plasma insulin concentration (mU/l)	arterial plasma glucose concentration (mg/dl)	splanchnic glucose uptake (mg/kg/min)
DeFronzo <i>et al.</i> (1983) [219]	37 ^a		13 ± 12	95 ± 6	
	4	0.25	37 ± 4	95 ± 8	0.38 ± 0.2
	3	0.5	53 ± 4	93 ± 5	0.37 ± 0.12
	6	1	101 ± 12	94 ± 7	0.46 ± 0.22
	3	5	428 ± 64	94 ± 5	} 0.68 ± 0.29
	2	10	1189 ± 20	94 ± 5	
		3 ^b	0	10 ± 2	224 ± 2
	3 ^b	0.30	40 ± 10	222 ± 4	1.02 ± 0.17
Basu <i>et al.</i> (2004) [220]	14 ^a		6 ± 3	99 ± 7	
	14	0.50	23 ± 5	168 ± 7	1.5 ± 0.9
	14	1	47 ± 11	168 ± 7	1.68 ± 0.7
	14	2	102 ± 25	2.0 ± 0.5	2.7 ± 0.8

^a basal glucose and insulin concentrations

^b insulin suppression via somatostatin infusion

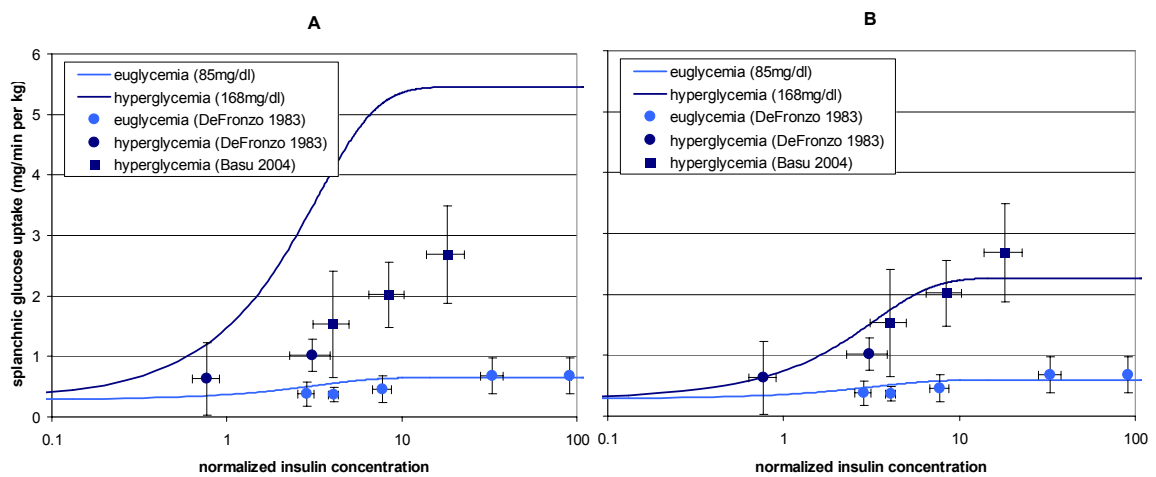


Figure 4.6: Steady-state rates of splanchnic glucose uptake at euglycemia (light blue) and hyperglycemia (dark blue) as a function of normalized insulin concentrations. The lines represent model estimates of uptake and points represent actual measurements. Panel A: model estimates

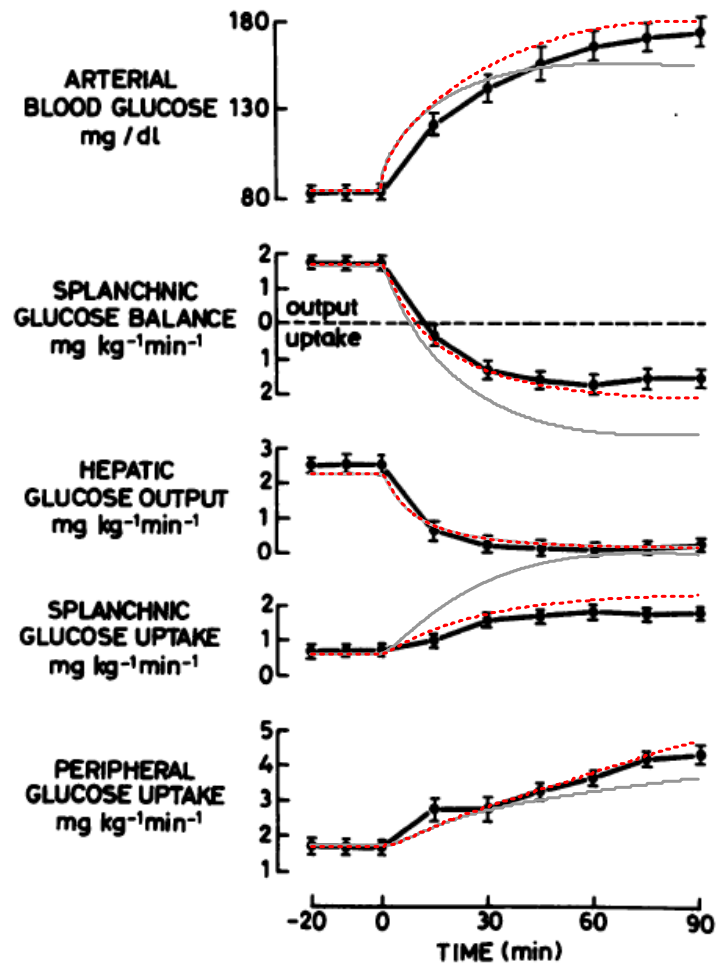


Figure 4.7: Model simulation (red dashed line) of a $6.5 \text{ mg kg}^{-1} \text{ min}^{-1}$ intravenous glucose infusion in normal man superimposed on plot of experimental data originally reported in [9] after adjustment of the function parameters of glucose-mediated hepatic glucose uptake (gray line represents the simulation data with original parameter values).

Increased circulating levels of glucagon, epinephrine and cortisol during stress profoundly alter glucose processing within the liver. The synergistic interactions of these hormones are responsible, at least in part, to an increase in endogenous glucose production that leads to stress-induced hyperglycemia. The infusion of either glucagon or epinephrine [8] causes a rapid but transient increase in endogenous glucose production while the infusion of cortisol [3] had no demonstrative effect on endogenous glucose

production. However, when combined, the infusion of these hormones produces a rapid and sustained increase in glucose production. Endogenous glucose production was 50 percent above basal levels despite concurrent hyperinsulinemia and hyperglycemia after 5 hours of a combined glucagon, epinephrine, and cortisol infusion [3]. Under similar conditions, Bessey et al. (1984) demonstrated that endogenous glucose production in subjects receiving the triple-hormone infusion remained elevated compared to controls after 72 hours (Table 4.7).

Table 4.7: The increase in endogenous glucose production (EGP) and circulating levels of glucagon, epinephrine, and cortisol after 5h [3] and 72h [4] of hormone infusion in healthy subjects

	Shamoon et al. (1981)	Bessey et al. (1984)
Number of Subjects	10	9
Hormone Infusion Rates		
Glucagon (ng kg ⁻¹ min ⁻¹)	3.0	3.0
Epinephrine (ng kg ⁻¹ min ⁻¹)	33 ^a	30
Cortisol (ug kg ⁻¹ min ⁻¹)	2.3 ^b	2.3
Basal Hormone Concentrations		
Glucagon (pg/ml)	90 ± 57	79 ± 42
Epinephrine (pg/ml)	28 ± 9	22 ± 15
Cortisol (ug/dl)	12 ± 3	12 ± 3
Hormone Concentrations During Triple-Hormone Infusion		
Glucagon (pg/ml)	313 ± 126	464 ± 165
Epinephrine (pg/ml)	377 ± 243	432 ± 339
Cortisol (ug/dl)	38 ± 9	38 ± 15
Endogenous Glucose Production (mg kg⁻¹ min⁻¹)		
Basal	1.8 ± 0.1	2.08 ± 0.05 ^c
Triple-Hormone Infusion	2.9 ± 0.3 ^d	2.55 ± 0.05 ^e
Percent Increase from Basal	61%	23%

^a infusion rate converted from 1.2 ug/m² min⁻¹ assuming 1.9 m² body surface area and 70 kg body weight

^b infusion rate converted from 5 mg/m² hr⁻¹ assuming 1.9 m² body surface area and 70 kg body weight

^c EGP determined in three control subjects after 72h saline infusion

^e EGP determined in three subjects after 72h of triple-hormone infusion

The relationship between stress hormones and endogenous glucose production has been documented in hospitalized patients. Dahn et al (1995) compared net hepatic output in healthy volunteers and hospitalized patients [221]. Patients were separated into two groups based on evidence of sepsis. They were studied in the postoperative intensive care unit 4-11 days after admission to the hospital. Volunteers were studied after an 18h fast. Glucagon levels in both patient groups were five-fold greater than those of the volunteers (507 ± 464 and 513 ± 423 vs. 93 ± 30 pg/ml) while plasma insulin and arterial glucose concentrations were similar in all subjects. Cortisol levels in the septic patients were also significantly elevated compared to non-septic patients and controls (34 ± 31 vs. 20 ± 7 and 15 ± 6 ug/dl). The net hepatic glucose output was significantly higher in septic patients (3.0 ± 1.0 mg/kg min⁻¹) when compared to volunteers (1.7 ± 0.5 mg/kg min⁻¹) and non-septic patients (1.9 ± 0.6 mg/kg min⁻¹). The concentrations of glucagon and cortisol hospitalized patients are comparable to those reported in the triple-hormone infusion studies discussed above. Associated with significant increases in cortisol levels and endogenous glucose production, septic patients are at greater risk for hyperglycemia.

Wilmore et al. (1980) also confirmed an association between sepsis and increased endogenous glucose production [222]. Nineteen burn patients (mean burn size: 51% total body surface, range 41-83.5%) were studied approximately 10 days post-injury. Patients were grouped as non-septic, septic and septic with complications. Catheterizations of the right hepatic vein were performed to study the metabolic response of the liver to injury. At the time of study, cardiac output for all patients was near maximal, doubling hepatic blood flow. Hepatic glucose production in the non-septic patients was elevated (2.9 ± 0.4 mg/kg min⁻¹). It was significantly greater in uncomplicated septic patients (4.1 ± 0.7

mg/kg min⁻¹) compared to non-septic patients while septic patients experiencing complications (*e.g.*, renal insufficiency) had normal hepatic glucose production (1.6 ± 0.5 mg/dl). Complicated sepsis was associated with an absolute mortality rate. Whether this return to baseline hepatic glucose production is a result of a decrease in the levels of stress hormones or a product of end-organ failure was not investigated.

CHAPTER 5. MODELING STRESS-INDUCED HYPERGLYCEMIA

The stress response is characterized by increased levels of circulating epinephrine, cortisol, growth hormone, and glucagon which lead to increased insulin resistance and increased endogenous glucose production. The imbalance in glucose flux created by increases in insulin resistance and endogenous glucose production often leads to hyperglycemia.

Simultaneous exogenous infusions of epinephrine, cortisol and glucagon have been shown to mimic the metabolic response to injury [4]. The concerted elevations in circulating levels of glucagon, epinephrine and cortisol during stress have profound effects on the processes that regulate glycemia. Collectively, these hormones suppress insulin release, decrease glucose disposal and increase glucose production. This chapter describes the kinetics and dynamics of epinephrine in the compartmental framework of the glucose metabolism model.

The terms *endogenous glucose production* and *hepatic glucose production* are used interchangeably in this chapter.

5.1. Epinephrine Kinetics

Epinephrine is synthesized from norepinephrine in the cytosol of adrenergic neurons and cells of the adrenal medulla. The majority, if not all, of circulating epinephrine originates from the cells found in the adrenal glands. However, under the extreme stress of cardiac arrest, significant epinephrine release from the heart, lungs, gut and liver has been demonstrated [223, 224].

Epinephrine release is controlled by the sympathetic nervous system acting via splanchnic nerves to the adrenal medulla. Acetylcholine released by preganglionic sympathetic fibers of these nerves acts on nicotinic acetylcholine receptors, causing cell depolarization and an influx of calcium through voltage-gated calcium channels. Calcium triggers the exocytosis of chromaffin granules and thus the release of epinephrine (and norepinephrine) into the bloodstream. The average release of epinephrine in man at rest has been measured in several studies (Table 5.1). The majority of these studies have employed radiolabeled epinephrine infused intravenously at very low rates in order to avoid the pharmacodynamic effects of elevated epinephrine levels [36, 223, 224]. In an extensive study of regional epinephrine kinetics, Eisenhofer et al. (1995) determined that 91% of circulating epinephrine originates from the adrenal glands while the gut, liver and kidneys had modest contributions of 3.1, 2.9 and 2.1 percent, respectively [224].

Table 5.1: Average (\pm SD) release rate and clearance of epinephrine in man at rest reported in the literature (n, number of subjects; ND, not determined).

n	Release Rate (ng/min)	Clearance (l/min)	Reference
95 ^a	197	ND	[224]
23	187 \pm 115	3.64 \pm 0.91	[223]
8	303 \pm 108	3.10 \pm 0.75	[36]
6	516 \pm 341	9.41 \pm 3.36	[24] ^b

^a 8 of the 95 subjects were surgical patients

^b kinetics were determined with intravenous infusions of unlabelled epinephrine at 0.01, 0.03, 0.05, 0.075 and 0.10 μ g/kg/ per min

Blood supplying the adrenal glands drains via the suprarenal veins: the right suprarenal vein drains into the inferior vena cava and the left suprarenal vein drains into the left renal vein or the left inferior phrenic vein which drains into the inferior vena cava. Upon entering systemic circulation, epinephrine is rapidly distributed through the extracellular

space. The liver, kidneys, and skeletal muscle are the primary sites responsible for clearing epinephrine from systemic circulation. The concentration of epinephrine in arterial blood is significantly greater than peripheral venous concentrations (Figure 5.1).

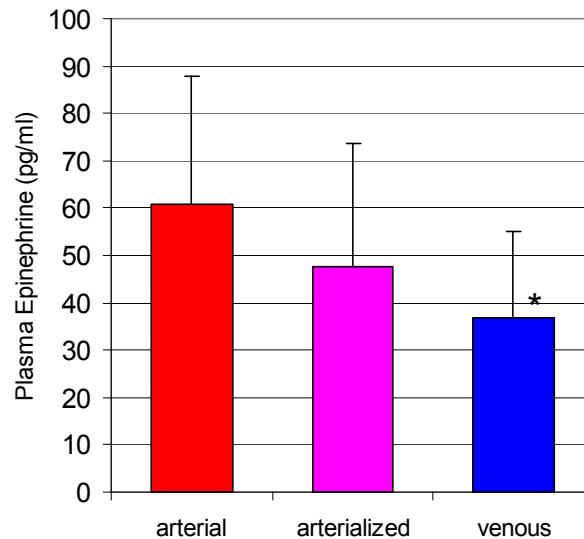


Figure 5.1: Average (\pm SD) plasma epinephrine concentrations in arterial, arterialized venous, and venous blood as reported in [3, 5, 10-33] (* $p < 0.005$ versus arterial)

The extraction of epinephrine is determined by measuring its concentration in the arterial blood supplying, and venous blood draining, the tissue. The exogenous administration of radiolabeled epinephrine is typically used to differentiate a tissue's extraction of circulating epinephrine from its release. Studies measuring the extraction of plasma epinephrine by the tissue compartments (brain, periphery, lungs, kidneys, gut, and liver) used in the glucose metabolism are summarized in Table 5.2.

Table 5.2: Fractional extraction of epinephrine for specific regions reported in the literature

Brain	Periphery^a	Lungs	Kidneys	Gut	Liver	Reference
	0.79	0.02	0.62	0.37	0.87	[224]
			0.45	0.83 ^b		[22]
			0.50	0.88 ^b		[225]
				0.90 ^b		[226]
			0.46			[20]
	0.70					[10]
	0.49					[29]
	0.75					[21]
	0.44					[23]
	0.46					[227]
	0.36					[11]
	0.39					[13]
		0				[228]
		0				[229]
0 ^c						[230, 231]
<i>0.00</i>	<i>0.55</i>	<i>0.00</i>	<i>0.51</i>	<i>0.37</i>	<i>0.87</i>	

^a periphery extraction extrapolated from appendicular studies

^b extraction reported for splanchnic region (liver and gut combined)

^c extraction inferred from reported animal studies

Epinephrine does not diffuse across the blood-brain barrier [230, 231]. The majority of epinephrine is cleared from the extracellular fluid by extraneuronal cells. These cells take up epinephrine and metabolize it via beta-adrenergic receptors [232]. Beta-adrenergic receptors have been found on a variety of blood cells (erythrocytes, lymphocytes and granulocytes) [233-235]. Epinephrine is stored in platelets with intracellular concentrations that are 500-fold higher than those found in erythrocytes or in plasma [17]. In dogs, epinephrine concentrations in whole blood were stable several hours after the samples were obtained which suggests that epinephrine is not metabolized to a significant amount by any constituent of blood [236].

Epinephrine is inactivated by O-methylation and sulfoconjugation. Catechol-O-methyl transferase (COMT) inactivates catecholamines by O-methylation [22]. This

extraneuronal enzyme is most abundant in liver and kidney [237]. Phenolsulfotransferase (PST) is the enzyme responsible for sulfoconjugation [238]. PST activity has been found in liver, kidney, intestine, brain, skeletal muscle, platelets and erythrocytes. In a study of eight normal subjects, the average free epinephrine level was 46% lower in venous than in arterial blood while average sulfated epinephrine level was 37% higher, suggesting that epinephrine sulfoconjugation occurs within the muscle of the forearm [227].

5.2. Epinephrine Pharmacodynamics

Epinephrine exerts control over several mechanisms which determine how glucose is handled within the body. Epinephrine displays a transient stimulatory effect on hepatic glucose production. It directly antagonizes the actions of insulin. The uptake of glucose by splanchnic and peripheral tissues is inhibited by epinephrine. These effects are amplified by synergistic interactions with other stress hormones.

5.2.1. Insulin Release

Epinephrine attenuates insulin secretion via an alpha-adrenergic mechanism [239-242]. Epinephrine (infused at 6 ug/min) abolished the first phase, and attenuated the second phase, of insulin secretion in response to a 5g intravenous glucose challenge [243]. Glucose clamp studies performed in eight male subjects demonstrated that epinephrine inhibits the first phase insulin response to 5g intravenous arginine in a dose-dependent manner [5]. When average glucose levels were raised (without exogenously infused epinephrine) to 156 mg/dl and 242 mg/dl using an intravenous glucose infusion, the peak first phase insulin response increased two- and four-fold, respectively, compared to the peak response of 77 ± 37 mU/l during euglycemia. Intravenous infusions of epinephrine at 1.05 and 5.60 ug/min progressively decreased the peak first phase insulin response

independent of glycemia (Table 5.3). Similarly, Morrow et al (1993) observed a progressive decrease in the first phase insulin response to an intravenous tolbutamide bolus (125-150 mg/m²) when epinephrine levels were increase via a constant intravenous infusion (at rates of 0.5, 1.0 and 2.0 ug/min) that was independent of age [244]. Clutter et al (1980) observed that plasma insulin levels doubled and quadrupled 15 minutes after the cessation of 2.5 and 5.0 ug/min epinephrine infusions, respectively, in response to plasma glucose levels 40 and 70 mg/dl above basal [103]. Combining the results from [5, 103, 243], the suppression of insulin release displays a dose-dependent response to epinephrine (Figure 5.2).

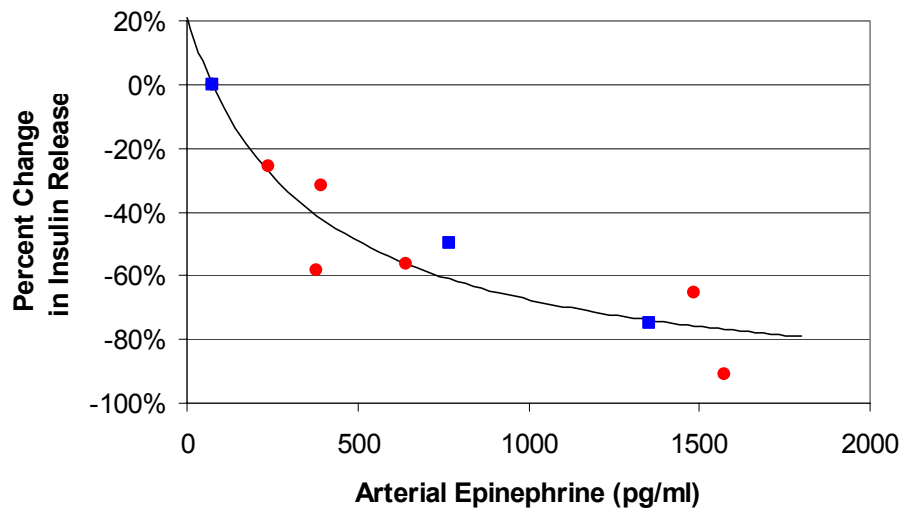


Figure 5.2: Percent decrease in first phase (red circles) and second phase (blue squares) insulin release as a function of arterial epinephrine concentration. The solid line represent the best fit of all data points to the equation $\Delta IR = V_{max}(x-1)/(K_m + x-1)$ where V_{max} and K_m are constants and x is the arterial epinephrine concentration divided by the basal arterial epinephrine concentration.

Table 5.3: Peak first-phase insulin response to a 5g intravenous arginine bolus at different plasma glucose (100, 150 and 250 mg/dl) and epinephrine concentrations [5].

Epinephrine Infusion (ug/min)	Venous Epinephrine (pg/ml)	Peak Insulin Response (mU/ml)		
		100 mg/dl	150 mg/dl	250 mg/dl
0.00	47 ± 20	77 ± 37	232 ± 99	388 ± 122
1.05	192 ± 54	49 ± 17	138 ± 48	319 ± 96
5.60	1140 ± 342	-	59 ± 31	170 ± 74

The fractional decrease in insulin release (ΔIR) as a function of arterial epinephrine concentrations was fit to the Michaelis-Menten equation

$$\Delta IR = \frac{V_{\max}(x-1)}{K_m + (x-1)} \quad 5.1$$

where x is the arterial epinephrine concentration divided by the basal arterial epinephrine concentration and V_{\max} and K_m are coefficients. The best fit (in a least-squares sense) between equation 5.1 and the published data from [5, 103, 243] was achieved with coefficient values -0.99 and 5.71 for V_{\max} and K_m , respectively ($R^2 = 0.9029$). A logarithmic relationship (i.e., $\Delta IR = A + B \log_{10}(x)$ where A and B are coefficients) originally proposed in [5] produces a similar fit ($R^2 = 0.9084$). However, equation 5.1 is preferred because its behavior is bounded at physiologically low epinephrine concentrations (for which no data exists) whereas the logarithm relationship increases to infinity when arterial epinephrine concentrations approach zero.

Conclusive evidence demonstrating a lag between a change in epinephrine concentration and its subsequent effect on pancreatic insulin release is not available. The two published studies that measured the effect of epinephrine on the first (acute) phase of insulin release [5, 243] began intravenous epinephrine infusions 45 to 60 minutes before administering

the insulin stimulus (either glucose or arginine). Clutter et al (1980) observed an increase in plasma insulin levels 15 minutes after the cessation of intravenous epinephrine [103]. If any lag exists between the pharmacological action of epinephrine upon insulin release, it is on the order of seconds to minutes. For modeling purposes, it will be assumed that no lag exists.

5.2.2. Endogenous Glucose Production

The ability of epinephrine to increase endogenous glucose production has been demonstrated. Epinephrine binds to beta adrenergic receptors in the liver to stimulate endogenous glucose production [15]. Direct stimulation increases the hepatic glucose output primarily through an increase in glycogenolysis [108]. In addition, epinephrine indirectly increases endogenous glucose production by increasing the abundance of gluconeogenic substrates (*e.g.*, alanine, lactate, and glycerol) [108, 109, 245].

Attempts to relate changes in endogenous glucose production to epinephrine per se are confounded by its complex interactions between glucose and other hormones. The work of Guy et al. (2005) illustrates this problem. Performing a hyperinsulinemic (1.3 mU/kg/min) euglycemic clamp with and without the concomitant infusion of epinephrine (0.06 ug/kg/min), insulin and glucose concentrations were fixed with a constant infusion of insulin and a variable infusion of glucose. The epinephrine infusion caused an eight-fold increase in endogenous glucose production as measured at the end of the two-hour experiment (1.51 ± 0.97 vs. 0.19 ± 0.42 mg/kg per min). However, the epinephrine infusion also altered circulating levels of glucagon and cortisol – final concentrations were increased compared to experiments without concomitant infusion of epinephrine in

nondiabetic subjects [16]. Since glucagon is a potent simulator of hepatic glycogenolysis, the increase in glucose production cannot be attributed solely to epinephrine.

Rizza et al. (1979) reported a transient increase in endogenous glucose production when epinephrine was infused over three hours (50 ng/kg per min) with a concomitant infusion of somatostatin [6]. Glucose appearance peaked 30 minutes after the start of the epinephrine infusion. It reached a maximum value of 3.8 ± 0.5 mg/kg per min from a baseline value of 1.7 ± 0.2 mg/kg per min to. Since glycemia was not clamped, venous plasma glucose concentrations rose from 89 ± 3 mg/dl at baseline to 217 ± 37 mg/dl at the end of the epinephrine infusion. As described by the model herewith in, the rise in glucose levels observed in these experiments alone would decrease glucose-mediated control of hepatic glucose (*i.e.*, M_{HGP}^G) production by 77 percent at the conclusion of the experiments. In addition, there was an incremental increase in plasma insulin concentrations from an average basal concentration of 8 mU/l to 11.5 mU/l and glucagon concentration fell 37 percent from their basal values. These conditions (*i.e.*, an increase in plasma glucose, an increase in plasma insulin and a decrease in plasma glucagon) will suppress endogenous glucose production. However, endogenous glucose production was at least 50 percent above basal for all measurements taken during the three-hour epinephrine infusion – demonstrating epinephrine’s ability to stimulate glucose release from the liver.

Definitive studies of epinephrine’s effect on endogenous glucose production do not exist. The confounding effect of glucose, insulin and glucagon has not been adequately controlled in the few reported studies. In order to determine a functional relationship

between epinephrine and hepatic glucose production, certain assumptions were adopted to analyze the available data. Epinephrine was assumed to independently modify the hepatic glucose production through $M_{\text{HGP}}^{\text{E}}$ in equation 5.2

$$r_{\text{HGP}} = r_{\text{HGP}}^{\text{B}} M_{\text{HGP}}^{\text{G}} M_{\text{HGP}}^{\text{I}} M_{\text{HGP}}^{\text{\Gamma}} M_{\text{HGP}}^{\text{E}} \quad 5.2$$

where r_{HGP} is the rate of hepatic glucose production, $r_{\text{HGP}}^{\text{B}}$ is the basal rate of hepatic glucose production, and $M_{\text{HGP}}^{\text{G}}$, $M_{\text{HGP}}^{\text{I}}$, and $M_{\text{HGP}}^{\text{\Gamma}}$ are determined from the reported glucose, insulin and glucagon concentrations using equations 5.3, 5.4 and 5.5 (which are modified versions of the auxiliary equations presented in chapter 4).

$$M_{\text{HGP}}^{\text{G}} = 1.42 - 1.41 \tanh[0.62(G^{\text{N}} - 0.497)] \quad 5.3$$

$$M_{\text{HGP}}^{\text{I}} = \left(1 - e^{-\frac{t}{\tau_1}}\right) \left(1.21 - 1.14 \tanh[1.66(I^{\text{N}} - 0.89)]\right) \quad 5.4$$

$$M_{\text{HGP}}^{\text{\Gamma}} = \left(1 - e^{-\frac{t}{\tau_{\Gamma}}}\right) 2.7 \tanh[0.39\Gamma^{\text{N}}] \quad 5.5$$

In equations above, G^{N} , I^{N} and Γ^{N} are glucose, insulin, and glucagon concentrations divided by their respective basal values as reported. The time constants, τ_1 and τ_{Γ} , are 25 and 65 min, respectively, as defined in [187] and $t = 0$ is defined as the start of the epinephrine infusion. Therefore, $M_{\text{HGP}}^{\text{E}}$ can be determined using available data using the equation:

$$M_{\text{HGP}}^{\text{E}} = \frac{\Gamma_{\text{HGP}}^{\text{N}}}{M_{\text{HGP}}^{\text{G}} M_{\text{HGP}}^{\text{I}} M_{\text{HGP}}^{\text{\Gamma}}} \quad 5.6$$

where $r_{\text{HGP}}^{\text{N}}$ is the normalized rate of hepatic glucose production reported in the study and all other variables have been described above.

Data from Rizza et al (1979), Deibert et al (1980) and Shamoon et al (1980, 1981) were used to investigate epinephrine's effect on hepatic glucose production. The first two studies infused somatostatin to suppress endogenous insulin and glucagon secretion and infused epinephrine at the same rate (~ 3.5 ug/min). In addition, Deibert et al performed a euglycemic hyperinsulinemic clamp and replaced glucagon to achieve physiological concentrations of the hormone. In contrast, Shamoon et al did not infuse somatostatin while infusing epinephrine at a lower rate (~ 2.3 ug/min) over five hours. More recently, Guy et al (2005) also published a study investigating the effect of epinephrine on endogenous glucose production. However, this report was excluded from the analyses because it lacked a basal measure of hepatic glucose production and did not have serial measurements throughout the two-hour epinephrine infusion.

Table 5.4 summarizes the calculations involved in the determination of $M_{\text{HGP}}^{\text{E}}$. Although plasma levels of glucagon (in the data from Rizza et al) and insulin (in the data from Deibert et al) were reasonably constant throughout the experiment, their effects on r_{HGP} (as measured by $M_{\text{HGP}}^{\text{I}}$ and $M_{\text{HGP}}^{\text{G}}$) were not. As modeled, both glucagon and insulin have first-order dynamics that do not equilibrate during the experiments. For the data from Rizza et al, the need to account for glucagon dynamics was in addition to adjustments for increasing glycemia. In ideal conditions, these confounding variables would be held constant in order to study the effect of epinephrine on hepatic glucose production. The data from Shamoon et al needed to adjust for all three confounding

variables. However, the length of the epinephrine infusion (5 hours) was invaluable in terms of elucidating the time course of epinephrine's effect on the liver. In fact, if the data from Shamoon et al is excluded from the analysis, the evolution of $M_{\text{HGP}}^{\text{E}}$ during the constant epinephrine infusion would appear to grow unbounded (Figure 5.3). The transient influence of epinephrine on hepatic glucose appearance appears to dissipate after several hours.

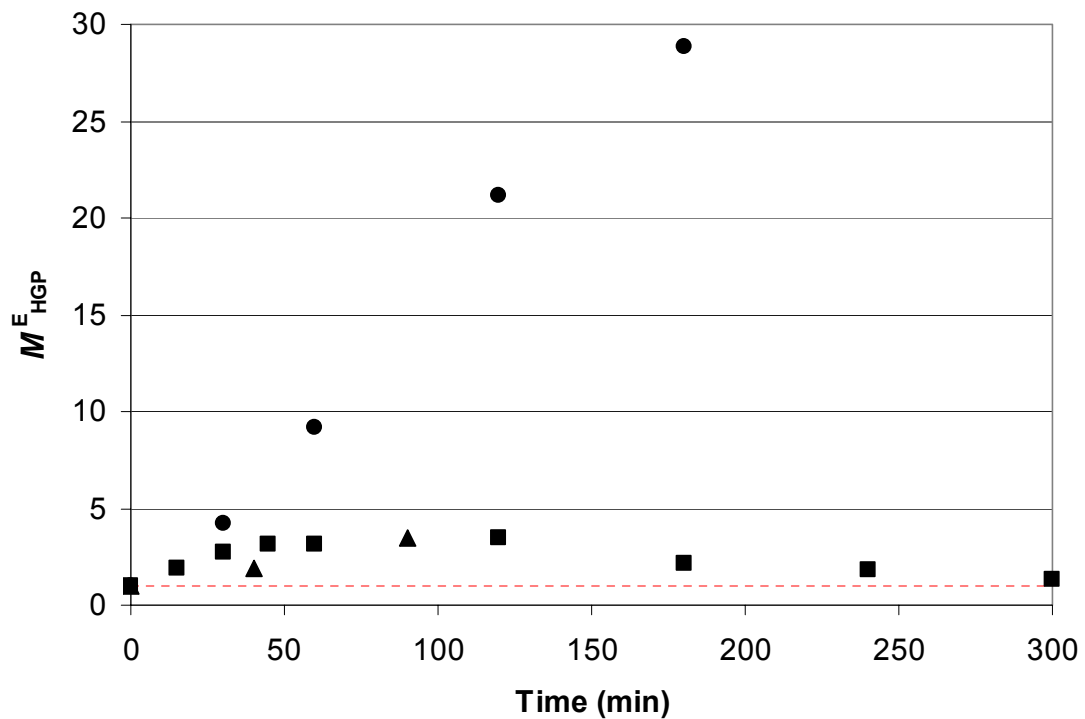


Figure 5.3: The time course of epinephrine-mediated hepatic glucose output in response to a constant intravenous epinephrine infusion as predicted from data from published by ●Rizza et al [6], ▲ Deibert [7] and ■ Shamoon [3, 8]. The red dashed line demarcates unity.

Table 5.4: Determination of the epinephrine modifier from data published by Rizza et al [6], Deibert [7] and Shamooun [3, 8].

	Rizza et al (1979)						Deibert et al (1980)						Shamooun et al (1980)								
Time* (min)	0	30	60	120	180		0	40	90				0	15	30	45	60	120	180	240	300
G (mg/dl)	84	120	170	211	217		86	88	88				91	107	119	126	126	126	121	117	115
I (mU/ml)	8	8.8	9.5	10.8	11.5		17	135	135				13.2	13.9	18.1	17.4	17.5	17.9	16.1	15	14.1
Γ (pg/ml)	128	86	78	78	75		69	74	74				75	86.4	96.6	85.9	95.9	70	77	80.7	83
E (pg/ml)	71	NA	850	875	941		25	736	736				24	NA	NA	NA	300	408	431	435	405
EGP (mg kg ⁻¹ min ⁻¹)	1.7	3.8	3.5	2.8	2.6		2.17	1.07	0.73				1.7	2.72	2.72	2.49	2.3	1.77	1.58	1.71	1.54
G^N	1.00	1.43	2.02	2.51	2.58		1.00	1.02	1.02				1.00	1.18	1.31	1.38	1.38	1.38	1.33	1.29	1.26
Γ^N	1.00	1.10	1.19	1.35	1.44		1.00	7.94	7.94				1.00	1.05	1.37	1.32	1.33	1.36	1.22	1.14	1.07
Γ^{-N}	1.00	0.67	0.61	0.61	0.59		1.00	1.07	1.07				1.00	1.15	1.29	1.15	1.28	0.93	1.03	1.08	1.11
r_{HGP}^N	1.00	2.24	2.06	1.65	1.53		1.00	0.49	0.34				1.00	1.60	1.60	1.46	1.35	1.04	0.93	1.01	0.91
M_{HGP}^G	0.99	0.69	0.38	0.22	0.21		0.99	0.98	0.98				0.99	0.86	0.77	0.71	0.71	0.71	0.75	0.78	0.80
M_{HGP}^I	1.00	0.89	0.79	0.69	0.64		1.00	1.03	1.03				1.00	0.96	0.73	0.63	0.57	0.48	0.63	0.76	0.87
M_{HGP}^F	1.00	0.88	0.75	0.50	0.40		1.00	0.26	0.10				1.00	1.03	1.05	1.03	1.05	0.87	0.92	0.95	0.96
M_{HGP}^E	1.00	4.18	9.19	21.12	28.85		1.01	1.90	3.51				1.01	1.89	2.72	3.16	3.14	3.51	2.15	1.81	1.36

* time (t = 0) is defined as the start of the epinephrine infusion; all measurements reported for t = 0 are basal values

A dose-dependent increase in $M_{\text{HGP}}^{\text{E}}$ is not evident from the three datasets analyzed. The estimates of $M_{\text{HGP}}^{\text{E}}$ from data of Rizza et al (1979) and Deibert et al (1980) differ greatly although the two studies use the same epinephrine infusion rate (Figure 5.3). Although no single human study has investigated the dose-dependent response of epinephrine, correlation between peak endogenous glucose production and plasma epinephrine concentrations has been demonstrated in pancreatic clamp experiments in dogs [109]. Here, the investigators used somatostatin to inhibit endogenous insulin and glucagon release and infused these hormones intraportally to achieve clamped physiological concentrations. However, glucose remained a confounding variable. In separate experiments, epinephrine was infused at a constant rate of 0.04, 0.16 or 0.23 $\mu\text{g}/\text{kg}$ per min over three hours. Arterial epinephrine levels reached plateau levels 447 ± 75 , $1,812 \pm 97$, and $2,495 \pm 428$ pg/ml , respectively. Endogenous glucose production increase 27, 67 and 132 percent above baseline 15 minutes after the start of the epinephrine infusion.

In order to derive a functional form for $M_{\text{HGP}}^{\text{E}}$, the data from Shamooin et al (1981) were used. In equation 5.7, $M_{\text{HGP}}^{\text{E}}$ is modeled as the difference of the two differential equations, f_1^{E} and f_2^{E} , if the difference is greater than or equal to one. The expression for $M_{\text{HGP}}^{\text{E}\infty}$ is arbitrary because there is insufficient data to establish a dose-dependent response of $M_{\text{HGP}}^{\text{E}}$ to epinephrine. Below the basal arterial epinephrine concentration, E_{H}^{B} , there is no epinephrine-mediated increase in hepatic glucose production, (*i.e.*, $M_{\text{HGP}}^{\text{E}\infty} = 1$) while $M_{\text{HGP}}^{\text{E}\infty}$ is modeled to increase in a linear fashion above E_{H}^{B} . The time

constants, τ_1^E and τ_2^E , were assigned values of 90 and 60 minutes, respectively. Figure

5.4 depicts the model's estimate of M_{HGP}^E .

$$M_{\text{HGP}}^E = \begin{cases} f_1^E - f_2^E, & f_1^E \geq f_2^E + 1 \\ 1, & \text{otherwise} \end{cases} \quad 5.7$$

$$\frac{d}{dt} f_1^E = \frac{1}{\tau_1^E} [M_{\text{HGP}}^{E\infty} - f_1^E] \quad 5.8$$

$$\frac{d}{dt} f_2^E = \frac{1}{\tau_2^E} [(f_1^E - 1) - f_2^E] \quad 5.9$$

$$M_{\text{HGP}}^{E\infty} = \begin{cases} 0.14 \frac{E_H}{E_H^B} + 0.86, & \frac{E_H}{E_H^B} \geq 1 \\ 1, & \text{otherwise} \end{cases} \quad 5.10$$

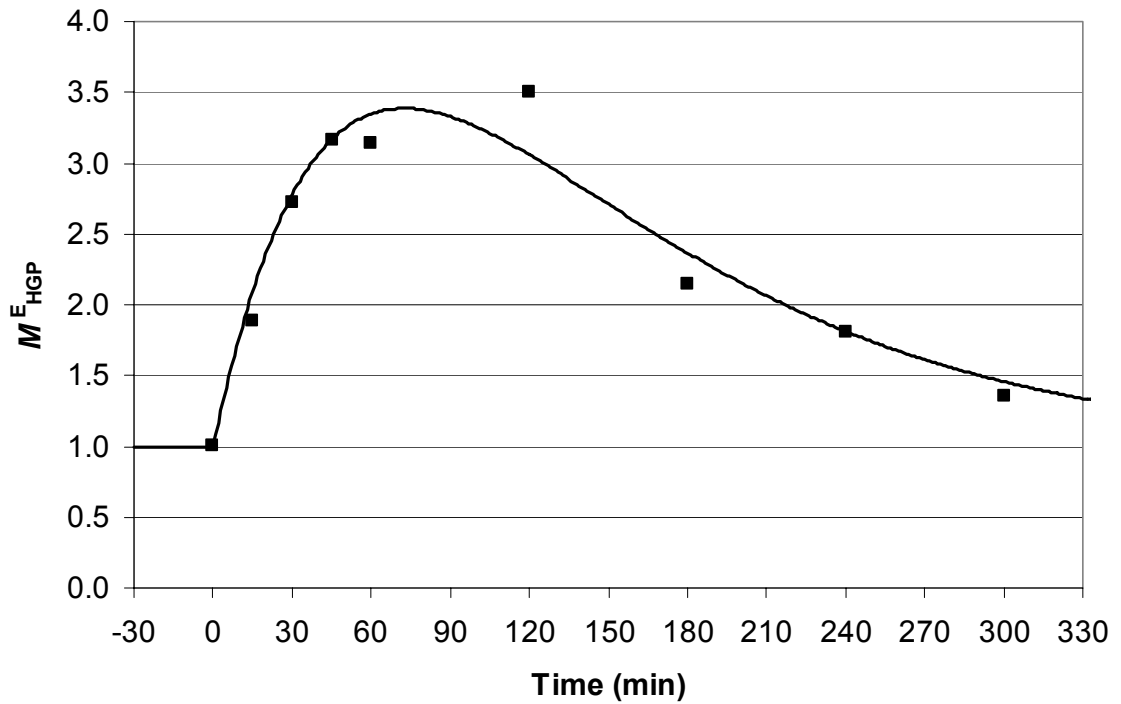


Figure 5.4: A model of the time course of epinephrine-mediated hepatic glucose output (solid line) compared to the experimental data (■) from published by Shamoon [3, 8].

5.2.3. Glucose Uptake

A physiological increase in epinephrine will decrease insulin-mediated glucose uptake by insulin-sensitive tissues [246]. Using an euglycemic insulin clamp technique, Deibert et al (1980) demonstrated a time-dependent reduction in whole body glucose utilization when epinephrine levels are increased [7]. Compared with the insulin infusion alone (~5U/hr), whole body glucose utilization declined 7 percent 0-20 minutes, 43 percent 20-40 minutes and 53 percent 60-120 minutes from the start of the concomitant infusion of epinephrine (3.5 ug/min).

5.2.3.1. Peripheral Glucose Uptake

A functional description of a dose-dependent effect of epinephrine on peripheral glucose uptake is sought. However, this description is complicated by epinephrine's complex interaction with the sigmoidal relationship between insulin and peripheral glucose uptake. As described in the previous chapter, the nonlinear relationship between insulin and peripheral glucose uptake can be adequately described by either the hyperbolic tangent equation or logistics equation. Laakso et al (1992) demonstrated that a physiological increase in circulating epinephrine will right shift the curve describing insulin-mediated peripheral glucose uptake (*i.e.*, it will significantly increase K_{50} in equation 5.3) whereas no significant changes were observed in the minimal and maximal responses (*i.e.*, V_{\min} and V_{\max} are not altered in equation 5.3) [201]. However, the marked reduction of peripheral glucose uptake observed at basal insulin concentrations (see [247]) contradicts the hypothesis that epinephrine's effect on peripheral insulin-mediated glucose uptake can be described by a right-shift in the insulin-mediated peripheral glucose curve alone.

Many published studies that investigated epinephrine's effect on peripheral glucose uptake failed to clamp insulin and glucose (*e.g.*, [32]), making it impossible to associate the change in glucose uptake with the increase in epinephrine concentration. Table 5.5 summarizes a handful of studies in man that clamped insulin and glucose levels and measured peripheral glucose uptake with and without concomitant epinephrine infusions. Whereas Laakso et al (1992) and Bessey et al (1983) used systemic intravenous infusions of insulin (at a constant rate) and glucose (at a variable rate) to achieve euglycemic hyperinsulinemic conditions [201, 248], Fryburg et al (1995) and Capaldo et al (1992) infused epinephrine (and insulin) directly into the brachial artery to raise forearm concentrations while maintaining basal concentrations of epinephrine, glucose and insulin throughout the rest of the body [247, 249]. Peripheral glucose uptake was reduced between 16 and 85 percent compared to experiments without a concomitant infusion of epinephrine. Epinephrine infusion rates were similar in the four experiments. The reduction in glucose uptake does not display a strong dose-dependency within this range of epinephrine concentrations (except for the data collected by Laakso et al (1992) under supra-physiological insulin concentrations). A systemic study that quantifies peripheral glucose uptake at different epinephrine and insulin concentrations is required to fully reveal the functional relationship between epinephrine and peripheral insulin-mediated glucose uptake.

Table 5.5: Summary of published euglycemic insulin clamp studies in man that report on the effect of epinephrine on peripheral glucose uptake

E_H (pg/ml)	I_{PI} (mU/l) ^a	G_H (mg/dl)	r_{PGU} (mg/min per 100ml)	$\frac{r_{PGU} _{\text{elevated } E_H}}{r_{PGU} _{\text{basal } E_H}}$	Reference
46	1114	81 ± 9	1.572	0.84	Laakso et al 1992
349	1865	81 ± 4	1.316		
48	32	79 ± 9	1.075	0.31	Laakso et al 1992
418	38	81 ± 4	0.332		
60 ^b	38	93 ± 3	0.660	0.27	Bessey et al 1983
643 ^c	34	99 ± 5	0.18		
60 ^b	33	79 ± 7	0.480	0.15	Capaldo et al 1992
660 ^d	26	79 ± 7	0.070		
60 ^b	4	83 ± 2	0.026	0.38	Fryburg et al 1995
935 ^d	4	85 ± 2	0.010		

^a estimated from reported arterial or venous insulin concentrations

^b no basal value reported - assumed to be the mean value of published basal epinephrine concentrations reported on herewith in.

^c estimated from reported systemic epinephrine infusion rate

^d estimated from reported peripheral venous epinephrine concentrations

^e glucose uptake reported in mg/min per leg (assumed a muscle weight per leg of 10kg in adult men and a muscle density of 0.106 kg/100ml)

Epinephrine may reduce the magnitude and right-shifts curve describing peripheral insulin-mediated glucose uptake. However, available data cannot adequately quantify this complex interaction. Therefore, it has been assumed that the rate of peripheral glucose uptake (r_{PGU}) is the product of a basal rate and separable epinephrine-, insulin- and glucose-dependent modifiers:

$$r_{PGU} = r_{PGU}^B M_{PGU}^G M_{PGU}^I M_{PGU}^E \quad 5.11$$

where the constant, r_{PGU}^B , and the functions, M_{PGU}^G and M_{PGU}^I , have been defined

previously. A hyperbolic expression was chosen for the epinephrine-dependent modifier,

M_{PGU}^E , to be consistent with other modifiers in the model.

$$M_{PGU}^E = \frac{1}{2} \left((V_{max} + V_{min}) + (V_{max} - V_{min}) \tanh \left(m \left(\frac{E_H}{E_H^B} - K_{50} \right) \right) \right). \quad 5.12$$

where E_H is the arterial epinephrine concentration, E_H^B is the basal epinephrine concentration; the parameters, V_{min} and V_{max} , determine the value of M_{PGU}^E as E_H approaches negative and positive infinity, respectively; the slope factor, m , determines the rate at which M_{PGU}^E transitions between V_{min} and V_{max} ; and K_{50} is the normalized epinephrine concentration where $M_{PGU}^E = \frac{1}{2}(V_{min} + V_{max})$. Figure 5.5 plots M_{PGU}^E ($E_H^B = 60$ pg/ml, $V_{min} = 1$, $V_{max} = 0.3$, $m = 1.5$, and $K_{50} = 6$) against the available data (first and fifth columns of Table 5.5).

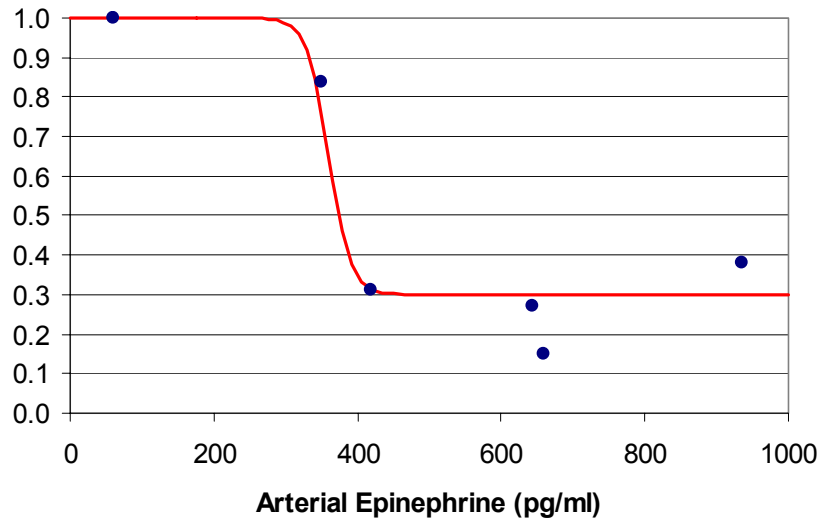


Figure 5.5: The epinephrine-dependent peripheral glucose uptake modifier. Blue circles represent the pooled clinical data from [201, 247-249] as shown in Table 5.5 and the red line represents equation 5.12 with $E_H^B = 60$ pg/ml, $V_{min} = 1$, $V_{max} = 0.3$, $m = 1.5$, and $K_{50} = 6$.

5.2.4. Blood Flow

Epinephrine increases blood flow to specific tissues in a dose-dependent manner by reducing vascular resistance and increasing in cardiac output [26, 28, 250]. The epinephrine-induced increase in cardiac output is due to an increase in both the frequency of contractions (heart rate) and the volume of blood pushed out of the heart per contraction (stroke volume) [24, 26, 28]. Cardiac output increases instantaneously (within one minute of the start of a intravenous infusion of epinephrine) [250] while cardiac responsiveness to epinephrine generally decreases with age [34]. Figure 5.6 summarizes observations from four published studies that investigated the effect of an intravenous epinephrine infusion on cardiac output. The fractional increase in cardiac output (ΔCO) as a function of arterial epinephrine concentrations was fit to the Michaelis-Menten equation

$$\Delta\text{CO} = \frac{V_{\max}(x-1)}{K_m + (x-1)} \quad 5.13$$

where x is the arterial epinephrine concentration divided by the basal arterial epinephrine concentration and V_{\max} and K_m are coefficients. The coefficient values for the four published studies are given in Table 5.6.

When epinephrine concentrations are elevated, blood flow to the splanchnic region (gut and liver) increases significantly via a beta-adrenergic mechanism [22]. Measured 10, 20 and 30 minutes into a 30-minute epinephrine infusion (0.10 ug/kg per min), hepatic blood flow increased 30 to 190 percent (average baseline hepatic blood flow rate 1.48 l/min) [251]. The infusion of exogenous epinephrine induces a dose-dependent increase in blood flow of the superior mesenteric artery and a selective decrease in superior mesenteric

artery resistance within 5 minutes of commencement [31]. These effects were observed before steady-state plasma levels of epinephrine were achieved and flow returned to baseline within 5 minutes of discontinuing the infusion.

Table 5.6: Coefficient values (V_{\max} and K_m) and goodness-of-fit for each published dataset and the average coefficient values. Fractional increase in cardiac output (ΔCO) and arterial epinephrine concentrations were fit to the equation $\Delta CO = V_{\max}(x-1)/(K_m + x-1)$ where V_{\max} and K_m are constants and x is the arterial epinephrine concentration divided by the basal arterial epinephrine concentration. Italicized coefficient values represent the values averaged from the four published studies.

V_{\max}	K_m	R^2	Reference
0.96	9.60	0.99698	[26]
1.01	8.55	0.99997	[28]
1.19	32.78	0.99733	[34]
1.07	27.91	0.96957	[35]
<i>1.06</i>	<i>19.71</i>	0.85935	

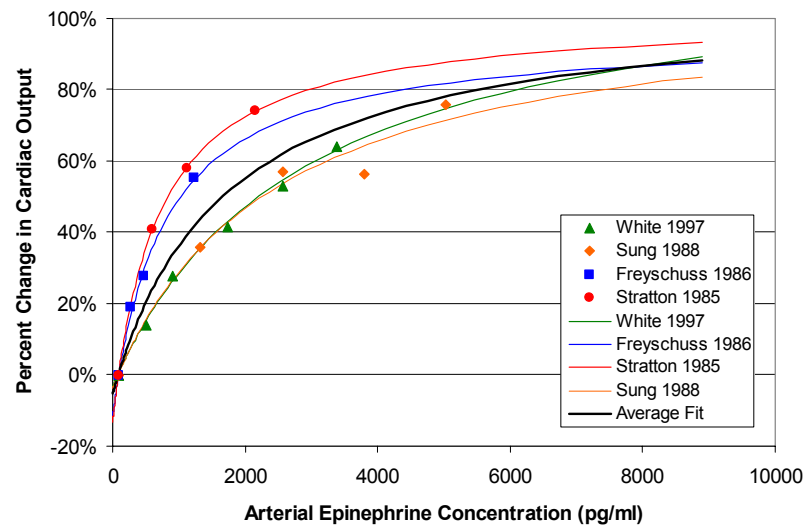


Figure 5.6: Percent change in cardiac output (l/min) as a function of arterial epinephrine concentration. The points represent data reported in [26, 28, 34, 35] and the lines represent the best fit to the equation $\Delta CO = V_{\max}(x-1)/(K_m + x-1)$ where V_{\max} and K_m are constants and x is the arterial epinephrine concentration divided by the basal arterial epinephrine concentration.

In contrast, renal blood flow did not significantly increase when plasma epinephrine concentrations were increased [22]. Stumvoll et al (1995) did not observed any significant increase in renal blood flow from baseline values (average renal blood flow rate 1.47 l/min at baseline and 1.58 l/min during the final 30 minutes of a 50 ng/kg per min intravenous epinephrine infusion) [252]. Similarly, a graded infusion of epinephrine that increased arterial epinephrine concentrations from 45 ± 38 pg/ml to 1177 ± 171 pg/ml in 12 male subjects did not have any noticeable impact on renal vascular resistance or blood flow [20].

Epinephrine increases blood flow to skeletal muscle and adipose tissue [26, 29, 253]. However, supraphysiological doses of epinephrine have caused vasoconstriction and decreased peripheral blood flow [254].

Epinephrine increases cerebral blood flow via a beta-adrenergic mechanism [255] but the data necessary to quantify this increase in man is not available. The ramped infusion of epinephrine in sheep (0-40 ug/min) significantly increased cerebral blood flow [256]. The intravenous infusion of epinephrine in rats (8 ug/kg/min) increased cerebral blood flow three-fold [257]. Both animal studies infused extreme quantities of epinephrine to observe the increase in cerebral blood flow.

5.2.5. Glucagon Release

The ability of epinephrine to promote glucagon release *in vivo* appears to be secondary to its abilities to enhance endogenous glucose production and inhibit insulin release. No significant changes to venous glucagon levels were observed during five separate 60-minute intravenous epinephrine infusions at 0.1, 0.5, 1.0, 2.5 and 5.0 ug/min in six healthy subjects (which produced circulating venous epinephrine concentrations of $54 \pm$

30, 114 ± 28 , 219 ± 83 , 412 ± 89 and 715 ± 228 pg/ml) [103]. However, resultant hyperglycemia observed at the two highest epinephrine infusion rates could have contributed to an inhibition of glucagon. Rizza et al (1979) observe a transient, yet significant, increase in venous glucagon concentrations that lasted 60 minutes after the start of an intravenous epinephrine infusion at 50ng/kg per min (~ 3.5 ug/min) [6]. However, this minor transient increase (50% above basal for 60 minutes) does not account for substantial increase in glucagon levels (300% increase over several hours or days) that can be encountered in severely stressed patients in the hospital.

5.3. Models of Epinephrine Kinetics

An accurate mathematical description of epinephrine kinetics is sought to integrate with the existing glucose metabolism model. Three kinetics models are described: a two-compartment model originally described by Rosen et al (1989), a six-compartment model with the same compartmental structure as the glucose metabolism model, and the same six-compartment model with a description of the hemodynamic changes that occur with changes in epinephrine concentrations. The ability of each model to estimate steady-state and transient epinephrine concentrations is assessed.

5.3.1. Two-compartment Model

A two-compartment model is necessary to accurately estimate arterial epinephrine kinetics [36]. Rosen et al (1989) published the parameters to a model in which sampling, endogenous epinephrine release (r_{AER}) and irreversible epinephrine loss (L_{01}) occurred from the same compartment (Figure 5.7). The distribution volume of this compartment (V_1) corresponds to the intravascular volume.

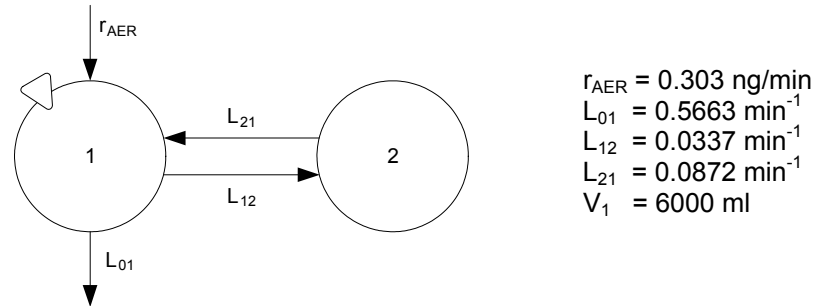


Figure 5.7: Two-compartment model of epinephrine kinetics adapted from [36].

5.3.2. Six-compartment Model

A descriptive model was developed in which each of the six compartments has a direct physiological interpretation representing either an organ or vascular space (Figure 5.8).

Irreversible loss of epinephrine occurs in the liver, kidneys, gut and peripheral tissues.

Endogenous epinephrine is released into the central venous blood supply from the adrenal glands. It travels through the heart and lungs without loss and then is distributed to the various organs.

The system of six differential equations describing epinephrine kinetics is given in Table 5.7 along with auxiliary equations. Parameter values are provided in Table 5.8. Here, r_{AER} and RE denote the rates of endogenous and exogenous epinephrine appearance and E_j , Q_j^E , V_j^E and r_{jEC} with $j = \{B, H, L, G, K, P, A\}$ denote organ epinephrine concentrations (pg/ml), volumetric flow rates (ml/min), distribution volumes (ml) and clearance rates (pg/min), respectively. The subscript j represents the compartment: brain (B), heart and lungs (H), liver (L), gut (G), kidneys (K), periphery (P), and hepatic artery (A). WCP and E_H^B represent the fraction of water in blood (water content percentage) and basal arterial epinephrine concentration. The epinephrine subsystem was formulated with and without a description of the hemodynamic changes that are associated with epinephrine.

Hemodynamic compensation is controlled through the epinephrine flow rate modifier, M_Q^E . With $M_Q^E = 1$, the system does not have hemodynamic compensation. Otherwise, the value of M_Q^E was defined $1 + \Delta\text{CO}$ where ΔCO is defined in equation 5.13. The values (1.06, 19.7) for V_{\max} and K_m , respectively, are the average values reported in Table 5.6.

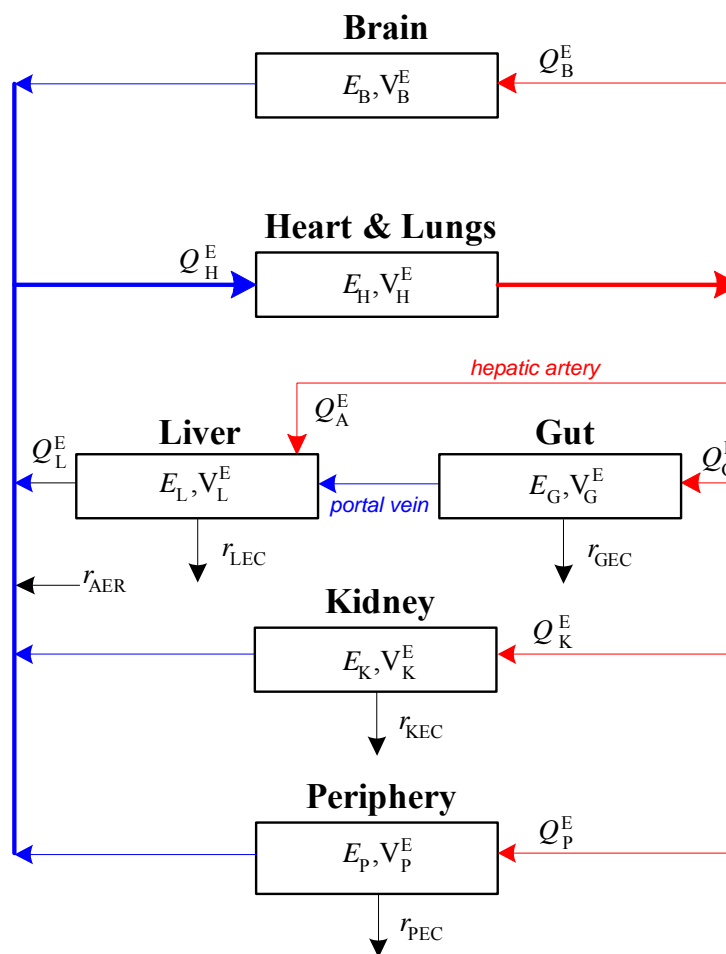


Figure 5.8: A six compartment model of epinephrine kinetics

Table 5.7: System of six first-order differential equations describing the kinetics of epinephrine.

<i>Differential Equations</i>	
$\frac{d}{dt} E_B = \frac{1}{V_B^E} [Q_B^E (E_H - E_B)]$	5.14
$\frac{d}{dt} E_H = \frac{1}{V_H^E} [Q_B^E E_B + Q_L^E E_L + Q_K^E E_K + Q_P^E E_{PV} - Q_H^E I_H + r_{AER} + RE]$	5.15
$\frac{d}{dt} E_G = \frac{1}{V_G^E} [Q_G^E (E_H - E_G) - r_{GEC}]$	5.16
$\frac{d}{dt} E_L = \frac{1}{V_L^E} [Q_A^E E_H + Q_G^E E_G - Q_L^E E_L - r_{LEC}]$	5.17
$\frac{d}{dt} E_K = \frac{1}{V_K^E} [Q_K^E (E_H - E_K) - r_{KEC}]$	5.18
$\frac{d}{dt} E_P = \frac{1}{V_P^E} [Q_P^E (E_H - E_P) - r_{PEC}]$	5.19

Clearance Rates (pg/min)

$r_{LEC} = F_{LEC} [Q_A^E E_H + Q_G^E E_G]$	5.20
$r_{GEC} = F_{GEC} Q_G^E E_G$	5.21
$r_{KEC} = F_{KEC} Q_K^E E_K$	5.22
$r_{PEC} = F_{PEC} Q_P^E E_P$	5.23

Table 5.8: Parameter Values for the 6th order model of epinephrine kinetics

<i>Distribution Volumes (ml)</i>	
$V_B^E = \frac{1000 \text{ ml}}{1} \times WCP \times V_{B,B}$	5.24
$V_H^E = \frac{1000 \text{ ml}}{1} \times WCP \times V_{H,B}$	5.25
$V_G^E = \frac{1000 \text{ ml}}{1} \times (WCP \times V_{G,B} + V_{G,ISF})$	5.26
$V_L^E = \frac{1000 \text{ ml}}{1} \times (WCP \times V_{L,B} + V_{L,ISF})$	5.27
$V_K^E = \frac{1000 \text{ ml}}{1} \times (WCP \times V_{K,B} + V_{K,ISF})$	5.28
$V_P^E = \frac{1000 \text{ ml}}{1} \times (WCP \times V_{P,B} + V_{P,ISF})$	5.29

Table 5.8 (continued)*Flow Rates (ml/min)*

$$Q_B^E = \frac{1000 \text{ ml}}{1} \times \text{WCP} \times M_Q^E \times Q_B \quad 5.30$$

$$Q_K^E = \frac{1000 \text{ ml}}{1} \times \text{WCP} \times Q_K \quad 5.31$$

$$Q_P^E = \frac{1000 \text{ ml}}{1} \times \text{WCP} \times M_Q^E \times Q_P \quad 5.32$$

$$Q_G^E = \frac{1000 \text{ ml}}{1} \times \text{WCP} \times M_Q^E \times Q_G \quad 5.33$$

$$Q_A^E = \frac{1000 \text{ ml}}{1} \times \text{WCP} \times M_Q^E \times Q_A \quad 5.34$$

$$Q_L^E = Q_A^E + Q_G^E \quad 5.35$$

$$Q_H^E = Q_B^E + Q_K^E + Q_P^E + Q_L^E \quad 5.36$$

Other Parameter Values

$$E_H^B = 75 \text{ pg/ml}, \text{WCP} = 0.84, F_{\text{LEC}} = 0.87, F_{\text{KEC}} = 0.51, F_{\text{PEC}} = 0.55, F_{\text{GEC}} = 0.37$$

Tissue or Organ	Subscript <i>j</i>	Q_j (l/min)	$V_{j,B}$ (l)	$V_{j,ISF}$ (l)
Brain	B	0.70	0.41	0.45
Heart & Lungs	H	(5.20)	1.64	-
Liver	L	(1.50)	0.90	0.60
Gut	G	1.20	0.71	0.52
Kidney	K	1.20	0.68	0.09
Periphery	P	1.80	1.26	6.74
Hepatic Artery	A	0.30	-	-

5.3.3. Model Accuracy in Steady-State and Transient Conditions

Published clinical data were pooled to investigate the accuracy of the three epinephrine kinetics models describe above. Model A, B and C will refer to the two-compartment model, the six-compartment model and the six-compartment model with hemodynamics, respectively. Published human studies that measured the concentration of epinephrine in the plasma of arterial, arterialized and/or venous blood in response to a constant intravenous epinephrine infusion were used to assess steady-state accuracy. A comprehensive list of the data used here is provided in Appendix B. Data reported by

Fitzgerald et al (1980) were used to assess each model's ability to estimate the transient response to a step-change in epinephrine appearance. The root mean square error (RMSE) was used to assess goodness-of-fit.

The results of the analyses are given in Figure 5.9 and Figure 5.10. The formulation of Model A does not differentiate between arterial or venous epinephrine concentrations. However, it is apparent that this model adequately describes arterial epinephrine concentrations. In order to assess goodness-of-fit to venous measurements in the steady-state and transient analyses, a correction factor of $1-F_{PEC}$ applied to the output of Model A. In all analyses, Model C provided the best fit to the data (Table 5.9). The limitation of Model A is apparent in the transient analysis (Figure 5.10) where it overestimated the speed by which venous epinephrine concentrations will reach steady-state after a step-change in the input.

Table 5.9: Goodness-of-Fit of epinephrine kinetics models to clinical data as assessed by the root mean square error (RMSE).

Accuracy Analysis	Model A	Model B	Model C
Arterial steady-state	114	307	109
Venous steady-state	131	318	119
Transient	261	233	63

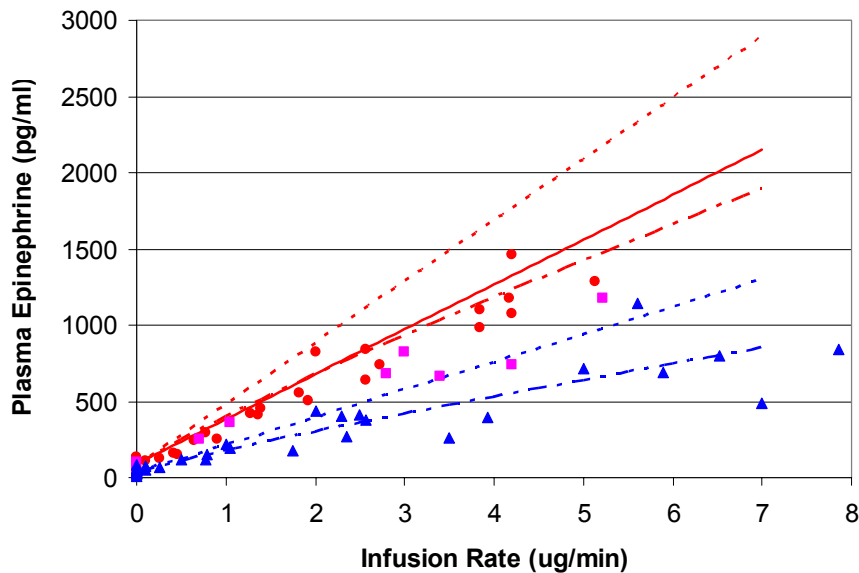


Figure 5.9: Model estimates of steady-state arterial (red circles) and venous (blue triangles) plasma epinephrine concentrations. Solid red line, arterial estimates of model A; red and blue dashed lines, arterial and venous estimates of model B; red and blue dot-dashed lines, arterial and venous estimates of model C; magenta squares, arterialized venous plasma epinephrine concentrations.

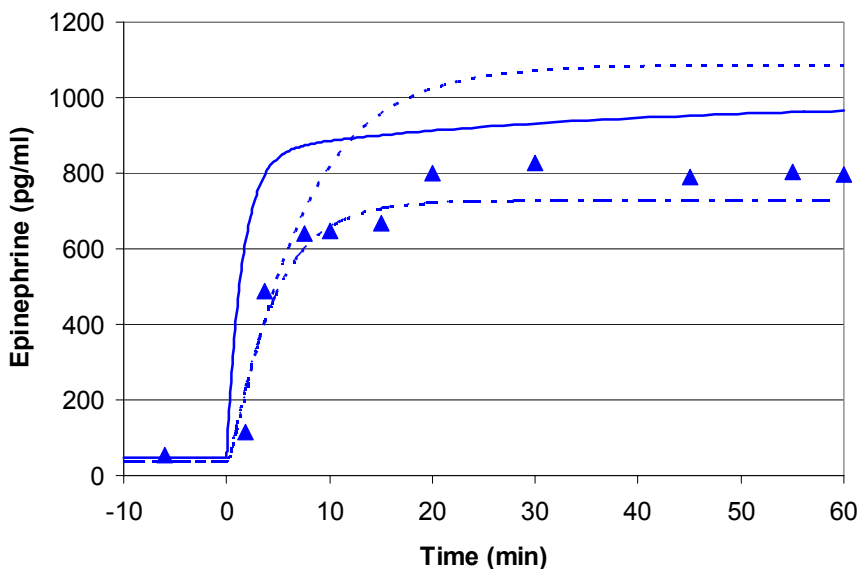


Figure 5.10: Comparison of experimental and simulated data for an intravenous epinephrine infusion at a rate of $0.83\mu\text{g}/\text{kg}$ per min over 60 minutes. Blue triangles, measured epinephrine levels from the brachial vein; solid blue line, model A; dashed blue line, model B; dot-dashed blue line, model C.

5.4. An Expanded Model of Glucose Metabolism

We have demonstrated the ability of the 6th-order subsystem with hemodynamic compensation to provide the best fit to experimental data. Next we must integrate the functional relationships between circulating epinephrine and the mechanisms of glycemic regulation that have been developed in this chapter into the existing glucose metabolism model. The complete system of equations appears in Figure 5.11 and the model parameters appear in Appendix C.

The functional relationship for the epinephrine-mediated modifier of pancreatic insulin release, M_{PIR}^E , was explored in section 5.2.1. It was determined that M_{PIR}^E acts collectively on the first and second phases of insulin secretion. As such, the rate of pancreatic insulin release it will appear as

$$r_{PIR} = r_{PIR}^B M_{PIR}^E \frac{S(G_H)}{S_\infty(G_H^B)}$$

with all other terms besides M_{PIR}^E defined in the original model. M_{PIR}^E is defined as $1 + \Delta IR$ where ΔIR is defined in equation 5.1 with coefficients -0.99 and 5.71 for V_{max} and K_m . The expression for M_{PIR}^E can be approximated as:

$$\begin{aligned}
M_{\text{PIR}}^{\text{E}} &= 1 - \frac{0.99 \left(\frac{E_{\text{H}}}{E_{\text{H}}^{\text{B}}} - 1 \right)}{5.71 + \left(\frac{E_{\text{H}}}{E_{\text{H}}^{\text{B}}} - 1 \right)} \\
&= \frac{5.71 + \left(\frac{E_{\text{H}}}{E_{\text{H}}^{\text{B}}} - 1 \right) - 0.99 \left(\frac{E_{\text{H}}}{E_{\text{H}}^{\text{B}}} - 1 \right)}{5.71 + \left(\frac{E_{\text{H}}}{E_{\text{H}}^{\text{B}}} - 1 \right)} \\
&\approx \frac{5.72}{5.71 + \left(\frac{E_{\text{H}}}{E_{\text{H}}^{\text{B}}} - 1 \right)} \\
&\approx \frac{5.72}{4.71 + \frac{E_{\text{H}}}{E_{\text{H}}^{\text{B}}}}
\end{aligned}$$

		Glucose Subsystem
1	$\frac{d}{dt} G_{BV} = \frac{1}{V_{BV}^G} \left[Q_B^G (G_H - G_{BV}) - \frac{V_{BI}^G}{T_B} (G_{BV} - G_{BI}) \right]$	
2	$\frac{d}{dt} G_{BI} = \frac{1}{V_{BI}^G} \left[\frac{V_{BI}^G}{T_B} (G_{BV} - G_{BI}) - r_{BGU} \right]$	
3	$\frac{d}{dt} G_H = \frac{1}{V_H^G} \left[Q_B^G G_{BV} + Q_L^G G_L + Q_K^G G_K + Q_P^G G_{PV} - Q_H^G G_H - r_{RBCU} + RG \right]$	
4	$\frac{d}{dt} G_G = \frac{1}{V_G^G} \left[Q_G^G (G_H - G_G) - r_{GGU} \right]$	
5	$\frac{d}{dt} G_L = \frac{1}{V_L^G} \left[Q_A^G G_H + Q_G^G G_G - Q_L^G I_L + r_{HGP} - r_{LIGU} \right]$	
5.1	$r_{HGP} = r_{HGP}^B M_{HGP}^G M_{HGP}^I M_{HGP}^T M_{HGP}^E$	
5.2	$M_{HGP}^G = 1.42 - 1.41 \tanh \left[0.62 \left(\frac{G_L}{G_L^B} - 0.497 \right) \right]$	
5.3	$M_{HGP}^{I\infty} = 1.21 - 1.14 \tanh \left[1.66 \left(\frac{I_L}{I_L^B} - 0.89 \right) \right]$	
5.4	$\frac{d}{dt} M_{HGP}^I = \frac{1}{\tau_1} \left[M_{HGP}^{I\infty} - M_{HGP}^I \right]$	
5.5	$\frac{d}{dt} f_2 = \frac{1}{\tau_f} \left[\frac{M_{HGP}^{I\infty} - 1}{2} - f_2 \right]$ $M_{HGP}^{I\infty} = 2.7 \tanh [0.39 \Gamma^N]$	
5.6	$M_{HGP}^T = M_{HGP}^{I\infty} - f_2$	
5.7	$\frac{d}{dt} f_1^E = \frac{1}{\tau_f^E} \left[M_{HGP}^{E\infty} - f_1^E \right]$ $M_{HGP}^{E\infty} = \begin{cases} 0.14 \frac{E_H}{E_H^B} + 0.86, & \frac{E_H}{E_H^B} \geq 1 \\ 1, & \text{otherwise} \end{cases}$	
5.8	$\frac{d}{dt} f_2^E = \frac{1}{\tau_f^E} \left[(f_1^E - 1) - f_2^E \right]$	
5.9	$M_{HGP}^E = \begin{cases} f_1^E - f_2^E, & f_1^E \geq f_2^E + 1 \\ 0, & \text{otherwise} \end{cases}$	
5.10	$r_{HGU} = r_{HGU}^B M_{HGU}^G M_{HGU}^I$	
5.11	$M_{HGU}^G = 1.89 + 1.89 \tanh \left[2.44 \left(\frac{G_L}{G_L^B} - 1.27 \right) \right]$	
5.12	$M_{HGU}^{I\infty} = 2.0 \tanh \left[0.55 \frac{I_L}{I_L^B} \right]$	
5.13	$\frac{d}{dt} M_{HGU}^I = \frac{1}{\tau_1} \left[M_{HGU}^{I\infty} - M_{HGU}^I \right]$	liver
6	$\frac{d}{dt} G_K = \frac{1}{V_K^G} \left[Q_K^G (G_H - G_K) - r_{KGE} \right]$	
6.1	$r_{KGE} = \begin{cases} 71 + 71 \tanh [0.011(G_K - 460)], & 0 \leq G_K \leq 460 \\ -330 + 0.872 G_K, & G_K > 460 \end{cases}$	
7	$\frac{d}{dt} G_{PV} = \frac{1}{V_{PV}^G} \left[Q_P^G (G_H - G_{PV}) - \frac{V_{PI}^G}{T_P} (G_{PV} - G_{PI}) \right]$	
8	$\frac{d}{dt} G_{PI} = \frac{1}{V_{PI}^G} \left[\frac{V_{PI}^G}{T_P} (G_{PV} - G_{PI}) - r_{PGU} \right]$	
8.1	$r_{PGU} = r_{PGU}^B M_{PGU}^G M_{PGU}^I M_{PGU}^E$	
8.1	$M_{PGU}^G = \frac{G_{PI}}{G_{PI}^B}$	
8.2	$M_{PGU}^I = 7.03 + 6.52 \tanh \left[0.338 \left(\frac{I_{PI}}{I_{PI}^B} - 5.82 \right) \right]$	
8.3	$M_{PGU}^E = 0.65 - 0.35 \tanh \left[1.5 \left(\frac{E_H}{E_H^B} - 6 \right) \right]$	periphery
9	$\frac{d}{dt} \Gamma^N = \frac{r_{MTC}}{V_T} \left[M_{PTT}^G M_{PTT}^I - \Gamma^N \right]$	Glucagon Subsystem
9.1	$M_{PTT}^G = 2.93 - 2.10 \tanh \left[4.18 \left(\frac{G_H}{G_H^B} - 0.61 \right) \right]$	
9.2	$M_{PTT}^I = 1.31 - 0.61 \tanh \left[1.06 \left(\frac{I_H}{I_H^B} - 0.47 \right) \right]$	

		Insulin Subsystem
10	$\frac{d}{dt} I_B = \frac{1}{V_B^I} \left[Q_B^I (I_H - I_B) \right]$	
11	$\frac{d}{dt} I_H = \frac{1}{V_H^I} \left[Q_B^I I_B + Q_L^I I_L + Q_K^I I_K + Q_P^I I_{PV} - Q_H^I I_H + RI \right]$	
12	$\frac{d}{dt} I_G = \frac{1}{V_G^I} \left[Q_G^I (I_H - I_G) \right]$	
13	$\frac{d}{dt} I_L = \frac{1}{V_L^I} \left[Q_A^I I_H + Q_G^I I_G - Q_L^I I_L + r_{PIR} - r_{LIC} \right]$	
13.1	$r_{LIC} = F_{LIC} \left[Q_A^I I_H + Q_G^I I_G + r_{PIR} \right]$	
13.2	$r_{PIR} = r_{PIR}^B M_{PIR}^E \frac{S(G_H)}{S_\infty(G_H^B)}$	
13.3	$S(G_H) = Q(M_1 Y + M_2 (X - I)^{0.4})$	
13.4	$S_\infty(G_H^B) = \frac{(P_\infty + KQ_0) M_1 Y}{K + M_1 Y}$	
13.5	$Y = P_\infty = X^{1.11}$	
13.6	$X(G) = \frac{G^{3.27}}{132^{3.27} + 5.93 G^{3.02}}$	
13.7	$\frac{d}{dt} P = \alpha(P_\infty - P)$	
13.8	$\frac{d}{dt} I = \beta(X - I)$	
13.8	$\frac{d}{dt} Q = K(Q_0 - Q) + \gamma P - S$	
13.9	$M_{PIR}^E = \frac{5.72}{4.71 + \frac{E_H}{E_H^B}}$	pancreas
14	$\frac{d}{dt} I_K = \frac{1}{V_K^I} \left[Q_K^I (I_H - I_K) - r_{KIC} \right]$	
14.1	$r_{KIC} = F_{KIC} Q_K^I I_K$	
15	$\frac{d}{dt} I_{PV} = \frac{1}{V_{PV}^I} \left[Q_P^I (I_H - I_{PV}) - \frac{V_{PI}^I}{T_P} (I_{PV} - I_{PI}) \right]$	
16	$\frac{d}{dt} I_{PI} = \frac{1}{V_{PI}^I} \left[\frac{V_{PI}^I}{T_P} (I_{PV} - I_{PI}) - r_{PIC} \right]$	
16.1	$r_{PIC} = \frac{I_{PI}}{\frac{1}{Q_P^I} \left(\frac{1 - F_{PIC}}{F_{PIC}} \right) - \frac{T_P^I}{V_{PI}^I}}$	

		Epinephrine Subsystem
17	$\frac{d}{dt} E_B = \frac{1}{V_B^E} \left[Q_B^E (E_H - E_B) \right]$	
18	$\frac{d}{dt} E_H = \frac{1}{V_H^E} \left[Q_B^E E_B + Q_L^E E_L + Q_K^E E_K + Q_P^E E_{PV} - Q_H^E E_H + r_{AER} + RE \right]$	
18.1	$M_Q^E = 1 - \frac{1.06 \frac{E_H}{E_H^B} - 1}{19.7 \frac{E_H}{E_H^B} - 1}$	
19	$\frac{d}{dt} E_G = \frac{1}{V_G^E} \left[Q_G^E (E_H - E_G) - r_{GEC} \right]$	
19.1	$r_{GEC} = F_{GEC} Q_G^E E_G$	
20	$\frac{d}{dt} E_L = \frac{1}{V_L^E} \left[Q_A^E E_H + Q_G^E E_G - Q_L^E E_L - r_{LEC} \right]$	
20.1	$r_{LEC} = F_{LEC} \left[Q_A^E E_H + Q_G^E E_G \right]$	
21	$\frac{d}{dt} E_K = \frac{1}{V_K^E} \left[Q_K^E (E_H - E_K) - r_{KEC} \right]$	
21.1	$r_{KEC} = F_{KEC} Q_K^E E_K$	
22	$\frac{d}{dt} E_P = \frac{1}{V_P^E} \left[Q_P^E (E_H - E_P) - r_{PEC} \right]$	
22.1	$r_{PEC} = F_{PEC} Q_P^E E_P$	

Figure 5.11: Extended model equations categorized by subsystem with equations highlight gray associated with a particular organ or tissue in each subsystem. Equations and variables highlighted in green and yellow identify our contribution to the extended model with green representing modifications to the original model (equation 5.11 and F_{LIC} in 13.1) and yellow representing new equations (5.7-5.9, 8.3, 13.9, and 17-22).

LIST OF REFERENCES

1. Rosenthal MH. Intraoperative fluid management--what and how much? *Chest*. 1999 May;115(5 Suppl):106S-12S.
2. Pandit MK, Burke J, Gustafson AB, Minocha A, Peiris AN. Drug-induced disorders of glucose tolerance. *Ann Intern Med*. 1993 April 1;118(7):529-39.
3. Shamoon H, Hendler R, Sherwin RS. Synergistic interactions among antiinsulin hormones in the pathogenesis of stress hyperglycemia in humans. *J Clin Endocrinol Metab*. 1981 Jun;52(6):1235-41.
4. Bessey PQ, Watters JM, Aoki TT, Wilmore DW. Combined hormonal infusion simulates the metabolic response to injury. *Ann Surg*. 1984 Sep;200(3):264-81.
5. Beard JC, Weinberg C, Pfeifer MA, Best JD, Halter JB, Porte D, Jr. Interaction of glucose and epinephrine in the regulation of insulin secretion. *Diabetes*. 1982 Sep;31(9):802-7.
6. Rizza R, Haymond M, Cryer P, Gerich J. Differential effects of epinephrine on glucose production and disposal in man. *Am J Physiol*. 1979 Oct;237(4):E356-62.
7. Deibert DC, DeFronzo RA. Epinephrine-induced insulin resistance in man. *J Clin Invest*. 1980 Mar;65(3):717-21.
8. Shamoon H, Hendler R, Sherwin RS. Altered responsiveness to cortisol, epinephrine, and glucagon in insulin-infused juvenile-onset diabetics. A mechanism for diabetic instability. *Diabetes*. 1980 Apr;29(4):284-91.
9. Sacca L, Cicala M, Trimarco B, Ungaro B, Vigorito C. Differential effects of insulin on splanchnic and peripheral glucose disposal after an intravenous glucose load in man. *J Clin Invest*. 1982 Jul;70(1):117-26.
10. Tack CJ, Lenders JW, Willemsen JJ, van Druten JA, Thien T, Lutterman JA, et al. Insulin stimulates epinephrine release under euglycemic conditions in humans. *Metabolism*. 1998 Mar;47(3):243-9.
11. Best J, Halter J. Release and clearance rates of epinephrine in man: Importance of arterial measurements. *J Clin Endocrinol Metab*. 1982 August 1;55(2):263-8.
12. Kjeldsen SE, Westheim A, Aakesson I, Eide I, Leren P. Plasma adrenaline and noradrenaline during orthostasis in man: The importance of arterial sampling. *Scand J Clin Lab Invest*. 1986 Sep;46(5):397-401.

13. Halter JB, Pflug AE, Tolas AG. Arterial-venous differences of plasma catecholamines in man. *Metabolism*. 1980 1;29(1):9-12.
14. Rosen SG, Sanfield JA, Morrow LA, Zweifler AJ. Relationship between plasma and platelet epinephrine concentrations in humans. *Am J Physiol Endocrinol Metab*. 1987 March 1;252(3):E334-339.
15. Rizza RA, Cryer PE, Haymond MW, Gerich JE. Adrenergic mechanisms for the effects of epinephrine on glucose production and clearance in man. *J Clin Invest*. 1980 Mar;65(3):682-9.
16. Guy DA, Sandoval D, Richardson MA, Tate D, Flakoll PJ, Davis SN. Differing physiological effects of epinephrine in type 1 diabetes and nondiabetic humans. *Am J Physiol Endocrinol Metab*. 2005 Jan;288(1):E178-86.
17. Ratge D, Kohse K, Steegmuller U, Wisser H. Distribution of free and conjugated catecholamines between plasma, platelets and erythrocytes: Different effects of intravenous and oral catecholamine administrations. *J Pharmacol Exp Ther*. 1991 April 1;257(1):232-8.
18. McCulloch RK, Vandongen R, Tunney AM, Beilin LJ, Rogers PB. Distribution of free and sulfate-conjugated catecholamines in human platelets. *Am J Physiol Endocrinol Metab*. 1987 September 1;253(3):E312-316.
19. Meyer C, Stumvoll M, Welle S, Woerle HJ, Haymond M, Gerich J. Relative importance of liver, kidney, and substrates in epinephrine-induced increased gluconeogenesis in humans. *Am J Physiol Endocrinol Metab*. 2003 Oct;285(4):E819-26.
20. Tidgren B, Hjemdahl P. Renal responses to mental stress and epinephrine in humans. *Am J Physiol*. 1989 Oct;257(4 Pt 2):F682-9.
21. Willemsen JJ, Ross HA, Jacobs MC, Lenders JW, Thien T, Swinkels LM, et al. Highly sensitive and specific HPLC with fluorometric detection for determination of plasma epinephrine and norepinephrine applied to kinetic studies in humans. *Clin Chem*. 1995 Oct;41(10):1455-60.
22. Sacca L, Hendler R, Picardi A, Sherwin RS. Splanchnic and renal contribution to disposal of infused epinephrine in humans. *Am J Physiol*. 1986 Sep;251(3 Pt 1):E285-9.
23. Liu D, Andreasson K, Lins PE, Adamson UC, Macdonald IA. Adrenaline and noradrenaline responses during insulin-induced hypoglycaemia in man: Should the hormone levels be measured in arterialized venous blood? *Acta Endocrinol (Copenh)*. 1993 Jan;128(1):95-8.

24. Fitzgerald GA, Barnes P, Hamilton CA, Dollery CT. Circulating adrenaline and blood pressure: The metabolic effects and kinetics of infused adrenaline in man. *Eur J Clin Invest*. 1980 Oct;10(5):401-6.
25. Insulander P, Juhlin-Dannfelt A, Freyschuss U, Vallin H. Electrophysiologic effects of mental stress in healthy subjects: A comparison with epinephrine infusion. *J Electrocardiol*. 2003 Oct;36(4):301-9.
26. Freyschuss U, Hjemdahl P, Juhlin-Dannfelt A, Linde B. Cardiovascular and metabolic responses to low dose adrenaline infusion: An invasive study in humans. *Clin Sci (Lond)*. 1986 Feb;70(2):199-206.
27. Fellows IW, Bennett T, MacDonald IA. The effect of adrenaline upon cardiovascular and metabolic functions in man. *Clin Sci (Lond)*. 1985 Aug;69(2):215-22.
28. Stratton JR, Pfeifer MA, Ritchie JL, Halter JB. Hemodynamic effects of epinephrine: Concentration-effect study in humans. *J Appl Physiol*. 1985 Apr;58(4):1199-206.
29. Lindqvist M, Kahan T, Melcher A, Bie P, Hjemdahl P. Forearm vasodilator mechanisms during mental stress: Possible roles for epinephrine and ANP. *Am J Physiol*. 1996 Mar;270(3 Pt 1):E393-9.
30. Stallknecht B, Bulow J, Frandsen E, Galbo H. Desensitization of human adipose tissue to adrenaline stimulation studied by microdialysis. *J Physiol*. 1997 Apr 1;500 (Pt 1)(Pt 1):271-82.
31. Braatvedt GD, Flynn MD, Stanners A, Halliwell M, Corrall RJ. Splanchnic blood flow in man: Evidence for mediation via a beta-adrenergic mechanism. *Clin Sci (Lond)*. 1993 Feb;84(2):201-7.
32. Simonsen L, Bulow J, Madsen J, Christensen NJ. Thermogenic response to epinephrine in the forearm and abdominal subcutaneous adipose tissue. *Am J Physiol*. 1992 Nov;263(5 Pt 1):E850-5.
33. Bachmann AW, Gordon RD, Bathgate RA, Thompson RE. Effect of graded adrenaline infusion on arterial adrenaline clearance in normotensive and hypertensive man. *Clin Exp Pharmacol Physiol*. 1990 Apr;17(4):257-61.
34. White M, Leenen FH. Effects of age on cardiovascular responses to adrenaline in man. *Br J Clin Pharmacol*. 1997 Apr;43(4):407-14.
35. Sung BH, Robinson C, Thadani U, Lee R, Wilson MF. Effects of 1-epinephrine on hemodynamics and cardiac function in coronary disease: Dose-response studies. *Clin Pharmacol Ther*. 1988 Mar;43(3):308-16.

36. Rosen SG, Linares OA, Sanfield JA, Zech LA, Lizzio VP, Halter JB. Epinephrine kinetics in humans: Radiotracer methodology. *J Clin Endocrinol Metab.* 1989 Oct;69(4):753-61.
37. Werb MR, Zinman B, Teasdale SJ, Goldman BS, Scully HE, Marliss EB. Hormonal and metabolic responses during coronary artery bypass surgery: Role of infused glucose. *J Clin Endocrinol Metab.* 1989 Nov;69(5):1010-8.
38. Clarke RS, Johnston H, Sheridan B. The influence of anaesthesia and surgery on plasma cortisol, insulin and free fatty acids. *Br J Anaesth.* 1970 Apr;42(4):295-9.
39. Allison SP, Tomlin PJ, Chamberlain MJ. Some effects of anaesthesia and surgery on carbohydrate and fat metabolism. 1969. *Br J Anaesth.* 1998 Aug;81(2):273,7; discussion 271-2.
40. Farkas-Hirsch R, Boyle PJ, Hirsch IB. Glycemic control of the surgical patient with IDDM. *Diabetes.* 1989;Suppl 2:39A.
41. Alberti KG, Thomas DJ. The management of diabetes during surgery. *Br J Anaesth.* 1979 Jul;51(7):693-710.
42. Van den Berghe G, Wilmer A, Hermans G, Meersseman W, Wouters PJ, Milants I, et al. Intensive insulin therapy in the medical ICU. *N Engl J Med.* 2006 Feb 2;354(5):449-61.
43. Van den Berghe G, Wouters P, Weekers F, Verwaest C, Bruyninckx F, Schetz M, et al. Intensive insulin therapy in the critically ill patients. *N Engl J Med.* 2001 Nov 8;345(19):1359-67.
44. Lazar HL, Chipkin S, Philippides G, Bao Y, Apstein C. Glucose-insulin-potassium solutions improve outcomes in diabetics who have coronary artery operations. *Ann Thorac Surg.* 2000 Jul;70(1):145-50.
45. Furnary AP, Zerr KJ, Grunkemeier GL, Starr A. Continuous intravenous insulin infusion reduces the incidence of deep sternal wound infection in diabetic patients after cardiac surgical procedures. *Ann Thorac Surg.* 1999 Feb;67(2):352,60; discussion 360-2.
46. Mangano CM, Diamondstone LS, Ramsay JG, Aggarwal A, Herskowitz A, Mangano DT. Renal dysfunction after myocardial revascularization: Risk factors, adverse outcomes, and hospital resource utilization. the multicenter study of perioperative ischemia research group. *Ann Intern Med.* 1998 Feb 1;128(3):194-203.
47. Rady MY, Ryan T, Starr NJ. Perioperative determinants of morbidity and mortality in elderly patients undergoing cardiac surgery. *Crit Care Med.* 1998 Feb;26(2):225-35.

48. Rosetti L, Giaccari A, DeFronzo RA. Glucose toxicity. *Diabetes Care*. 1990;13:610-30.
49. Centers for disease control and prevention. national diabetes fact sheet: General information and national estimates on diabetes in the united states [homepage on the Internet]. Atlanta, GA: US Dept Health & Human Services, Centers for Disease Control & Prevention. 2005 Feb. 2007. Available from: http://www.cdc.gov/diabetes/pubs/pdf/ndfs_2005.pdf.
50. Centers for disease control and prevention. national diabetes fact sheet errata [homepage on the Internet]. Atlanta, GA: . Feb. 2007 [cited June 2005]. Available from: : <http://www.cdc.gov/diabetes/pubs/pdf/errata05.pdf>.
51. Hogan P, Dall T, Nikolov P, American Diabetes Association. Economic costs of diabetes in the US in 2002. *Diabetes Care*. 2003 Mar;26(3):917-32.
52. DeFrances CJ, Hall MJ. 2002 national hospital discharge survey. *Adv Data*. 2004 May 21;(342)(342):1-29.
53. Murkin JM. Pro: Tight intraoperative glucose control improves outcome in cardiovascular surgery. *J Cardiothorac Vasc Anesth*. 2000 Aug;14(4):475-8.
54. Gogou G, Maglaveras N, Ambrosiadou BV, Goulis D, Pappas C. A neural network approach in diabetes management by insulin administration. *J Med Syst*. 2001 Apr;25(2):119-31.
55. Hirsch IB, McGill JB, Cryer PE, White PF. Perioperative management of surgical patients with diabetes mellitus. *Anesthesiology*. 1991 Feb;74(2):346-59.
56. Levetan CS, Passaro M, Jablonski K, Kass M, Ratner RE. Unrecognized diabetes among hospitalized patients. *Diabetes Care*. 1998 Feb;21(2):246-9.
57. Roghi A, Palmieri B, Crivellaro W, Faletra F, Puttini M. Relationship of unrecognized myocardial infarction, diabetes mellitus and type of surgery to postoperative cardiac outcomes in vascular surgery. *Eur J Vasc Endovasc Surg*. 2001 Jan;21(1):9-16.
58. Capes SE, Hunt D, Malmberg K, Gerstein HC. Stress hyperglycaemia and increased risk of death after myocardial infarction in patients with and without diabetes: A systematic overview. *Lancet*. 2000 Mar 4;355(9206):773-8.
59. Van den Berghe G, Wouters PJ, Bouillon R, Weekers F, Verwaest C, Schetz M, et al. Outcome benefit of intensive insulin therapy in the critically ill: Insulin dose versus glycemic control. *Crit Care Med*. 2003 Feb;31(2):359-66.
60. Rybka J, Mistrik J, Szabo M. Preoperative and postoperative care in diabetics. *Vnitr Lek*. 2001 May;47(5):333-6.

61. Kalin MF, Tranbaugh RF, Salas J, Zumoff B. Intensive intervention by an endocrinologist-directed diabetes team diminishes excess mortality in patients with diabetes who undergo coronary artery bypass graft. *Diabetes*. 1998;47(Suppl 1):A87.
62. Shojanian KG, Duncan BW, McDonald KM, Wachter RM, Markowitz AJ. Making health care safer: A critical analysis of patient safety practices. *Evid Rep Technol Assess (Summ)*. 2001;(43)(43):i,x, 1-668.
63. Barash PG, Cullen BF, Stoelting RK. *Clinical anesthesia*. 3rd ed. Lippincott-Raven; 1997.
64. Jacober SJ, Sowers JR. An update on perioperative management of diabetes. *Arch Intern Med*. 1999 Nov 8;159(20):2405-11.
65. Zerr KJ, Furnary AP, Grunkemeier GL, Bookin S, Kanhere V, Starr A. Glucose control lowers the risk of wound infection in diabetics after open heart operations. *Ann Thorac Surg*. 1997 Feb;63(2):356-61.
66. Golden SH, Peart-Vigilance C, Kao WH, Brancati FL. Perioperative glycemic control and the risk of infectious complications in a cohort of adults with diabetes. *Diabetes Care*. 1999 Sep;22(9):1408-14.
67. Pomposelli JJ, Baxter JK, 3rd, Babineau TJ, Pomfret EA, Driscoll DF, Forse RA, et al. Early postoperative glucose control predicts nosocomial infection rate in diabetic patients. *JPEN J Parenter Enteral Nutr*. 1998 Mar-Apr;22(2):77-81.
68. Rassias AJ, Marrin CA, Arruda J, Whalen PK, Beach M, Yeager MP. Insulin infusion improves neutrophil function in diabetic cardiac surgery patients. *Anesth Analg*. 1999 May;88(5):1011-6.
69. Weintraub WS, Stein B, Kosinski A, Douglas JS, Jr, Ghazzal ZM, Jones EL, et al. Outcome of coronary bypass surgery versus coronary angioplasty in diabetic patients with multivessel coronary artery disease. *J Am Coll Cardiol*. 1998 Jan;31(1):10-9.
70. Influence of diabetes on 5-year mortality and morbidity in a randomized trial comparing CABG and PTCA in patients with multivessel disease: The bypass angioplasty revascularization investigation (BARI). *Circulation*. 1997 Sep 16;96(6):1761-9.
71. Marcus AO, Perkowski DJ, Littlefield S. Use of metabolic interventions to reduce risk of CABG complications in patients with diabetes mellitus. *Diabetes*. 1998;47:322A.
72. Strategic approaches in coronary interventions. Ellis SG and Holmes DR, editors. Philadelphia: Lippincott, Williams and Wilkins; 2000.

73. Mak KH, Moliterno DJ, Granger CB, Miller DP, White HD, Wilcox RG, et al. Influence of diabetes mellitus on clinical outcome in the thrombolytic era of acute myocardial infarction. GUSTO-I investigators. global utilization of streptokinase and tissue plasminogen activator for occluded coronary arteries. *J Am Coll Cardiol*. 1997 Jul;30(1):171-9.
74. Granger CB, Califf RM, Young S, Candela R, Samaha J, Worley S, et al. Outcome of patients with diabetes mellitus and acute myocardial infarction treated with thrombolytic agents. the thrombolysis and angioplasty in myocardial infarction (TAMI) study group. *J Am Coll Cardiol*. 1993 Mar 15;21(4):920-5.
75. Akasaka T, Yoshida K, Hozumi T, Takagi T, Kaji S, Kawamoto T, et al. Retinopathy identifies marked restriction of coronary flow reserve in patients with diabetes mellitus. *J Am Coll Cardiol*. 1997 Oct;30(4):935-41.
76. Bohlen HG, Nase GP. Arteriolar nitric oxide concentration is decreased during hyperglycemia-induced betaII PKC activation. *Am J Physiol Heart Circ Physiol*. 2001 Feb;280(2):H621-7.
77. Cosentino F, Luscher TF. Endothelial dysfunction in diabetes mellitus. *J Cardiovasc Pharmacol*. 1998;32 Suppl 3:S54-61.
78. Kuntschen FR, Taillens C, Galletti PM, Hauf E, Hahn C. Coronary surgery in diabetics: Metabolic aspects of glycemia control by an artificial pancreas. *Trans Am Soc Artif Intern Organs*. 1982;28:236-9.
79. Abbud ZA, Shindler DM, Wilson AC, Kostis JB. Effect of diabetes mellitus on short- and long-term mortality rates of patients with acute myocardial infarction: A statewide study. myocardial infarction data acquisition system study group. *Am Heart J*. 1995 Jul;130(1):51-8.
80. Malmberg K, Norhammar A, Ryden L, DIGAAMI study. Insulin treatment post myocardial infarction: The DIGAMI study. *Adv Exp Med Biol*. 2001;498:279-84.
81. Malmberg K, McGuire DK. Diabetes and acute myocardial infarction: The role of insulin therapy. *Am Heart J*. 1999 Nov;138(5 Pt 1):S381-6.
82. Malmberg K. Prospective randomised study of intensive insulin treatment on long term survival after acute myocardial infarction in patients with diabetes mellitus. DIGAMI (diabetes mellitus, insulin glucose infusion in acute myocardial infarction) study group. *BMJ*. 1997 May 24;314(7093):1512-5.
83. Malmberg K, Ryden L, Efendic S, Herlitz J, Nicol P, Waldenstrom A, et al. Randomized trial of insulin-glucose infusion followed by subcutaneous insulin treatment in diabetic patients with acute myocardial infarction (DIGAMI study): Effects on mortality at 1 year. *J Am Coll Cardiol*. 1995 Jul;26(1):57-65.

84. Malmberg K, Ryden L. Myocardial infarction in patients with diabetes mellitus. *Eur Heart J*. 1988 Mar;9(3):259-64.
85. Hirsch IB, Paauw DS, Brunzell J. Inpatient management of adults with diabetes. *Diabetes Care*. 1995 Jun;18(6):870-8.
86. Dazzi D, Taddei F, Gavarini A, Uggeri E, Negro R, Pezzarossa A. The control of blood glucose in the critical diabetic patient: A neuro-fuzzy method. *J Diabetes Complications*. 2001 Mar-Apr;15(2):80-7.
87. Top 50 drug products associated with medication errors [homepage on the Internet]. Rockville, MD: United States Pharmacopeia [cited November 2007]. Available from: <http://www.usp.org/hqi/patientSafety/resources/top50DrugErrors.html>.
88. Queale WS, Seidler AJ, Brancati FL. Glycemic control and sliding scale insulin use in medical inpatients with diabetes mellitus. *Arch Intern Med*. 1997 Mar 10;157(5):545-52.
89. Hiss RG, Davis WK. Intensified glycemic control and changes in training and continuing education of physicians. *Diabetes Rev*. 1994;2:310,310-321.
90. Galloway JA, Spradlin CT, Howey DC, Dupre J. Intrasubject differences in pharmacokinetics and pharmacodynamic responses: The immutable problem of present-day treatment? In: Serrano-Rios M, Lefebvre PJ, editors. *Diabetes*. Amsterdam: Excerpta Medica; 1986. p. 877,877-886.
91. Matz R. Inpatient management of adults with diabetes. *Diabetes Care*. 1996 Jan;19(1):90-2.
92. Meyers EF, Alberts D, Gordon MO. Perioperative control of blood glucose in diabetic patients: A two-step protocol. *Diabetes Care*. 1986 Jan-Feb;9(1):40-5.
93. Turner RC, Grayburn JA, Newman GB, Nabarro JD. Measurement of the insulin delivery rate in man. *J Clin Endocrinol Metab*. 1971 Aug;33(2):279-86.
94. Levetan CS, Magee MF. Hospital management of diabetes. *Endocrinol Metab Clin North Am*. 2000 Dec;29(4):745-70.
95. Meijering S, Corstjens AM, Tulleken JE, Meertens JH, Zijlstra JG, Ligtenberg JJ. Towards a feasible algorithm for tight glycaemic control in critically ill patients: A systematic review of the literature. *Crit Care*. 2006 Feb;10(1):R19.
96. Goldberg PA, Siegel MD, Sherwin RS, Halickman JI, Lee M, Bailey VA, et al. Implementation of a safe and effective insulin infusion protocol in a medical intensive care unit. *Diabetes Care*. 2004 Feb;27(2):461-7.

97. Davidson PC, Steed RD, Bode BW. Glucomander: A computer-directed intravenous insulin system shown to be safe, simple, and effective in 120,618 h of operation. *Diabetes Care*. 2005 Oct;28(10):2418-23.
98. Anesthesia. 5th ed. Miller RD, editor. Philadelphia, PA: Churchill Livingstone; 2000.
99. Garber AJ, Moghissi ES, Bransome ED, Jr, Clark NG, Clement S, Cobin RH, et al. American college of endocrinology position statement on inpatient diabetes and metabolic control. *Endocr Pract*. 2004 Jan-Feb;10(1):77-82.
100. ACE/ADA Task Force on Inpatient Diabetes. American college of endocrinology and american diabetes association consensus statement on inpatient diabetes and glycemic control. *Endocr Pract*. 2006 Jul-Aug;12(4):458-68.
101. Bessler H, Bergman M, Salman H. Interleukin-3 and stress. *Biomed Pharmacother*. 2000 Jul;54(6):299-304.
102. Maier SF, Ryan SM, Barksdale CM, Kalin NH. Stressor controllability and the pituitary-adrenal system. *Behav Neurosci*. 1986 Oct;100(5):669-74.
103. Clutter WE, Bier DM, Shah SD, Cryer PE. Epinephrine plasma metabolic clearance rates and physiologic thresholds for metabolic and hemodynamic actions in man. *J Clin Invest*. 1980 Jul;66(1):94-101.
104. Kolettis TM, Psarros E, Kyriakides ZS, Katsouras CS, Michalis LK, Sideris DA. Haemodynamic and catecholamine response to simulated ventricular tachycardia in man: Effect of baseline left ventricular function. *Heart*. 2003 Mar;89(3):306-10.
105. Engelman RM, Haag B, Lemeshow S, Angelo A, Rousou JH. Mechanism of plasma catecholamine increases during coronary artery bypass and valve procedures. *J Thorac Cardiovasc Surg*. 1983 Oct;86(4):608-15.
106. Linsell CR, Lightman SL, Mullen PE, Brown MJ, Causon RC. Circadian rhythms of epinephrine and norepinephrine in man. *J Clin Endocrinol Metab*. 1985 Jun;60(6):1210-5.
107. Wortsman J, Frank S, Cryer PE. Adrenomedullary response to maximal stress in humans. *Am J Med*. 1984 Nov;77(5):779-84.
108. Chu CA, Sindelar DK, Neal DW, Allen EJ, Donahue EP, Cherrington AD. Comparison of the direct and indirect effects of epinephrine on hepatic glucose production. *J Clin Invest*. 1997 Mar 1;99(5):1044-56.
109. Stevenson RW, Steiner KE, Connolly CC, Fuchs H, Alberti KG, Williams PE, et al. Dose-related effects of epinephrine on glucose production in conscious dogs. *Am J Physiol*. 1991 Mar;260(3 Pt 1):E363-70.

110. Silverberg AB, Shah SD, Haymond MW, Cryer PE. Norepinephrine: Hormone and neurotransmitter in man. *Am J Physiol.* 1978 Mar;234(3):E252-6.
111. Connolly CC, Steiner KE, Stevenson RW, Neal DW, Williams PE, Alberti KG, et al. Regulation of glucose metabolism by norepinephrine in conscious dogs. *Am J Physiol.* 1991 Dec;261(6 Pt 1):E764-72.
112. Reves JG, Karp RB, Buttner EE, Tosone S, Smith LR, Samuelson PN, et al. Neuronal and adrenomedullary catecholamine release in response to cardiopulmonary bypass in man. *Circulation.* 1982 Jul;66(1):49-55.
113. De Kloet ER, Derijk R. Signaling pathways in brain involved in predisposition and pathogenesis of stress-related disease: Genetic and kinetic factors affecting the MR/GR balance. *Ann N Y Acad Sci.* 2004 Dec;1032:14-34.
114. Rizza RA, Mandarino LJ, Gerich JE. Cortisol-induced insulin resistance in man: Impaired suppression of glucose production and stimulation of glucose utilization due to a postreceptor defect of insulin action. *J Clin Endocrinol Metab.* 1982 Jan;54(1):131-8.
115. Marco J, Calle C, Roman D, Diaz-Fierros M, Villanueva ML, Valverde I. Hyperglucagonism induced by glucocorticoid treatment in man. *N Engl J Med.* 1973 Jan 18;288(3):128-31.
116. Wise JK, Hendler R, Felig P. Influence of glucocorticoids on glucagon secretion and plasma amino acid concentrations in man. *J Clin Invest.* 1973 Nov;52(11):2774-82.
117. McGregor VP, Banarer S, Cryer PE. Elevated endogenous cortisol reduces autonomic neuroendocrine and symptom responses to subsequent hypoglycemia. *Am J Physiol Endocrinol Metab.* 2002 Apr;282(4):E770-7.
118. Davis SN, Shavers C, Costa F, Mosqueda-Garcia R. Role of cortisol in the pathogenesis of deficient counterregulation after antecedent hypoglycemia in normal humans. *J Clin Invest.* 1996 Aug 1;98(3):680-91.
119. Takahashi Y, Kipnis DM, Daughaday WH. Growth hormone secretion during sleep. *J Clin Invest.* 1968 Sep;47(9):2079-90.
120. Vogeser M, Felbinger TW, Kilger E, Roll W, Fraunberger P, Jacob K. Corticosteroid-binding globulin and free cortisol in the early postoperative period after cardiac surgery. *Clin Biochem.* 1999 Apr;32(3):213-6.
121. Hamrahian AH, Oseni TS, Arafah BM. Measurements of serum free cortisol in critically ill patients. *N Engl J Med.* 2004 Apr 15;350(16):1629-38.

122. Braams R, Koppeschaar HP, van de Pavoordt HD, van Vroonhoven TJ. Adrenocortical function in patients with ruptured aneurysm of the abdominal aorta. *Intensive Care Med.* 1998 Feb;24(2):124-7.
123. Lecocq FR, Mebane D, Madison LL. The acute effect of hydrocortisone on hepatic glucose output and peripheral glucose utilization. *J Clin Invest.* 1964 Feb;43:237-46.
124. Wright PD, Johnston ID. The effect of surgical operation on growth hormone levels in plasma. *Surgery.* 1975 Apr;77(4):479-86.
125. Moller N, Jorgensen JO, Schmitz O, Moller J, Christiansen J, Alberti KG, et al. Effects of a growth hormone pulse on total and forearm substrate fluxes in humans. *Am J Physiol.* 1990 Jan;258(1 Pt 1):E86-91.
126. Moller N, Schmitz O, Porksen N, Moller J, Jorgensen JO. Dose-response studies on the metabolic effects of a growth hormone pulse in humans. *Metabolism.* 1992 Feb;41(2):172-5.
127. Bratusch-Marrain PR, Smith D, DeFronzo RA. The effect of growth hormone on glucose metabolism and insulin secretion in man. *J Clin Endocrinol Metab.* 1982 Nov;55(5):973-82.
128. Fowelin J, Attvall S, von Schenck H, Smith U, Lager I. Characterization of the insulin-antagonistic effect of growth hormone in man. *Diabetologia.* 1991 Jul;34(7):500-6.
129. Ghanaat F, Tayek JA. Growth hormone administration increases glucose production by preventing the expected decrease in glycogenolysis seen with fasting in healthy volunteers. *Metabolism.* 2005 May;54(5):604-9.
130. Teng Chung T, Hinds CJ. Treatment with GH and IGF-1 in critical illness. *Crit Care Clin.* 2006 Jan;22(1):29,40, vi.
131. Farah AE. Glucagon and the circulation. *Pharmacol Rev.* 1983 Sep;35(3):181-217.
132. Unger RH, Orci L. Glucagon and the A cell: Physiology and pathophysiology (second of two parts). *N Engl J Med.* 1981 Jun 25;304(26):1575-80.
133. Russell RC, Walker CJ, Bloom SR. Hyperglucagonaemia in the surgical patient. *Br Med J.* 1975 Jan 4;1(5948):10-2.
134. Matsubara Y, Iwafuchi M, Muto T, Ito S, Hayashi M. Plasma glucagon changes in surgical patients. *Jpn J Surg.* 1979 Dec;9(4):327-34.
135. Marliss EB, Aoki TT, Unger RH, Soeldner JS, Cahill GF, Jr. Glucagon levels and metabolic effects in fasting man. *J Clin Invest.* 1970 Dec;49(12):2256-70.

136. Chhibber VL, Soriano C, Tayek JA. Effects of low-dose and high-dose glucagon on glucose production and gluconeogenesis in humans. *Metabolism*. 2000 Jan;49(1):39-46.
137. Mittelman SD, Fu YY, Rebrin K, Steil G, Bergman RN. Indirect effect of insulin to suppress endogenous glucose production is dominant, even with hyperglucagonemia. *J Clin Invest*. 1997 Dec 15;100(12):3121-30.
138. Ferrannini E, DeFronzo RA, Sherwin RS. Transient hepatic response to glucagon in man: Role of insulin and hyperglycemia. *Am J Physiol*. 1982 Feb;242(2):E73-81.
139. Dirlewanger M, Schneiter PH, Paquot N, Jequier E, Rey V, Tappy L. Effects of glucocorticoids on hepatic sensitivity to insulin and glucagon in man. *Clin Nutr*. 2000 Feb;19(1):29-34.
140. Huypens P, Ling Z, Pipeleers D, Schuit F. Glucagon receptors on human islet cells contribute to glucose competence of insulin release. *Diabetologia*. 2000 Aug;43(8):1012-9.
141. Sherwin RS, Sacca L. Effect of epinephrine on glucose metabolism in humans: Contribution of the liver. *Am J Physiol*. 1984 Aug;247(2 Pt 1):E157-65.
142. Abraham E. Effects of stress on cytokine production. *Methods Achiev Exp Pathol*. 1991;14:45-62.
143. Thorell A, Loftenius A, Andersson B, Ljungqvist O. Postoperative insulin resistance and circulating concentrations of stress hormones and cytokines. *Clin Nutr*. 1996 Apr;15(2):75-9.
144. Stanley TH, Berman L, Green O, Robertson D. Plasma catecholamine and cortisol responses to fentanyl-oxygen anesthesia for coronary-artery operations. *Anesthesiology*. 1980 Sep;53(3):250-3.
145. Lattermann R, Schrickler T, Wachter U, Georgieff M, Goertz A. Understanding the mechanisms by which isoflurane modifies the hyperglycemic response to surgery. *Anesth Analg*. 2001 Jul;93(1):121-7.
146. Nishiyama T, Yamashita K, Yokoyama T. Stress hormone changes in general anesthesia of long duration: Isoflurane-nitrous oxide vs sevoflurane-nitrous oxide anesthesia. *J Clin Anesth*. 2005 Dec;17(8):586-91.
147. Furuya K, Shimizu R, Hirabayashi Y, Ishii R, Fukuda H. Stress hormone responses to major intra-abdominal surgery during and immediately after sevoflurane-nitrous oxide anaesthesia in elderly patients. *Can J Anaesth*. 1993 May;40(5 Pt 1):435-9.
148. Boyd O, Grounds M, Bennett D. The dependency of oxygen consumption on oxygen delivery in critically ill postoperative patients is mimicked by variations in sedation. *Chest*. 1992 Jun;101(6):1619-24.

149. Nygren J, Thorell A, Ljungqvist O. Preoperative oral carbohydrate nutrition: An update. *Curr Opin Clin Nutr Metab Care*. 2001 Jul;4(4):255-9.
150. Soop M, Nygren J, Myrenfors P, Thorell A, Ljungqvist O. Preoperative oral carbohydrate treatment attenuates immediate postoperative insulin resistance. *Am J Physiol Endocrinol Metab*. 2001 Apr;280(4):E576-83.
151. Boden G. Role of fatty acids in the pathogenesis of insulin resistance and NIDDM. *Diabetes*. 1997 Jan;46(1):3-10.
152. Bock JC, Barker BC, Clinton AG, Wilson MB, Lewis FR. Post-traumatic changes in, and effect of colloid osmotic pressure on the distribution of body water. *Ann Surg*. 1989 Sep;210(3):395,403; discussion 403-5.
153. Holte K, Sharrock NE, Kehlet H. Pathophysiology and clinical implications of perioperative fluid excess. *Br J Anaesth*. 2002 Oct;89(4):622-32.
154. Shippy CR, Shoemaker WC. Hemodynamic and colloid osmotic pressure alterations in the surgical patient. *Crit Care Med*. 1983 Mar;11(3):191-5.
155. Watters JM, Bessey PQ, Dinarello CA, Wolff SM, Wilmore DW. Both inflammatory and endocrine mediators stimulate host responses to sepsis. *Arch Surg*. 1986 Feb;121(2):179-90.
156. Brandstrup B. Fluid therapy for the surgical patient. *Best Pract Res Clin Anaesthesiol*. 2006 Jun;20(2):265-83.
157. Lobo DN, Macafee DA, Allison SP. How perioperative fluid balance influences postoperative outcomes. *Best Pract Res Clin Anaesthesiol*. 2006 Sep;20(3):439-55.
158. Brater DC. Diuretic therapy. *N Engl J Med*. 1998 Aug 6;339(6):387-95.
159. Hildebrand F, Giannoudis PV, van Griensven M, Chawda M, Pape HC. Pathophysiologic changes and effects of hypothermia on outcome in elective surgery and trauma patients. *Am J Surg*. 2004 Mar;187(3):363-71.
160. Schulster L, Chinn RY, CDC, HICPAC. Guidelines for environmental infection control in health-care facilities. recommendations of CDC and the healthcare infection control practices advisory committee (HICPAC). *MMWR Recomm Rep*. 2003 Jun 6;52(RR-10):1-42.
161. Terao Y, Miura K, Saito M, Sekino M, Fukusaki M, Sumikawa K. Quantitative analysis of the relationship between sedation and resting energy expenditure in postoperative patients. *Crit Care Med*. 2003 Mar;31(3):830-3.
162. Hynson JM, Sessler DI. Intraoperative warming therapies: A comparison of three devices. *J Clin Anesth*. 1992 May-Jun;4(3):194-9.

163. Lehot JJ, Piriz H, Villard J, Cohen R, Guidollet J. Glucose homeostasis. comparison between hypothermic and normothermic cardiopulmonary bypass. *Chest*. 1992 Jul;102(1):106-11.
164. Kuntschen FR, Galletti PM, Hahn C. Glucose-insulin interactions during cardiopulmonary bypass. hypothermia versus normothermia. *J Thorac Cardiovasc Surg*. 1986 Mar;91(3):451-9.
165. Curry DL, Curry KP. Hypothermia and insulin secretion. *Endocrinology*. 1970 Oct;87(4):750-5.
166. Black PR, van Devanter S, Cohn LH. Effects of hypothermia on systemic and organ system metabolism and function. *J Surg Res*. 1976 Jan;20(1):49-63.
167. Chaney MA, Nikolov MP, Blakeman BP, Bakhos M. Attempting to maintain normoglycemia during cardiopulmonary bypass with insulin may initiate postoperative hypoglycemia. *Anesth Analg*. 1999 Nov;89(5):1091-5.
168. Oltmanns KM, Gehring H, Rudolf S, Schultes B, Rook S, Schweiger U, et al. Hypoxia causes glucose intolerance in humans. *Am J Respir Crit Care Med*. 2004 Jun 1;169(11):1231-7.
169. Punjabi NM, Polotsky VY. Disorders of glucose metabolism in sleep apnea. *J Appl Physiol*. 2005 Nov;99(5):1998-2007.
170. Reynolds RM, Walker BR. Human insulin resistance: The role of glucocorticoids. *Diabetes Obes Metab*. 2003 Jan;5(1):5-12.
171. Jacob S, Rett K, Henriksen EJ. Antihypertensive therapy and insulin sensitivity: Do we have to redefine the role of beta-blocking agents? *Am J Hypertens*. 1998 Oct;11(10):1258-65.
172. Helderman JH, Elahi D, Andersen DK, Raizes GS, Tobin JD, Shocken D, et al. Prevention of the glucose intolerance of thiazide diuretics by maintenance of body potassium. *Diabetes*. 1983 Feb;32(2):106-11.
173. Menzies DJ, Dorsainvil PA, Cunha BA, Johnson DH. Severe and persistent hypoglycemia due to gatifloxacin interaction with oral hypoglycemic agents. *Am J Med*. 2002 Aug 15;113(3):232-4.
174. Lin G, Hays DP, Spillane L. Refractory hypoglycemia from ciprofloxacin and glyburide interaction. *J Toxicol Clin Toxicol*. 2004;42(3):295-7.
175. Yip C, Lee AJ. Gatifloxacin-induced hyperglycemia: A case report and summary of the current literature. *Clin Ther*. 2006 Nov;28(11):1857-66.

176. Shankar SS, Considine RV, Gorski JC, Steinberg HO. Insulin sensitivity is preserved despite disrupted endothelial function. *Am J Physiol Endocrinol Metab.* 2006 Oct;291(4):E691-6.
177. Walli R, Herfort O, Michl GM, Demant T, Jager H, Dieterle C, et al. Treatment with protease inhibitors associated with peripheral insulin resistance and impaired oral glucose tolerance in HIV-1-infected patients. *AIDS.* 1998 Oct 22;12(15):F167-73.
178. Behrens G, Dejam A, Schmidt H, Balks HJ, Brabant G, Korner T, et al. Impaired glucose tolerance, beta cell function and lipid metabolism in HIV patients under treatment with protease inhibitors. *AIDS.* 1999 Jul 9;13(10):F63-70.
179. Dahn MS, Lange MP, Mitchell RA, Lobdell K, Wilson RF. Insulin production following injury and sepsis. *J Trauma.* 1987 Sep;27(9):1031-8.
180. Marchuk JB, Finley RJ, Groves AC, Wolfe LI, Holliday RL, Duff JH. Catabolic hormones and substrate patterns in septic patients. *J Surg Res.* 1977 Sep;23(3):177-82.
181. Marana E, Scambia G, Maussier ML, Parpaglioni R, Ferrandina G, Meo F, et al. Neuroendocrine stress response in patients undergoing benign ovarian cyst surgery by laparoscopy, minilaparotomy, and laparotomy. *J Am Assoc Gynecol Laparosc.* 2003 May;10(2):159-65.
182. Karayiannakis AJ, Makri GG, Mantzioka A, Karousos D, Karatzas G. Systemic stress response after laparoscopic or open cholecystectomy: A randomized trial. *Br J Surg.* 1997 Apr;84(4):467-71.
183. Glaser F, Sannwald GA, Buhr HJ, Kuntz C, Mayer H, Klee F, et al. General stress response to conventional and laparoscopic cholecystectomy. *Ann Surg.* 1995 Apr;221(4):372-80.
184. Thorell A, Nygren J, Ljungqvist O. Insulin resistance: A marker of surgical stress. *Curr Opin Clin Nutr Metab Care.* 1999 Jan;2(1):69-78.
185. Jones HJ, de Cossart L. Risk scoring in surgical patients. *Br J Surg.* 1999 Feb;86(2):149-57.
186. Copeland GP. The POSSUM system of surgical audit. *Arch Surg.* 2002 Jan;137(1):15-9.
187. Sorensen JT. A physiologic model of glucose metabolism in man and its use to design and assess improved insulin therapies for diabetes [dissertation]. Boston, MA: Massachusetts Institute of Technology; 1985.

188. Fairbanks VF, Tefferi A. Normal ranges for packed cell volume and hemoglobin concentration in adults: Relevance to 'apparent polycythemia'. *Eur J Haematol*. 2000 Nov;65(5):285-96.
189. Hipszer B, Joseph J, Kam M. Pharmacokinetics of intravenous insulin delivery in humans with type 1 diabetes. *Diabetes Technol Ther*. 2005 Feb;7(1):83-93.
190. Ferrannini E, Wahren J, Faber OK, Felig P, Binder C, DeFronzo RA. Splanchnic and renal metabolism of insulin in human subjects: A dose-response study. *Am J Physiol*. 1983 Jun;244(6):E517-27.
191. Laakso M, Edelman SV, Brechtel G, Baron AD. Decreased effect of insulin to stimulate skeletal muscle blood flow in obese man. A novel mechanism for insulin resistance. *J Clin Invest*. 1990 Jun;85(6):1844-52.
192. Louard RJ, Fryburg DA, Gelfand RA, Barrett EJ. Insulin sensitivity of protein and glucose metabolism in human forearm skeletal muscle. *J Clin Invest*. 1992 Dec;90(6):2348-54.
193. Bonadonna RC, Saccomani MP, Seely L, Zych KS, Ferrannini E, Cobelli C, et al. Glucose transport in human skeletal muscle. the in vivo response to insulin. *Diabetes*. 1993 Jan;42(1):191-8.
194. Williams KV, Price JC, Kelley DE. Interactions of impaired glucose transport and phosphorylation in skeletal muscle insulin resistance: A dose-response assessment using positron emission tomography. *Diabetes*. 2001 Sep;50(9):2069-79.
195. Bonadonna RC, Del Prato S, Saccomani MP, Bonora E, Gulli G, Ferrannini E, et al. Transmembrane glucose transport in skeletal muscle of patients with non-insulin-dependent diabetes. *J Clin Invest*. 1993 Jul;92(1):486-94.
196. Yki-Jarvinen H, Young AA, Lamkin C, Foley JE. Kinetics of glucose disposal in whole body and across the forearm in man. *J Clin Invest*. 1987 Jun;79(6):1713-9.
197. Fugmann A, Lind L, Andersson PE, Millgard J, Hanni A, Berne C, et al. The effect of euglycaemic hyperinsulinaemia on forearm blood flow and glucose uptake in the human forearm. *Acta Diabetol*. 1998 Dec;35(4):203-6.
198. Brooks DC, Bessey PQ, Black PR, Aoki TT, Wilmore DW. Post-traumatic insulin resistance in uninjured forearm tissue. *J Surg Res*. 1984 Aug;37(2):100-7.
199. Fuller NJ, Hardingham CR, Graves M, Screaton N, Dixon AK, Ward LC, et al. Predicting composition of leg sections with anthropometry and bioelectrical impedance analysis, using magnetic resonance imaging as reference. *Clin Sci (Lond)*. 1999 Jun;96(6):647-57.

200. Little RA, Henderson A, Frayn KN, Galasko CS, White RH. The disposal of intravenous glucose studied using glucose and insulin clamp techniques in sepsis and trauma in man. *Acta Anaesthesiol Belg.* 1987;38(4):275-9.
201. Laakso M, Edelman SV, Brechtel G, Baron AD. Effects of epinephrine on insulin-mediated glucose uptake in whole body and leg muscle in humans: Role of blood flow. *Am J Physiol.* 1992 Aug;263(2 Pt 1):E199-204.
202. Taylor R, Magnusson I, Rothman DL, Cline GW, Caumo A, Cobelli C, et al. Direct assessment of liver glycogen storage by ¹³C nuclear magnetic resonance spectroscopy and regulation of glucose homeostasis after a mixed meal in normal subjects. *J Clin Invest.* 1996 Jan 1;97(1):126-32.
203. DeFronzo RA, Jacot E, Jequier E, Maeder E, Wahren J, Felber JP. The effect of insulin on the disposal of intravenous glucose. results from indirect calorimetry and hepatic and femoral venous catheterization. *Diabetes.* 1981 Dec;30(12):1000-7.
204. Rothman DL, Magnusson I, Katz LD, Shulman RG, Shulman GI. Quantitation of hepatic glycogenolysis and gluconeogenesis in fasting humans with ¹³C NMR. *Science.* 1991 Oct 25;254(5031):573-6.
205. Wahren J, Ekberg K. Splanchnic regulation of glucose production. *Annu Rev Nutr.* 2007;27:329-45.
206. Landau BR, Wahren J, Chandramouli V, Schumann WC, Ekberg K, Kalhan SC. Contributions of gluconeogenesis to glucose production in the fasted state. *J Clin Invest.* 1996 Jul 15;98(2):378-85.
207. Petersen KF, Laurent D, Rothman DL, Cline GW, Shulman GI. Mechanism by which glucose and insulin inhibit net hepatic glycogenolysis in humans. *J Clin Invest.* 1998 Mar 15;101(6):1203-9.
208. Moore MC, Connolly CC, Cherrington AD. Autoregulation of hepatic glucose production. *Eur J Endocrinol.* 1998 Mar;138(3):240-8.
209. Davidson MB. Autoregulation by glucose of hepatic glucose balance: Permissive effect of insulin. *Metabolism.* 1981 3;30(3):279-84.
210. Barthel A, Schmoll D. Novel concepts in insulin regulation of hepatic gluconeogenesis. *Am J Physiol Endocrinol Metab.* 2003 October 1;285(4):E685-692.
211. Adkins A, Basu R, Persson M, Dicke B, Shah P, Vella A, et al. Higher insulin concentrations are required to suppress gluconeogenesis than glycogenolysis in nondiabetic humans. *Diabetes.* 2003 Sep;52(9):2213-20.
212. Jiang G, Zhang BB. Glucagon and regulation of glucose metabolism. *Am J Physiol Endocrinol Metab.* 2003 Apr;284(4):E671-8.

213. Khani S, Tayek JA. Cortisol increases gluconeogenesis in humans: Its role in the metabolic syndrome. *Clin Sci (Lond)*. 2001 Dec;101(6):739-47.
214. Kraus-Friedmann N. Hormonal regulation of hepatic gluconeogenesis. *Physiol Rev*. 1984 January 1;64(1):170-259.
215. Pessin JE, Bell GI. Mammalian facilitative glucose transporter family: Structure and molecular regulation. *Annu Rev Physiol*. 1992 10/27;54(1):911-30.
216. Magnuson M. Glucokinase gene structure. functional implications of molecular genetic studies. *Diabetes*. 1990 May 1;39(5):523-7.
217. Vella A, Shah P, Basu R, Basu A, Camilleri M, Schwenk WF, et al. Effect of enteral vs. parenteral glucose delivery on initial splanchnic glucose uptake in nondiabetic humans. *Am J Physiol Endocrinol Metab*. 2002 Aug;283(2):E259-66.
218. Bergman RN, Beir JR, Hourigan PM. Intraportal glucose infusion matched to oral glucose absorption. lack of evidence for "gut factor" involvement in hepatic glucose storage. *Diabetes*. 1982 Jan;31(1):27-35.
219. DeFronzo RA, Ferrannini E, Hendler R, Felig P, Wahren J. Regulation of splanchnic and peripheral glucose uptake by insulin and hyperglycemia in man. *Diabetes*. 1983 Jan;32(1):35-45.
220. Basu R, Basu A, Johnson CM, Schwenk WF, Rizza RA. Insulin dose-response curves for stimulation of splanchnic glucose uptake and suppression of endogenous glucose production differ in nondiabetic humans and are abnormal in people with type 2 diabetes. *Diabetes*. 2004 Aug;53(8):2042-50.
221. Dahn MS, Mitchell RA, Lange MP, Smith S, Jacobs LA. Hepatic metabolic response to injury and sepsis. *Surgery*. 1995 May;117(5):520-30.
222. Wilmore DW, Goodwin CW, Aulick LH, Powanda MC, Mason AD, Jr, Pruitt BA, Jr. Effect of injury and infection on visceral metabolism and circulation. *Ann Surg*. 1980;192(4):491-504.
223. Esler M, Eisenhofer G, Chin J, Jennings G, Meredith I, Cox H, et al. Is adrenaline released by sympathetic nerves in man? *Clin Auton Res*. 1991 Jun;1(2):103-8.
224. Eisenhofer G, Rundquist B, Aneman A, Friberg P, Dakak N, Kopin IJ, et al. Regional release and removal of catecholamines and extraneuronal metabolism to metanephrines. *J Clin Endocrinol Metab*. 1995 Oct;80(10):3009-17.
225. Henriksen JH, Ring-Larsen H, Kanstrup IL, Christensen NJ. Splanchnic and renal elimination and release of catecholamines in cirrhosis. evidence of enhanced sympathetic nervous activity in patients with decompensated cirrhosis. *Gut*. 1984 Oct;25(10):1034-43.

226. Keller U, Gerber PP, Buhler FR, Stauffacher W. Role of the splanchnic bed in extracting circulating adrenaline and noradrenaline in normal subjects and in patients with cirrhosis of the liver. *Clin Sci (Lond)*. 1984 Jul;67(1):45-9.
227. Joyce DA, Beilin LJ, Vandongen R, Davidson L. Epinephrine sulfation in the forearm: Arteriovenous differences in free and conjugated catecholamines. *Life Sci*. 1982 Nov 29;31(22):2513-7.
228. Hoffmann JJ, Lenders JW, Pijls NH, Benraad TJ, Thien T. Vascular distribution of plasma catecholamines--pulmonary extraction, arterio-venous differences and effect of age. *Scand J Clin Lab Invest*. 1987 Apr;47(2):179-83.
229. Sole MJ, Drobac M, Schwartz L, Hussain MN, Vaughan-Neil EF. The extraction of circulating catecholamines by the lungs in normal man and in patients with pulmonary hypertension. *Circulation*. 1979 Jul;60(1):160-3.
230. Weil-Malherbe H, Axelrod J, Tomchick R. Blood-brain barrier for adrenaline. *Science*. 1959 May 1;129(3357):1226-7.
231. Steinman AM, Smerin SE, Barchas JD. Epinephrine metabolism in mammalian brain after intravenous and intraventricular administration. *Science*. 1969 Aug 8;165(893):616-7.
232. Cryer PE, Rizza RA, Haymond MW, Gerich JE. Epinephrine and norepinephrine are cleared through beta-adrenergic, but not alpha-adrenergic, mechanisms in man. *Metabolism*. 1980 Nov;29(11 Suppl 1):1114-8.
233. Bree F, Gault I, d'Athis P, Tillement JP. Beta adrenoceptors of human red blood cells, determination of their subtypes. *Biochem Pharmacol*. 1984 Dec 15;33(24):4045-50.
234. Galant SP, Underwood S, Duriseti L, Insel PA. Characterization of high-affinity beta2-adrenergic receptor binding of (-)-[3H]-dihydroalprenolol to human polymorphonuclear cell particulates. *J Lab Clin Med*. 1978 Oct;92(4):613-8.
235. Williams LT, Snyderman R, Lefkowitz RJ. Identification of beta-adrenergic receptors in human lymphocytes by (-) (3H) alprenolol binding. *J Clin Invest*. 1976 Jan;57(1):149-55.
236. Jones RT, Blake WD. Dynamics of epinephrine distribution in the dog. *Am J Physiol*. 1958 May;193(2):365-70.
237. Axelrod J, Tomchick R. Enzymatic O-methylation of epinephrine and other catechols. *J Biol Chem*. 1958 September 1;233(3):702-5.
238. Kuchel O, Buu N, Hamet P, Larochelle P, Bourque M, Genest J. Essential hypertension with low conjugated catecholamines imitates pheochromocytoma. *Hypertension*. 1981 May 1;3(3):347-55.

239. Porte D, Jr. A receptor mechanism for the inhibition of insulin release by epinephrine in man. *J Clin Invest.* 1967 Jan;46(1):86-94.
240. Samols E, Weir GC. Adrenergic modulation of pancreatic A, B, and D cells alpha-adrenergic suppression and beta-adrenergic stimulation of somatostatin secretion, alpha-adrenergic stimulation of glucagon secretion in the perfused dog pancreas. *J Clin Invest.* 1979 Feb;63(2):230-8.
241. Rizza RA, Cryer PE, Haymond MW, Gerich JE. Adrenergic mechanisms of catecholamine action on glucose homeostasis in man. *Metabolism.* 1980 Nov;29(11 Suppl 1):1155-63.
242. Natali A, Gastaldelli A, Galvan AQ, Sironi AM, Ciociaro D, Sanna G, et al. Effects of acute alpha 2-blockade on insulin action and secretion in humans. *Am J Physiol.* 1998 Jan;274(1 Pt 1):E57-64.
243. Lerner RL, Porte D, Jr. Epinephrine: Selective inhibition of the acute insulin response to glucose. *J Clin Invest.* 1971 Nov;50(11):2453-7.
244. Morrow LA, Morganroth GS, Herman WH, Bergman RN, Halter JB. Effects of epinephrine on insulin secretion and action in humans. interaction with aging. *Diabetes.* 1993 Feb;42(2):307-15.
245. Sacca L, Vigorito C, Cicala M, Corso G, Sherwin RS. Role of gluconeogenesis in epinephrine-stimulated hepatic glucose production in humans. *Am J Physiol.* 1983 Sep;245(3):E294-302.
246. Baron AD, Wallace P, Olefsky JM. In vivo regulation of non-insulin-mediated and insulin-mediated glucose uptake by epinephrine. *J Clin Endocrinol Metab.* 1987 May;64(5):889-95.
247. Fryburg DA, Gelfand RA, Jahn LA, Oliveras D, Sherwin RS, Sacca L, et al. Effects of epinephrine on human muscle glucose and protein metabolism. *Am J Physiol.* 1995 Jan;268(1 Pt 1):E55-9.
248. Bessey PQ, Brooks DC, Black PR, Aoki TT, Wilmore DW. Epinephrine acutely mediates skeletal muscle insulin resistance. *Surgery.* 1983 Aug;94(2):172-9.
249. Capaldo B, Napoli R, Di Marino L, Sacca L. Epinephrine directly antagonizes insulin-mediated activation of glucose uptake and inhibition of free fatty acid release in forearm tissues. *Metabolism.* 1992 Oct;41(10):1146-9.
250. Allwood MJ, Keck EW, Marshall RJ, Shepherd JT. Correlation of hemodynamic events during infusion of epinephrine in man. *J Appl Physiol.* 1962 Jan;17:71-4.
251. Bearn AG, Billing B, Sherlock S. The effect of adrenaline and noradrenaline on hepatic blood flow and splanchnic carbohydrate metabolism in man. *J Physiol.* 1951 December 28;115(4):430-41.

252. Stumvoll M, Chintalapudi U, Perriello G, Welle S, Gutierrez O, Gerich J. Uptake and release of glucose by the human kidney. postabsorptive rates and responses to epinephrine. *J Clin Invest.* 1995 Nov;96(5):2528-33.
253. Samra JS, Simpson EJ, Clark ML, Forster CD, Humphreys SM, Macdonald IA, et al. Effects of epinephrine infusion on adipose tissue: Interactions between blood flow and lipid metabolism. *Am J Physiol.* 1996 Nov;271(5 Pt 1):E834-9.
254. Baltzan MA, Andres R, Cader G, Zieler KL. Effects of epinephrine on forearm blood flow and metabolism in man. *J Clin Invest.* 1965 Jan;44:80-92.
255. Bryan RM, Jr. Cerebral blood flow and energy metabolism during stress. *Am J Physiol.* 1990 Aug;259(2 Pt 2):H269-80.
256. Myburgh JA, Upton RN, Grant C, Martinez A. The effect of infusions of adrenaline, noradrenaline and dopamine on cerebral autoregulation under propofol anaesthesia in an ovine model. *Intensive Care Med.* 2003 May;29(5):817-24.
257. Dahlgren N, Rosén I, Sakabe T, Siesjö BK. Cerebral functional, metabolic and circulatory effects of intravenous infusion of adrenaline in the rat. *Brain Research.* 1980 2/17;184(1):143-52.

APPENDIX A: ORIGINAL MODEL EQUATIONS

The equations for the model of glucose metabolism as they appear in the 1985 doctoral thesis of John Sorensen are provided here. In general, time-varying variables (*e.g.*, G_H and r_{PIR}) are italicized whereas time-invariant quantities (*e.g.*, Q_L^1 and r_{RBCU}) are not. Some minor corrections and clarifications are provided for the reader. In equation A.A.45 (a description of the kidney glucose excretion rate r_{KGE}), the quantity 0.011 multiplying the expression (G_K-460) within the hyperbolic tangent function was incorrectly reported in some sections of Sorensen's thesis. In the equations for pancreatic insulin release (equations A.34-A.41), the superscript 0+ in the expression $(X-I)^{0+}$ denotes that the expression only takes on positive values and is zero otherwise.

Glucose Subsystem

$$\frac{d}{dt} G_{BV} = \frac{1}{V_{BV}^G} \left[Q_B^G (G_H - G_{BV}) - \frac{V_{BI}^G}{T_B} (G_{BV} - G_{BI}) \right] \quad A.1$$

$$\frac{d}{dt} G_{BI} = \frac{1}{V_{BI}^G} \left[\frac{V_{BI}^G}{T_B} (G_{BV} - G_{BI}) - r_{BGU} \right] \quad A.2$$

$$\frac{d}{dt} G_H = \frac{1}{V_H^G} \left[Q_B^G G_{BV} + Q_L^G G_L + Q_K^G G_K + Q_P^G G_{PV} - Q_H^G G_H - r_{RBCU} \right] \quad A.3$$

$$\frac{d}{dt} G_G = \frac{1}{V_G^G} \left[Q_G^G (G_H - G_G) - r_{GGU} \right] \quad A.4$$

$$\frac{d}{dt} G_L = \frac{1}{V_L^G} \left[Q_A^G G_H + Q_G^G G_G - Q_L^G I_L + r_{HGP} - r_{HGU} \right] \quad A.5$$

$$\frac{d}{dt} G_K = \frac{1}{V_K^G} \left[Q_K^G (G_H - G_K) - r_{KGE} \right] \quad A.6$$

$$\frac{d}{dt} G_{PV} = \frac{1}{V_{PV}^G} \left[Q_P^G (G_H - G_{PV}) - \frac{V_{PI}^G}{T_P} (G_{PV} - G_{PI}) \right] \quad A.7$$

$$\frac{d}{dt} G_{PI} = \frac{1}{V_{PI}^G} \left[\frac{V_{PI}^G}{T_P} (G_{PV} - G_{PI}) - r_{PGU} \right] \quad A.8$$

$$r_{\text{KGE}} = \begin{cases} 71 + 71 \tanh[0.011(G_{\text{K}} - 460)], & 0 \leq G_{\text{K}} \leq 460 \\ -330 + 0.872G_{\text{K}}, & G_{\text{K}} > 460 \end{cases} \quad \text{A.45}$$

$$r_{\text{PGU}} = \Gamma_{\text{PGU}}^{\text{B}} M_{\text{PGU}}^{\text{G}} M_{\text{PGU}}^{\text{I}} \quad \text{A.10}$$

$$M_{\text{PGU}}^{\text{G}} = \frac{G_{\text{PI}}}{G_{\text{PI}}^{\text{B}}} \quad \text{A.11}$$

$$M_{\text{PGU}}^{\text{I}} = 7.03 + 6.52 \tanh \left[0.338 \left(\frac{I_{\text{PI}}}{I_{\text{PI}}^{\text{B}}} - 5.82 \right) \right] \quad \text{A.12}$$

$$r_{\text{HGU}} = \Gamma_{\text{HGU}}^{\text{B}} M_{\text{HGU}}^{\text{G}} M_{\text{HGU}}^{\text{I}} \quad \text{A.13}$$

$$M_{\text{HGU}}^{\text{G}} = 5.66 + 5.66 \tanh \left[2.44 \left(\frac{G_{\text{L}}}{G_{\text{L}}^{\text{B}}} - 1.48 \right) \right] \quad \text{A.14}$$

$$\frac{d}{dt} M_{\text{HGU}}^{\text{I}} = \frac{1}{\tau_1} [M_{\text{HGU}}^{\text{I}\infty} - M_{\text{HGU}}^{\text{I}}] \quad \text{A.15}$$

$$M_{\text{HGU}}^{\text{I}\infty} = 2.0 \tanh \left[0.55 \frac{I_{\text{L}}}{I_{\text{L}}^{\text{B}}} \right] \quad \text{A.16}$$

$$r_{\text{HGP}} = \Gamma_{\text{HGP}}^{\text{B}} M_{\text{HGP}}^{\text{G}} M_{\text{HGP}}^{\text{I}} M_{\text{HGP}}^{\Gamma} \quad \text{A.17}$$

$$M_{\text{HGP}}^{\text{G}} = 1.42 - 1.41 \tanh \left[0.62 \left(\frac{G_{\text{L}}}{G_{\text{L}}^{\text{B}}} - 0.497 \right) \right] \quad \text{A.18}$$

$$\frac{d}{dt} M_{\text{HGP}}^{\text{I}} = \frac{1}{\tau_1} [M_{\text{HGP}}^{\text{I}\infty} - M_{\text{HGP}}^{\text{I}}] \quad \text{A.19}$$

$$M_{\text{HGP}}^{\text{I}\infty} = 1.21 - 1.14 \tanh \left[1.66 \left(\frac{I_{\text{L}}}{I_{\text{L}}^{\text{B}}} - 0.89 \right) \right] \quad \text{A.20}$$

$$M_{\text{HGP}}^{\Gamma} = M_{\text{HGP}}^{\Gamma 0} - f_2 \quad \text{A.21}$$

$$M_{\text{HGP}}^{\Gamma 0} = 2.7 \tanh[0.39\Gamma^{\text{N}}] \quad \text{A.22}$$

$$\frac{d}{dt} f_2 = \frac{1}{\tau_{\Gamma}} \left[\frac{M_{\text{HGP}}^{\Gamma 0} - 1}{2} - f_2 \right] \quad \text{A.23}$$

$$\begin{array}{llll}
V_{BV}^G = 3.5 \text{ dl} & Q_B^G = 5.9 \text{ dl/min} & T_B = 2.1 \text{ min} & G_H^B = 91.89 \text{ mg/dl} \\
V_{BI}^G = 4.5 \text{ dl} & Q_A^G = 2.5 \text{ dl/min} & T_P^G = 5.0 \text{ min} & G_L^B = 101.0 \text{ mg/dl} \\
V_H^G = 13.8 \text{ dl} & Q_H^G = 43.7 \text{ dl/min} & & G_{PI}^B = 86.81 \text{ mg/dl} \\
V_L^G = 25.1 \text{ dl} & Q_L^G = 12.6 \text{ dl/min} & \tau_I = 25 \text{ min} & r_{PGU}^B = 35 \text{ mg/min} \\
V_G^G = 11.2 \text{ dl} & Q_G^G = 10.1 \text{ dl/min} & \tau_T = 65 \text{ min} & r_{HGU}^B = 20 \text{ mg/min} \\
V_K^G = 6.6 \text{ dl} & Q_K^G = 10.1 \text{ dl/min} & & r_{HGP}^B = 155 \text{ mg/min} \\
V_{PV}^G = 10.4 \text{ dl} & Q_P^G = 15.1 \text{ dl/min} & & r_{BGU} = 70 \text{ mg/min} \\
V_{PI}^G = 67.4 \text{ dl} & & & r_{BCU} = 10 \text{ mg/min} \\
& & & r_{GGU} = 20 \text{ mg/min}
\end{array}$$

Insulin Subsystem

$$\frac{d}{dt} I_B = \frac{1}{V_B^I} [Q_B^I (I_H - I_B)] \quad \text{A.24}$$

$$\frac{d}{dt} I_H = \frac{1}{V_H^I} [Q_B^I I_B + Q_L^I I_L + Q_K^I I_K + Q_P^I I_{PV} - Q_H^I I_H] \quad \text{A.25}$$

$$\frac{d}{dt} I_G = \frac{1}{V_G^I} [Q_G^I (I_H - I_G)] \quad \text{A.26}$$

$$\frac{d}{dt} I_L = \frac{1}{V_L^I} [Q_A^I I_H + Q_G^I I_G - Q_L^I I_L + r_{PIR} - r_{LIC}] \quad \text{A.27}$$

$$\frac{d}{dt} I_K = \frac{1}{V_K^I} [Q_K^I (I_H - I_K) - r_{KIC}] \quad \text{A.28}$$

$$\frac{d}{dt} I_{PV} = \frac{1}{V_{PV}^I} \left[Q_P^I (I_H - I_{PV}) - \frac{V_{PI}^I}{T_P^I} (I_{PV} - I_{PI}) \right] \quad \text{A.29}$$

$$\frac{d}{dt} I_{PI} = \frac{1}{V_{PI}^I} \left[\frac{V_{PI}^I}{T_P^I} (I_{PV} - I_{PI}) - r_{PIC} \right] \quad \text{A.30}$$

$$r_{LIC} = F_{LIC} [Q_A^I I_H + Q_G^I I_G + r_{PIR}] \quad \text{A.31}$$

$$r_{KIC} = F_{KIC} Q_K^I I_K \quad \text{A.32}$$

$$r_{PIC} = \frac{I_{PI}}{\frac{1}{Q_P^I} \left(\frac{1 - F_{PIC}}{F_{PIC}} \right) - \frac{T_P^I}{V_{PI}^I}} \quad \text{A.33}$$

$$r_{PIR} = r_{PIR}^B \frac{S(G_H)}{S_\infty(G_H^B)} \quad \text{A.34}$$

$$S(G_H) = Q(M_1 Y + M_2 (X - I)^{0+}) \quad \text{A.35}$$

$$S_\infty(G_H^B) = \frac{(\gamma P_\infty + K Q_0) M_1 Y}{K + M_1 Y} \quad \text{A.36}$$

$$X(G) = \frac{G^{3.27}}{132^{3.27} + 5.93G^{3.02}} \quad \text{A.37}$$

$$Y = P_\infty = X^{1.11} \quad \text{A.38}$$

$$\frac{d}{dt} P = \alpha(P_\infty - P) \quad \text{A.39}$$

$$\frac{d}{dt} I = \beta(X - I) \quad \text{A.40}$$

$$\frac{d}{dt} Q = K(Q_0 - Q) + \gamma P - S \quad \text{A.41}$$

$V_B^I = 0.261$	$Q_B^I = 0.45 \text{ l/min}$	$T_P^I = 20 \text{ min}$	$\alpha = 0.0482 \text{ min}^{-1}$
$V_H^I = 0.991$	$Q_H^I = 3.12 \text{ l/min}$	$F_{LIC} = 0.40$	$\beta = 0.931 \text{ min}^{-1}$
$V_L^I = 0.941$	$Q_L^I = 0.90 \text{ l/min}$	$F_{KIC} = 0.30$	$\gamma = 0.575 \text{ U/min}$
$V_G^I = 1.141$	$Q_G^I = 0.72 \text{ l/min}$	$F_{PIC} = 0.15$	$K = 0.00794 \text{ min}^{-1}$
$V_K^I = 0.511$	$Q_K^I = 0.72 \text{ l/min}$	$I_H^B = 15.15 \text{ mU/l}$	$M_1 = 0.00747 \text{ min}^{-1}$
$V_{PV}^I = 0.741$	$Q_P^I = 1.05 \text{ l/min}$	$I_L^B = 21.43 \text{ mU/l}$	$M_2 = 0.0958 \text{ min}^{-1}$
$V_{PI}^I = 6.741$	$Q_A^I = 0.18 \text{ l/min}$	$I_{PI}^B = 5.304 \text{ mU/l}$	$Q_0 = 6.33 \text{ U}$
			$r_{PIR}^B = 20 \text{ mU/min}$

Glucagon Subsystem

$$\frac{d}{dt} \Gamma^N = \frac{r_{MFC}}{V^\Gamma} [M_{PT\Gamma}^G M_{PT\Gamma}^I - \Gamma^N] \quad \text{A.42}$$

$$M_{PT\Gamma}^G = 2.93 - 2.10 \tanh \left[4.18 \left(\frac{G_H}{G_B} - 0.61 \right) \right] \quad \text{A.43}$$

$$M_{PT\Gamma}^I = 1.31 - 0.61 \tanh \left[1.06 \left(\frac{I_H}{I_B} - 0.47 \right) \right] \quad \text{A.44}$$

$$V^\Gamma = 11310 \text{ ml} \quad r_{MFC} = 9.10 \text{ ml/min}$$

APPENDIX B: EPINEPHRINE INFUSION STUDIES IN MAN

Subjects (Male/Female)	Infusion Rate (ug/min)	Average (\pm SD) Epinephrine Concentration (pg/ml)			Reference
		Arterial	Arterialized	Venous	
6M	0.00	71 \pm 32		50 \pm 17	[11]
6M	0.10	112 \pm 22		77 \pm 27	
6M	2.00	826 \pm 174		437 \pm 161	
16	0.00	57 \pm 21		29 \pm 15	[12]
13M/1F	0.00	132 \pm 63		80 \pm 37	[13]
40	0.00	27 \pm 12		7 \pm 5	[21]
6M	0.00	62 \pm 36		35 \pm 18	[23]
12	0.00	53 \pm 44		13 \pm 6	[10]
12	0.00	46 \pm 19		16 \pm 13	
12M	0.00	35 \pm 19		24 \pm 19	[29]
12M	0.26 ^b	125 \pm 19		66 \pm 19	
12M	0.77 ^b	291 \pm 63		115 \pm 44	
12M	2.56 ^b	842 \pm 164		382 \pm 70	
8	0.00	49			[19]
8	3.40	668			
12M	0.00	45 \pm 38			[20]
12M	0.42	163 \pm 70			
12M	1.39	456 \pm 82			
12M	4.18	1177 \pm 171			
10M	0.00	55 \pm 35			[25]
10M	0.32 ^b	152 \pm 20			
10M	3.85 ^b	1130 \pm 119			
11M	0.00	49 \pm 24			[26]
11M	0.64 ^b	245 \pm 42			
11M	1.28 ^b	421 \pm 55			
11M	3.85 ^b	1102 \pm 164			
8M/3F	0.00	78			[30]
8M/3F	1.92 ^b	504			
8M/3F	3.85 ^b	981			
6M	0.00	37 \pm 22			[31]
6M	0.70 ^b	251 \pm 130			
6M	2.80 ^b	683 \pm 179			
1M/6F	0.00	29 \pm 12			[32]
1M/6F	2.56 ^b	636 \pm 150			
1M/6F	5.13 ^b	1283 \pm 156			

8	0.00	100 ± 28	[103]
6M/3F	0.00	84 ± 33	[14]
6M/3F	1.05 ^a	360 ± 72	
6M/3F	5.23 ^a	1177 ± 165	
5F	0.00	26 ± 9	[15]
5F	3.00 ^b	822 ± 134	
8M/9F	0.00	31 ± 17	[16]
8M/9F	4.20 ^b	736 ± 230	
6	0.10	54 ± 30	[103]
6	0.50	114 ± 28	
6	1.00	219 ± 83	
6	2.50	412 ± 89	
6	5.00	715 ± 228	
5M/7F	0.00	38	[17]
5	0.00	37 ± 13	[18]
8	0.00	28 ± 8	[8]
8	2.30 ^a	375-425	
6M	0.00	49 ± 13	[24]
6M	0.00	53 ± 27	
6M	0.79	155 ± 45	
6M	2.36	267 ± 107	
6M	3.93	391 ± 897	
6M	5.90	692 ± 1004	
6M	6.52	797 ± 480	
6M	7.86	844 ± 256	
8M	0.00	47 ± 20	[5]
8M	1.05 ^b	192 ± 54	
8M	5.60 ^b	1140 ± 342	
7M	0.00	27 ± 15	[27]
7M	0.70 ^b	134 ± 39	
7M	3.50 ^b	401 ± 73	
95	0.00	55 ± 22	[28]
5M	1.75 ^b	178 ± 34	
10M	3.50 ^b	259 ± 76	
5M	7.00 ^b	484 ± 154	

^a intravenous epinephrine infusion rate reported per m² body surface area without subject body surface area reported (1.9m² body surface area assumed)

^b intravenous epinephrine infusion rate reported per kg body weight without average subject weight reported (assumed 60kg and 70kg body mass for female and male subjects, respectively)

APPENDIX C: VALUES FOR EXTENDED MODEL PARAMETERS

Subscript j	Q_j (l/min)	$V_{j,B}$ (l)	$V_{j,ISF}$ (l)	$V_{j,ICF}$
B	0.70	0.41	0.45	8.60
H	(5.20)	1.64	-	-
L	(1.50)	0.90	0.60	1.15
G	1.20	0.71	0.52	1.01
K	1.20	0.68	0.09	0.18
P	1.80	1.26	6.74	19.65
A	0.30	-	-	-

$$WCP = 0.84$$

$$HCT = 0.40$$

Glucose Subsystem

$$V_{BV}^G = \frac{10 \text{ dl}}{1} \times WCP \times V_{B,B}$$

$$Q_B^G = \frac{10 \text{ dl}}{1} \times WCP \times M_Q^E \times Q_B$$

$$V_{BI}^G = \frac{10 \text{ dl}}{1} \times V_{B,ISF}$$

$$Q_K^G = \frac{10 \text{ dl}}{1} \times WCP \times Q_K$$

$$V_H^G = \frac{10 \text{ dl}}{1} \times WCP \times V_{H,B}$$

$$Q_P^G = \frac{10 \text{ dl}}{1} \times WCP \times M_Q^E \times Q_P$$

$$V_L^G = \frac{10 \text{ dl}}{1} (WCP \times V_{L,B} + V_{L,ISF} + V_{L,ICF})$$

$$Q_G^G = \frac{10 \text{ dl}}{1} \times WCP \times M_Q^E \times Q_G$$

$$V_G^G = \frac{10 \text{ dl}}{1} (WCP \times V_{G,B} + V_{G,ISF})$$

$$Q_A^G = \frac{10 \text{ dl}}{1} \times WCP \times M_Q^E \times Q_A$$

$$V_K^G = \frac{10 \text{ dl}}{1} (WCP \times V_{K,B} + V_{K,ISF})$$

$$Q_L^G = Q_A^G + Q_G^G$$

$$Q_H^G = Q_B^G + Q_K^G + Q_P^G + Q_L^G$$

$$V_{PV}^G = \frac{10 \text{ dl}}{1} \times WCP \times V_{P,B}$$

$$V_{PI}^G = \frac{10 \text{ dl}}{1} \times V_{P,ISF}$$

Insulin Subsystem

$$V_B^I = (1 - HCT) \times V_{B,B}$$

$$Q_B^I = (1 - HCT) \times M_Q^E \times Q_B$$

$$V_H^I = (1 - HCT) \times V_{H,B}$$

$$Q_K^I = (1 - HCT) \times Q_K$$

$$V_L^I = (1 - HCT) \times V_{L,B} + V_{L,ISF}$$

$$Q_P^I = (1 - HCT) \times M_Q^E \times Q_P$$

$$V_G^I = (1 - HCT) \times V_{G,B} + V_{G,ISF}$$

$$Q_G^I = (1 - HCT) \times M_Q^E \times Q_G$$

$$V_K^I = (1 - HCT) \times V_{K,B} + V_{K,ISF}$$

$$Q_A^I = (1 - HCT) \times M_Q^E \times Q_A$$

$$V_{PV}^I = (1 - HCT) \times V_{P,B}$$

$$Q_L^I = Q_A^I + Q_G^I$$

$$V_{PI}^I = V_{P,ISF}$$

$$Q_H^I = Q_B^I + Q_K^I + Q_P^I + Q_L^I$$

Glucagon Subsystem

$$V^\Gamma = \frac{1000 \text{ ml}}{1} \times \sum_j V_j^1 \text{ for } j = \{B, H, L, G, K, PV, PI\}$$

Epinephrine Subsystem

$$\begin{aligned} V_B^E &= \frac{1000 \text{ ml}}{1} \times \text{WCP} \times V_{B,B} & Q_B^E &= \frac{1000 \text{ ml}}{1} \times \text{WCP} \times M_Q^E \times Q_B \\ V_H^E &= \frac{1000 \text{ ml}}{1} \times \text{WCP} \times V_{H,B} & Q_K^E &= \frac{1000 \text{ ml}}{1} \times \text{WCP} \times Q_K \\ V_G^E &= \frac{1000 \text{ ml}}{1} \times (\text{WCP} \times V_{G,B} + V_{G,ISF}) & Q_P^E &= \frac{1000 \text{ ml}}{1} \times \text{WCP} \times M_Q^E \times Q_P \\ V_L^E &= \frac{1000 \text{ ml}}{1} \times (\text{WCP} \times V_{L,B} + V_{L,ISF}) & Q_G^E &= \frac{1000 \text{ ml}}{1} \times \text{WCP} \times M_Q^E \times Q_G \\ V_K^E &= \frac{1000 \text{ ml}}{1} \times (\text{WCP} \times V_{K,B} + V_{K,ISF}) & Q_A^E &= \frac{1000 \text{ ml}}{1} \times \text{WCP} \times M_Q^E \times Q_A \\ V_P^E &= \frac{1000 \text{ ml}}{1} \times (\text{WCP} \times V_{P,B} + V_{P,ISF}) & Q_L^E &= Q_A^E + Q_G^E \\ & & Q_H^E &= Q_B^E + Q_K^E + Q_P^E + Q_L^E \end{aligned}$$

Additional Subsystem-specific Parameter Values

Glucose (G)	Insulin (I)	Glucagon (Γ)	Epinephrine (E)
$G_H^B = 91.89 \text{ mg/dl}$	$T_P^I = 20 \text{ min}$	$r_{MFC} = 9.10 \text{ ml/min}$	$E_H^B = 75 \text{ pg/ml}$
$G_L^B = 101.0 \text{ mg/dl}$	$F_{LIC} = 0.40$		$F_{LEC} = 0.87$
$G_{PI}^B = 86.81 \text{ mg/dl}$	$F_{KIC} = 0.30$		$F_{KEC} = 0.51$
$r_{PGU}^B = 35 \text{ mg/min}$	$F_{PIC} = 0.15$		$F_{PEC} = 0.55$
$r_{HGU}^B = 20 \text{ mg/min}$	$I_H^B = 15.15 \text{ mU/l}$		$F_{GEC} = 0.37$
$r_{HGP}^B = 155 \text{ mg/min}$	$I_L^B = 21.43 \text{ mU/l}$		
$r_{BGU} = 70 \text{ mg/min}$	$I_{PI}^B = 5.304 \text{ mU/l}$		
$r_{RBCU} = 10 \text{ mg/min}$	$\alpha = 0.0482 \text{ min}^{-1}$		
$r_{GGU} = 20 \text{ mg/min}$	$\beta = 0.931 \text{ min}^{-1}$		
$T_B = 2.1 \text{ min}$	$\gamma = 0.575 \text{ U/min}$		
$T_P^G = 5.0 \text{ min}$	$K = 0.00794 \text{ min}^{-1}$		
$\tau_I = 25 \text{ min}$	$M_1 = 0.00747 \text{ min}^{-1}$		
$\tau_\Gamma = 65 \text{ min}$	$M_2 = 0.0958 \text{ min}^{-1}$		
	$Q_0 = 6.33 \text{ U}$		
	$r_{PIR}^B = 20 \text{ mU/min}$		

VITA

Brian Ray Hipszer

Born in Abington, Pennsylvania on November 27, 1974

A citizen of the United States of America

Education:

1993-98 BSc Drexel University (Electrical Engineering)

1998-01 MSc Drexel University (Electrical Engineering and Biomedical Engineering)

Awards, Honors and Membership in Honorary Societies:

1993-98 A.J. Drexel Scholarship, Drexel University

1998-03 Calhoun Fellowship, School of Biomedical Engineering, Science, and Health Systems, Drexel University

Memberships in Professional and Scientific Societies:

1996- Member, IEEE

Editorial Positions:

2008 Reviewer, Journal of Diabetes Science and Technology

Academic Committees:

2008 - Member, Diabetes Working Group. Thomas Jefferson University Hospital Committee charged with developing guidelines and protocols to improve blood glucose control at TJUH.

Lectures by Invitation:

October 26, 2007 “The Utility of Simultaneous Glucose Sensor Measurements” Diabetes Technology Meeting, October 2007, San Francisco, CA

Peer-reviewed Publications:

1. **Hipszer B**, Joseph J, Kam M., Pharmacokinetics of Intravenous Insulin Delivery in Humans with Type 1 Diabetes. *Diabetes Technology & Therapeutics*, 2005;7(1):83-93.
2. Ganesh A, **Hipszer B**, Loomba N, Simon B, Torjman MC, Joseph JI. Evaluation of the VIA[®] Blood Chemistry Monitor for Glucose in Healthy and Diabetic Volunteers. *Journal of Diabetes Science and Technology*, 2008;2(2):182-193.
3. Simon B, Treat V, Marco C, Rosenberg D, Joseph JI, **Hipszer B**, Li Y, Chervoneva I, Padron-Massara L, Jabbour S. A comparison of glycemic variability in CSII versus MDI treated type 1 diabetic patients using CGMS. *International Journal of Clinical Practice*. 2008;62(12):1858-1863.
4. Mraovic B, Joseph JI, **Hipszer B**, Epstein RH, Pulido L, Parvizi J, Pequignot E, Chervoneva I, Grunwald Z. Preadmission hyperglycemia is an independent risk factor for in-hospital symptomatic pulmonary embolism after major orthopedic surgery. *The Journal of Arthroplasty*, 2008; *in press*

